

M-AM-MinA1 ATP β S DIASTEREOMERS AS SUBSTRATES OF ION TRANSPORTING ATPASES. M. Cohn, and A. Scarpa. Dept. Biochem-Biophysics, University of Pennsylvania, Philadelphia, PA 19104 USA.

The greater free energy of hydrolysis of the thioanalog of ATP, adenosine 5'-O-(2-thiotriphosphate) (ATP β S) relative to ATP ($\Delta\Delta F \sim 2.5$ Kcal/mole), permits the investigation of the coupling between ATPase and ion transport, in particular, an aspect of the thermodynamics of maintenance of ion concentration gradients for ion transporting ATPases. Of the three systems investigated, fragmented sarcoplasmic reticulum from rabbit skeletal muscle (SR), mitochondrial ATPase (Mw), and chromaffin granule ghost ATPase (CG), the SR ATPase is unique in that the steady state rates of the Ca-dependent hydrolysis are the same for ATP and for both diastereomers of ATP β S, R and S. For Mw ATPase, the relative rates of hydrolysis of ATP, ATP β S (R) and ATP β S (S) are approximately 100, 3, and 0, respectively. Similarly for CG ATPase, relative rates of ATP, ATP β S(R) and (S) are 100, 30, and 0, respectively. For the SR system, the kinetics of E-P formation were followed by fast quench using (γ - 32 P) ATP and (γ - 32 P) ATP β S(S) and the rate was ~ 2 -fold greater for the thioanalog. The basal ATPase activity (in EGTA) and the ATPase activity resulting from the low affinity site were undetectable for the ATP β S substrates. The rate and the steady state level of Ca $^{++}$ transport by SR are within experimental error identical for ATP and both ATP β S isomers. Thus, the increased free energy of hydrolysis of the thioanalog substrates was not reflected in an observable increase in the Ca $^{++}$ concentration gradient across the vesicle. On the other hand, under conditions leading to nucleoside triphosphate synthesis by reversal of the pump, much greater net synthesis of ATP than of ATP β S was achieved with identical concentrations of intravesicular Ca $^{++}$.

M-AM-MinA2 STRUCTURE, FUNCTION, AND COUPLING IN CYTOCHROME OXIDASE. B. Chance, Johnson Research Foundation, University of PA, Philadelphia, Pennsylvania.

Cytochrome oxidase has now emerged as the best known energy conserving transmembrane protein of the respiratory chain. Recent work on the membrane profile and location of the dimer by image-processed EMG(1,2), the amino acid sequence of the subunit II(3), the homologies of the portions of the sequence with well-known Cu proteins(3), and the intimate geometries of the two pairs of bimetallic clusters obtained from X-ray synchrotron and resonance scattering studies(4) identifies the electron transport reaction as unilateral rather than transmembrane(5). The details of the structure of the redox site, a S-bridged complex unreactive to ligands until reduction and oxygen binding can occur, explain much of the hitherto mysterious chemistry of the oxidase reactions. The spacing of the components of the bimetallic cluster is appropriate to a highly energetic reaction involving peroxide bridge formation and rupture of the O-O bond, together with changes in the relative distances in the Fe-Cu cluster atoms of 3.75 to over 4.00 Å, makes an even more favorable case for mechanical coupling to changes of structural features of the protein than in the case of the "honorary enzyme", hemoglobin. The unilateral location of electron transport in cytochrome oxidase emphasizes the need for a proton pumping mechanism linked to bond making and bond breaking processes and structural changes of the redox center of the enzyme itself(5).

(1) T. Frey et al., *J. Biol. Chem.* 253:4389-4395, 1979. (2) R. Capaldi et al, in *Interaction Between Iron and Proteins in Oxygen and Electron Transport* (C. Ho, ed) Elsevier/North Holland, in press. (3) G. Buse et al, in *Frontiers of Biological Energetics* (P. L. Dutton et al, eds), Academic, NY, 799-809, 1979. (4) L. Powers et al, Abstract, this vol. (5) B. Chance, Abstract, this vol. NIH GM27308, 27476, 38385, HLSCOR15061; SSRL Project 423B (NSF, DDR, DOE).

M-AM-MinA3 THE MITOCHONDRIAL OXIDATIVE PHOSPHORYLATION SYSTEM, YOUSSEF HATEFI, Scripps Clinic and Research Foundation, La Jolla, California 92037

The bovine heart oxidative phosphorylation system is composed of 5 enzyme complexes. Complexes I to IV catalyze the following electron transfer reaction. I: NAD(P)H \rightarrow Q (ubiquinone), II: succinate \rightarrow Q, III: reduced Q \rightarrow ferricytochrome c, and IV: ferrocyt. c \rightarrow O $_2$. Complex V catalyzes ATP synthesis and hydrolysis. Complexes I to V are present in beef-heart mitochondria in the approximate ratio of 1:2:3:7:3, respectively. I, III, IV and V are each capable of energy transduction (vectorial proton translocation) coupled to electron transfer (I, III, IV) or ATP hydrolysis (V). Details of their molecular weight (minimum) and composition are: Complex I - $M_r \sim 700,000$, 22-24 polypeptides, contains FMN and 5 iron-sulfur (FeS) centers in 5 separate polypeptides. Complex II - $M_r \sim 150,000$, 4 polypeptides. It is composed of succinate dehydrogenase (FeS flavoprotein; $M_r = 97,000$; 1 FAD:7-8 Fe:7-8 S $^{2-}$; 2 subunits, $M_r = 70,000$ and 27,000; larger subunit carries FAD plus half of FeS, smaller subunit contains the remainder of FeS) and a low potential cyt. b (b $_{560}$) (2 polypeptides $M_r \sim 15,500$ and 13,500). Complex III - $M_r \sim 250,000$; 8-9 subunits; 2 b cytochromes (b $_{562}$ and b $_{566}$), 1 cyt. c $_1$ ($M_r \sim 30,000$), and one FeS protein ($M_r = 24,500$, 1 2Fe-2S center). Complex IV - M_r (per mol a + a $_3$) $140-180 \times 10^3$, 7 subunits, 2 g atoms of Cu per a + a $_3$. Complex V - $M_r \sim 500,000$; 12-14 unlike subunits; contains F $_1$ -ATPase (5 unlike subunits), oligomycin sensitivity-conferring protein, uncoupler-binding protein, dicyclohexylcarbodiimide-binding protein, coupling factors F $_6$ and probably B, ATPase inhibitor protein, and two polypeptides of $M_r \sim 22-24,000$. Energy communication among the energy transducing Complexes I, III, IV and V occurs by way of the electrochemical potential of protons ($\Delta\mu_H^+$). Results of recent studies on the manner in which $\Delta\mu_H^+$ is utilized by Complex V for ATP synthesis and by the respiratory chain for reverse electron transfer (succinate \rightarrow NAD) will be discussed.

M-AM-MinA4 THE ACTIVE FORM OF CYTOCHROME OXIDASE S. Ferguson-Miller, M. Suarez-Villafane and D.A. Thompson, Biochemistry Department, Michigan State University, E. Lansing, MI 48824

To clarify the relationship between the function of cytochrome oxidase and its interaction with the membrane and with itself, we have studied the kinetic behavior of rat liver cytochrome oxidase in the intact membrane, solubilized membrane, purified form and reconstituted state. The kinetic parameters of the enzyme are altered in each of these conditions and reconstitution into liposomes does not reestablish the kinetic behavior observed in the native membrane.

The size of the active form of cytochrome oxidase has been examined by gel filtration and radiation inactivation analysis. Enzyme forms with apparent molecular weights of 650, 320, and 130 kd are observed in beef heart oxidase preparations and are found to have identical high activity. By irradiating the oxidase with high energy electrons, a target size can be obtained representing the volume of protein required for activity. Using a highly active oxidase preparation ($T_N = 700 \text{ s}^{-1}$), it was found that loss of activity and ability to bind cytochrome c occurred in parallel and was dependent on a molecular weight unit of approximately 85 (± 20) kd (average of two separate determinations at -70° and -170° C).

These results suggest that neither a dimer nor even a complete monomer of cytochrome oxidase is required for high turnover or normal binding of cytochrome c, and that the intact membrane plays a role in determining the kinetic characteristics of cytochrome oxidase (Thompson *et al.* *Biophysical J.* in press, Jan. 1982). This work was supported by NIH Grant GM 26916. The authors are indebted to Ray Narlock of Dow Chemical Co. (Midland, MI) for assistance with the radiation experiments.

M-AM-MinA5 ENERGY-LINKED RESPONSES OF MEMBRANE pH AND MEMBRANE POTENTIAL OPTICAL PROBES IN OPEN FRAGMENT SUBMITOCHONDRIAL PARTICLES. Bayard T. Storey, Depts. of Obstetrics & Gynecology and Physiology, University of Pennsylvania School of Medicine, Philadelphia, PA 19104.

Submitochondrial particles (SMP) prepared from skeletal muscle mitochondria have permeability properties of open fragments of the inner mitochondrial membrane, yet retain the capacity for energy coupling (Storey, Scott, and Lee (1980) *J. Biol. Chem.* **255**, 5224-5229). Energization of these SMP by the O_2 pulse method in the presence of either of the membrane pH optical probes, quinacrine (QA) or bromthymol blue (BTB), results in a spectral shift corresponding to acidification of the dye bound to the membrane: $\text{QAH}^+ + \text{H}^+ \rightarrow \text{QAH}_2^{2+}$ or $\text{BTB}^- + \text{H}^+ \rightarrow \text{BTBH}$. The former reaction is markedly enhanced, while the latter is inhibited, by SCN^- . The membrane potential probe Safranin O (Saf) responds to energization of these SMP with a spectral shift similar to that seen with intact mitochondria (Åkerman and Wikström (1976) *FEBS Lett.* **68**, 191-197). Oxonol VI (Ox) responds to energization with a spectral shift like that seen with beef heart SMP (Smith and Chance (1979) *J. Membr. Biol.* **46**, 255-282). The fluorescent membrane probes 3,3'-dipropylthiocarbocyanine and Merocyanine 540 show energy-linked fluorescent decreases with these SMP, but the responses are slow. The responses of Saf, QA (+ SCN^-), and BTB, are quite rapid, with $t_{1/2}$ of about 2-3 sec. The response of Ox has $t_{1/2} < 0.4$ sec. Since these SMP cannot sustain a transmembrane $\Delta\tilde{\mu}_{\text{H}^+}$, these energy-linked responses must be due to direct interaction of the dyes with the energized membrane, presumably in limited energy transfer domains (Ernster (1977), *Ann. Rev. Bioch.* **46**, 981-985).

Supported by NIH grant HL-19737 and the Muscular Dystrophy Association, Inc.

M-AM-MinA6 HOW CAN A PROTEIN MOLECULE CHANGE THE CHEMICAL POTENTIAL OF A TRANSPORTED ION? Charles Tanford, Dept. of Physiology, Duke Univ. Med. Center, Durham, N.C. 27710.

In active transport and related chemiosmotic processes the transport protein binds one or more ions at an electrochemical potential $\tilde{\mu}_1$ on one side of the membrane, and then releases the ions at a much higher (or lower) potential $\tilde{\mu}_2$ on the opposite side. This occurs without chemical change in the ion or direct interaction of the ion with ATP or other free energy donor. The simplest way a protein can catalyze such a process is if it has ion binding sites that have different binding constants when facing the two sides of the membrane, such that the standard potentials of the bound ions ($\mu_{1,b}$ and $\mu_{2,b}$) are approximately equal to μ_1 and μ_2 , respectively. The question of mechanism then reduces to the question of how μ_b^0 for a bound ion can be altered in synchrony with the translocation of the binding site. The value of μ_b^0 depends on the amino acid side chains and peptide groups that constitute the ion binding site and quantitative data are available for most ions of interest. There are also well-established examples of protein conformational changes that alter the organization of ligand binding sites and thereby change μ_b^0 , but they apply to water-soluble proteins. Using the structure of bacteriorhodopsin as a general model for a transport protein, the same principle can be applied to the present problem, and it becomes apparent that this particular structure is well designed to promote a cyclic change in μ_b^0 in synchrony with alternation in the exposure of the binding site between the two sides of the membrane. Transport of more than one ion per reaction cycle is readily accommodated. The underlying thermodynamic principle ($\Delta\mu_b^0 \approx \mu_1 - \mu_2$) is consistent with experimental data for ATP-driven Ca and Na,K pumps. Supported by NIH and NSF.

M-AM-MinA7 STIMULATION OF MITOCHONDRIAL K^+ FLUX BY DIBUTYLCHLOROMETHYLtin CHLORIDE. Joyce J. Diwan, Biology Department, Rensselaer Polytechnic Institute, Troy, NY 12181.

Three different inhibitors of oxidative phosphorylation, dicyclohexylcarbodiimide (DCCD), oligomycin, and dibutylchloromethyltin chloride (DBCT), have been shown to affect respiration-dependent K^+ flux into rat liver mitochondria (Gauthier & Diwan, BBRC 87:1072, 1979; Diwan, J. Bioener. Biomembr., in press). DCCD inhibits K^+ influx, increasing the apparent K_m of the transport mechanism for K^+ . While oligomycin alone has no apparent effect on K^+ flux, oligomycin enhances the stimulatory effect of mersalyl on K^+ influx. DBCT stimulates K^+ influx, and elicits a further stimulation of K^+ influx in the presence of mersalyl. In these studies, unidirectional K^+ flux into isolated rat liver mitochondria has been measured in the presence of succinate as energy source, by means of ^{42}K . Kinetic studies show that DBCT increases the apparent V_{max} of K^+ influx. The stimulatory effect of DBCT shows little dependence on the pH (7.0-8.0) of the medium. When mitochondria pretreated with 20-30 nmoles DCCD per mg protein are exposed to 5-8 nmoles DBCT per mg protein, the stimulated rate of K^+ influx is the same as that observed with control mitochondria exposed to DBCT. Thus the inhibitory effect of DCCD is not expressed in the presence of DBCT. Oligomycin (0.4-0.5 μ g/mg protein) has no apparent effect on the stimulation of K^+ influx by DBCT. Although the results are consistent with interaction of the mechanism mediating respiration-dependent K^+ influx with the ATP synthase complex, it is possible that DBCT and the other two oxidative phosphorylation inhibitors tested all have multiple sites of reaction with the mitochondrial inner membrane. The findings suggest some interaction between the sites of action of DBCT and DCCD. Supported by USPHS Grant GM-20726; DBCT was supplied by D. Griffiths.

M-AM-MinA8 ATP SYNTHESIS COUPLED TO K^+ INFLUX IN MITOCHONDRIA. Kathleen Walsh Kinnally and Henry Tedeschi, Department of Biological Sciences, State University of New York at Albany, Albany, N.Y. 12222.

In the presence of valinomycin the influx of K^+ in swollen, partially K^+ -depleted mitochondria, was found to be coupled to the synthesis of ATP from ADP and P_i . The synthesis was found to be as high as 16 μ moles ATP/g protein. The mitochondrial metabolism was blocked either with rotenone and antimycin or cyanide. The sidedness of the mitochondrial membrane was unchanged in these preparations as shown by the sensitivity of the phosphorylation to atractyloside which is presumed to block adenine nucleotide transport. The synthesis was found to be critically dependent on the valinomycin concentration and the external K^+ . With increasing valinomycin, the synthesis increases, reaching an optimum at a valinomycin concentration of 240 μ g/g protein. Any additional increase causes a precipitous drop in phosphorylation. This finding suggests that valinomycin acts at two separate sites, one the transducing site and another which short-circuits the transducing mechanism. The synthesis was found to be insensitive to oligomycin, probably as the result of the high ionic strength of the medium. Furthermore, it is relatively insensitive to uncouplers. The synthesis of 1 ATP was found to be accompanied by the disappearance from the medium of approximately 1 H^+ . The results are not readily explained by the chemiosmotic hypothesis. Aided by NIH grant GM 27053. We thank Daniel Pope for the use of his Aminco Chem-glow photometer and Joyce Diwan for K^+ analyses.

M-AM-MinA9 DEFECTIVE MITOCHONDRIA AND MODIFIED LACTATE DEHYDROGENASE IN TRANSFORMED CELL LINES. Ann E. Kaplan, Philip Hanna, Bruce Hochstadt and Harold Amos, National Cancer Institute, NIH, Bethesda, MD 20205 and Dept. of Microbiology, Harvard Medical School, Boston, MA 02115.

The increased rate of synthesis of lactic acid as a function of tumor cell growth is a common property of malignant cells. Though long-recognized, alterations in the bioenergetic pathway leading to this phenomenon are still incompletely understood. We examined this question with a chemically transformed rat hepatocyte line, NMU-3, which produces slow-growing carcinomas in vivo, and its control line, TRL 12-13, and with a virally (polyoma) transformed fibroblast line, NIL-PY, which produces sarcomas in vivo, and its control line, NIL. Ultrastructural differences in NMU-3 show one-third fewer mitochondria at confluence with incomplete cristae and fragmented matrices. In NMU-3, lactate dehydrogenase (LDH, EC 1.1.1.27) activity rises four-fold while the rate of synthesis and transport rises three-fold. Kinetic analyses identify a much decreased sensitivity to inhibition with NAD^+ in LDH from NMU-3 with a higher, longer-sustained initial reaction rate and a higher steady-state rate, supporting the increased rate of synthesis and export of lactic acid in the transformed cells. Gel electrophoresis and isoelectric focussing show increases in only one molecular type of LDH in both transformed cells compared with their control enzymes. Following incubation of LDH from TRL 12-13 and NMU-3 with alkaline phosphatase, each enzyme retains full LDH activity, but LDH from TRL 12-13 separates with molecular patterns of LDH from NMU-3. The results suggest that the increased rates of synthesis and export of lactic acid in these mitochondria-deficient transformed cells are associated with decreased phosphorylation of LDH identified through molecular and kinetic modifications of the enzyme.

M-AM-MinB1 THE SITES AND SOURCES OF COOPERATIVE ENERGY TRANSDUCTION IN THE HUMAN HEMOGLOBIN MOLECULE. Gary K. Ackers, Donald W. Pettigrew, Michael L. Smith, Amy Chu & Benjamin W. Turner, The Johns Hopkins University, Dept. of Biology, Baltimore, MD 21218.

The major sites of free energy transduction for the regulation of oxygen binding affinity have been determined by an extensive study of twenty two mutant and chemically modified human hemoglobins. For these hemoglobins we have measured the effects of structural alterations at individual amino acid sites on the total free energy used by the tetrameric molecule for regulation of oxygen affinity. We find that the regulatory energy is drastically altered by all structural alterations within the $\alpha^1\beta^2$ interface region of the molecule. By contrast the regulatory energy is essentially normal when the structural alterations are at other locations, including the region of the heme pocket. These results indicate the $\alpha^1\beta^2$ interface region (including intersubunit contacts $\alpha^1\alpha^2$, $\alpha^1\beta^2$, and $\alpha^2\beta^1$) to be the major site of the free energy changes which comprise cooperativity in oxygen binding.

Recent experimental work on the thermodynamics of ligand-linked subunit assembly has led to an evaluation of the possible types of noncovalent interactions which act as dominant sources of the regulatory energy. The results argue against hydrophobic interactions and salt bridges, but are consistent with hydrogen bonding and van der Waals interactions as dominant sources of regulatory energy. The regulatory energy is both enthalpic and entropic in origin and the enthalpic component is attributable almost entirely to the heats of Bohr proton release. (Supported by grants from NIH and NSF).

M-AM-MinB2 FREE ENERGY CONTRIBUTION OF ELECTROSTATIC INTERACTIONS TO COOPERATIVITY IN HUMAN HEMOGLOBIN. Frank R. N. Gurd, Margaret A. Flanagan, James B. Matthew, Mary Crowl Powers, and Stephen H. Friend, Department of Chemistry and Medical Sciences Program, Indiana University, Bloomington, IN 47405

Contributions of electrostatic interactions are observed in three aspects of ligand binding by human hemoglobin: those resulting from ligand binding, the binding of allosteric effectors and differential free energy gain on dimer-tetramer assembly of liganded and unliganded forms. The Tanford-Kirkwood treatment as modified by Shire was used to estimate the electrostatic contributions to cooperativity in each aspect. The contribution to ligand binding resulting from structural rearrangements was estimated from the liganded and deoxy quaternary structures, the liganded form having the more stable electrostatic configuration. Modelling of hydrogen ion and 2,3-diphosphoglycerate binding correctly predicted the alkaline Bohr effect and the binding energy of the organic phosphate in the β -cleft. The observed competition between diphosphoglycerate binding and formation of the Val-1 β carbamino adduct was predicted. The pH dependence and effects of specifically bound chloride ions on the electrostatic contribution to the energetics of the dimer-tetramer assembly were computed for deoxy and liganded hemoglobin. The electrostatic contributions correctly model the observed contrasting pH dependence of the assembly processes, that for the liganded assembly system representing a much larger fraction of the observed value than does that for the deoxy assembly system. These results, together with other recent work, suggest that salt bridge formation is not the dominant energetic factor favoring deoxyhemoglobin dimer-tetramer assembly. (Supported by U.S. Public Health Service Research Grant HL-05556.)

M-AM-MinB3 MEASUREMENT OF ENERGETIC STRUCTURE CHANGES IN HEMOGLOBIN BY DIFFERENCE H-EXCHANGE METHODS. S.W. Englander, J.R. Rogero and J.J. Englander. Department of Biochemistry and Biophysics, University of Pennsylvania, Phila, PA

The essence of allosteric mechanism is the transduction of binding energy and its translocation in the form of free energy of protein structure change. Understanding of this fundamental biological control mechanism therefore requires the measurement not only of individual structure changes but also the free energy of each. H-exchange (HX) methods appear to provide this capability. HX experiments now indicate that slow H-exchange is due to H-bonding, that the HX process involves a localized, H-bond breaking unfolding of short segments of structure (breathing), and that each local unfolding enters HX kinetics as a preequilibrium step so that its free energy can be computed from measured HX rate. Individual static structure (allosteric) changes affect individual breathing units, thus their free energy is expressed as a change in affected local unfolding equilibrium constants. A difference HX method can characterize individual HX rate changes, therefore can measure the change in structural free energy felt by the individual local unfoldings that generate them. Associated methods make it possible to isolate and identify individual breathing units, if they in fact exist. We have now isolated two allosterically sensitive breathing units in Hb. This appears to validate the view and approaches just outlined, which may make accessible the energy dimension of allostery and other protein functions. (Supported by NIH AM 11295)

M-AM-MinB4 ^1H NMR INVESTIGATION OF THE COOPERATIVE EVENTS DURING THE LIGATION OF HEMOGLOBIN.

Chien Ho, Department of Biological Sciences, Carnegie-Mellon University, Pittsburgh, PA 15213.

During the past several years, we have investigated the detailed molecular basis for the cooperative oxygenation of hemoglobin. We have found that high-resolution proton nuclear magnetic resonance (NMR) spectroscopy can provide unique insights into the cooperative ligand binding process in normal human adult hemoglobin (Hb A). By using ^1H NMR spectroscopy, with the help of appropriate mutant and chemically modified hemoglobins and Perutz's atomic models of hemoglobin, we have been able to assign a number of proton resonances to specific amino acid residues in the hemoglobin molecule. In addition, the use of mutant and chemically modified hemoglobins also permits us to gain information about the structural changes associated with the ligation of Hb A, and to investigate the ionization properties of specific surface histidyl residues of the Hb A molecule in going from the deoxy to the liganded form of Hb A under a variety of experimental conditions. Based on our experimental results, we can draw the following conclusions: (i) the structural changes during the oxygenation process of Hb A are not concerted; (ii) the molecular mechanisms based on two-state allosteric models do not adequately describe the cooperative oxygenation of Hb A; and (iii) the molecular mechanism for the Bohr effect as proposed by Perutz [Nature 228, 726 (1970)] is not unique and depends on the solvent media. The relation between our experimental results and the current models of the structure-function relationship in hemoglobin will be discussed. (Supported by research grants from the NIH and NSF).

M-AM-MinB5 STRETCHING AND BENDING NEAR THE IRON IN HEMOGLOBIN. Todd M. Schuster, University of Connecticut, Biochemistry & Biophysics, U-125, Storrs, Connecticut 06268

An understanding of the cooperative mechanism of oxygen binding by hemoglobin requires an evaluation of the energy contributions of all coupled reactions. Recent spectroscopic studies have been directed toward identifying optical markers at or near the iron atom in order to evaluate the ligand and effector linked energy changes at specific bonds. Other such studies have revealed spectroscopic changes near the heme accompanying changes in subunit interactions in normal and mutant human hemoglobins. Results from resonance Raman and absorption spectroscopy measurements on deoxy, liganded and met-hemoglobins will be reviewed and discussed in light of particular bonds as possible sources of cooperative energy in hemoglobin.

Supported by research grants from the National Science Foundation and the National Institutes of Health.

M-AM-A1 PICOSECOND MOTIONAL AVERAGING OF NMR AND FLUORESCENCE PROBES OF PROTEIN DYNAMICS.
R.M. Levy, Department of Chemistry, Rutgers University, New Brunswick, New Jersey 08903

A wide variety of experimental and theoretical techniques are providing an increasingly detailed picture of the internal dynamics of proteins. Time resolved fluorescence depolarization, NMR relaxation and linewidth experiments can provide information about fast (ps-ns) protein motions. The motions of aromatic amino acid side chains in proteins have been the subject of several recent experimental and theoretical studies. A relatively large number of experimental techniques can be used to study the ring motions including ^{13}C dipolar NMR relaxation studies of protonated and non protonated ring carbons, ^2H lineshape studies, chemical shift anisotropy relaxation and lineshape studies, as well as fluorescence depolarization experiments. Theoretical studies using molecular dynamics simulation methods have demonstrated that significant atomic fluctuations occur in the protein interior on a picosecond time scale and that the phenylalanine and tyrosine rings can undergo orientational fluctuations of up $\sim \pm 30^\circ$ from the average position. We examine the effect of these ring librations on a variety of spectroscopic probes of ring motion. Associated with each probe is an order parameter for the distribution of probe orientations on the picosecond time scale. We evaluate these order parameters for the different probes using both protein molecular dynamics trajectories and simple models for the motion. We demonstrate that the picosecond librations can have a significant effect on the probe order parameters and that the results depend on the details of the probe orientation with respect to the ring libration Axes.

M-AM-A2 INTRAMOLECULAR MOTIONS IN A SUPERCOOLED PROTEIN - THE STRUCTURE OF MYOGLOBIN AT 80K.
 Dagmar Ringe Ponzi and Gregory A. Petsko, Department of Chemistry, M.I.T.; Hans Frauenfelder, Department of Physics, University of Illinois; Herman Hauptmann and Fritz Parak, Technische Universität, München, FDR.

The crystal structure of sperm whale met myoglobin has been determined at a temperature of 80K at 2\AA resolution. The crystal was frozen by rapid immersion in liquid propane followed by further cooling with liquid nitrogen. Refinement of the structure has been carried out by the restrained least-squares method of Konnert and Hendrickson; the current R-factor is 0.26 with 0.027\AA root-mean-square deviation from ideal bond distances. The overall isotropic temperature factor, B, is 6.3\AA^2 for the protein at 80K, in contrast to a value of 14.2\AA^2 for crystals at room temperature. This dramatic reduction demonstrates that, in contrast to long-held beliefs, in some crystalline proteins the largest component of the apparent temperature factor is actual atomic motion. The refinement also demonstrates that cooling to 80K has reduced the volume of the protein by several percent. This fact is also reflected in a 4.5% contraction of the volume of the unit cell of the crystals from its room temperature value. Examination of the interatomic contact distances in the interior of the molecule suggests that hydrophobic interactions, particularly those where helices cross, have become stronger. Refinement of individual isotropic temperature factors for all of the 1261 non-hydrogen atoms shows that the mean-square displacements at 80K range from 0.035\AA^2 to 0.165\AA^2 .

M-AM-A3 MEDIUM RESOLUTION HYDROGEN EXCHANGE STUDIES OF THE CATALYTIC SUBUNIT (c_3) OF *E. COLI* ASPARTATE TRANSAMYLASE. M.Lennick and N.M. Allewell, Wesleyan University, Middletown, CT 06457.

Both ligand binding and subunit association reduce the overall rate of exchange from $c_3(1)$. In order to characterize the conformational dynamics of various segments of the structure and to identify responsive protons, we have begun to apply the medium resolution hydrogen exchange technique of Rosa and Richards (2). Digestion of c_3 with pepsin (0.8 mg/ml in 100 mM Na-malonate, pH 2.8, 0°C , 10 min) generates peptides which can be resolved into at least 30 peaks by HPLC on a Waters Bondapak C18 column. Under the elution conditions used (acetonitrile flowing at 0.3 ml/min to a reservoir of 50 mM NaPO_4 , 4.5% acetonitrile, pH 2.8, flowing to column at 1 ml/min), several peaks appear well-resolved and homogeneously by N-terminal analysis. The specific activities of peptides derived from ^3H -labeled protein decrease exponentially with time, as expected, and the bisubstrate analog, PALA, reduces rates of exchange from all observable peaks. In both cases, the overall kinetics of exchange are similar to those observed by classical methods. The changes produced by PALA in rates of exchange from individual peptides are smaller by several orders of magnitude than those produced by binding of S-peptide to S-protein (2); however, in contrast to the effects of 2'-CMP on RNase-S (3), they appear to be distributed throughout the structure. This approach will be extended to both the regulatory subunit and mutant proteins.

1. Lennick, M., and Allewell, N.M., *Proc. Natl. Acad. Sci. USA*, in press.

2. Rosa, J.J., and Richards, F.M., *J. Mol. Biol.* **145**, 835 (1981).

3. Rosa, J.J., and Richards, F.M., *Biophys. J.* **33**, 259a (1981).

Supported by USPHS Grant AM-17335.

M-AM-A4 α -KETOGLOUTARATE DEHYDROGENASE MULTIENZYME COMPLEX MAY BE HETEROGENEOUS IN QUATERNARY STRUCTURE. T. Wagenknecht, N. Francis and D.J. DeRosier, Department of Biology and Rosenstiel Basic Medical Sciences Research Center, Brandeis University, Waltham, MA 02254.

The α -ketoglutarate dehydrogenase multienzyme complex (KGDC) from *E. coli* consists of three enzymes: α -ketoglutarate dehydrogenase (E1), dihydrolipoyl transsuccinylase (E2), dihydrolipoyl dehydrogenase (E3). Under physiological conditions purified E2 is a cube-shaped molecule having octahedral (O_h) symmetry and consisting of 24 subunits. In KGDC, E2 forms a central core to which 6 subunits (dimers) each of E1 and E3 are noncovalently bonded; this stoichiometry precludes O_h symmetry for KGDC. In order to determine the symmetry of KGDC we have analyzed by electron microscopy subcomplexes consisting of E2 and one or two bound E1 or E3 subunits. The advantage of studying subcomplexes is that their images are more easily interpreted than images of KGDC. Images in which only one bound E1 or E3 is present allow us to map the positions on the E2 where the E1 and E3 bind. We find that both the E1 and E3 bind on the faces of the cube-shaped E2 between its 4- and 2-fold rotation axes; there are 24 such sites per E2 molecule. Images of subcomplexes consisting of E2 and 2 bound E1 subunits were also studied in order to determine if there are any preferred relative spatial arrangements of the 2 bound subunits as would be expected if the KGDC molecule belongs to one of the symmetric point groups. The results indicate that the subcomplexes assemble so that no more than one E1 binds per face of E2, but, surprisingly, the particular site occupied out of the 4 possible per face, is selected at random. These results are consistent with the hypothesis that KGDC does not have a unique quaternary structure, but rather consists of a family of structural isomers. Supported by NIH grants GM21189 (DJD) and GM06665 (TW).

M-AM-A5 LOW RESOLUTION MAPS OF THE HISTONE POSITIONS WITHIN A NUCLEOSOME. C.J. Stoeckert, Jr., J.W. Wiggins & M. Beer, Johns Hopkins University, Baltimore, Md. 21218

Low resolution maps have been obtained which localize within a nucleosome each of the four core histones: H2A, H2B, H3 and H4. The method used (M. Beer et al, Ultramicroscopy (In press)) involved selective labeling of histones with chloroglycyl-L-methionine platinum(II) (Pt-GLM) and imaging nucleosomes containing the labeled histones in the Johns Hopkins scanning transmission electron microscope (STEM). Selective labeling was obtained by first modifying histone lysines with the platinum-binding compound, methyl(methylthio)acetimidate, and then reconstituting nucleosomes in which only one or two of the histones were modified. The combinations of imidated histones reconstituted were: H2A-H2B, H3-H4, H3-H2B, H2A alone and H4 alone. The reconstituted nucleosomes were reacted with Pt-GLM, and high resolution (5Å) digitally recorded micrographs taken of each reconstitute in the STEM. The short cylindrically shaped nucleosome was found to lie on its flat face, and, thus, the nucleosome images obtained were projections down the cylinder axis. Picture elements (pixels) of high electron scattering intensity and high spatial frequency were selected as most likely to represent the Pt atom label. The distribution of these pixels was obtained for each micrograph using computer processing techniques, and an average distribution determined for each reconstitute. Through a linear comparison of the average distributions, 24 Å difference maps were constructed for each histone. These maps contain statistically significant peaks which indicate the histone positions. This research was supported by NIH grant# 5P41 RR01214-02 and NSF grant# PCM77-24912.

M-AM-A6 NMR EXAMINATION OF LAMBDA PHAGE CRO REPRESSOR COMPLEXES WITH DNA. K. T. Arndt, F. Boschelli, H. Nick, S. Cheung, P. Lu, Chemistry Department, University of Pennsylvania, Philadelphia, PA 19104 and Y. Takeda, Chemistry Department, University of Maryland, Baltimore Campus, Catonsville, MD.

The *cro* protein exists as a dimer of 66 amino acids per subunit and regulates lambda phage development by binding specifically to the lambda operators. We have performed high resolution proton NMR on the lambda *cro* repressor at 360 MHz. We are able to resolve the resonances for each of the 3 tyrosines or each of the 3 phenylalanines in the *cro* subunit by selective deuteration. In addition, the single histidine in the *cro* protein subunit was assigned by pH titration. When the *cro* protein binds to DNA fragments, 2 of the 3 tyrosine resonances and the single histidine resonance shift downfield, an observation similar to what we have reported for the *lac* repressor (Nick et al., Proc. Natl. Acad. Sci., USA, in press 1981). We have performed selective 1-D NOE and 2-D NMR experiments to probe the bound and free *cro* solution structure and compare it to the crystal structure (Anderson et al. (1981), Nature **290**, 754758). Experiments with the specific lambda operator, O_R3 , derived from a cloned chemically synthesized DNA sequence, are in progress. Supported by grants from the American Cancer Society and Natl. Inst. of Health.

M-AM-A7 STRUCTURAL STUDY OF GP32*I CRYSTAL BY ELECTRON DIFFRACTION. W. Chiu, H. Cohen and J. Hosoda*, Dept. of Cellular and Developmental Biology, Univ. of Arizona, Tucson, Arizona 85721 and *Lawrence Berkeley Laboratory, Univ. of California, Berkeley, California 94721

Gp32*I is a T4 DNA helix destabilizing protein obtained by a proteolytic removal of 51 amino acids from the carboxyl terminal of gp32. Very thin crystals of gp32*I, suitable for low dose electron diffraction study have been prepared. Electron diffraction patterns from unstained, hydrated crystals can routinely be obtained to 3.0 Å resolution. By using a computer processing technique, we have reconstructed a two dimensional projected density map of gp32*I crystal based on reflections extending to 7.6 Å. The map shows four asymmetric units in pgg symmetry. A plausible interpretation of the projected density map is that each asymmetric unit consists of two gp32*I monomers. The dimension of each monomer would then be ~ 15 by 30 by 90 Å which is consistent with the estimates derived from hydrodynamic measurements. The dimer in the asymmetric unit may represent the type of molecular interaction of the molecules in *in vivo* condition. We have also obtained a three dimensional map of the gp32*I stained with uranyl acetate at 15 Å resolution. This 3D reconstruction allows us to conclude the space group of the crystal to be $P2_12_12$ and to suggest the polarity of the molecules in each asymmetric unit of the crystal.

Acknowledgement: This work is supported by NIH Grant Nos. GM 27061 and GM 23563 and The University of Arizona Computer Center.

M-AM-A8 THE STRUCTURE OF POLYOMA VIRUS CAPSIDS AT 22.5 Å RESOLUTION. I. Rayment, T.S. Baker, D.L.D. Caspar and W.T. Murakami. Rosenstiel Basic Medical Sciences Research Center and Biochemistry Department, Brandeis University, Waltham, MA 02254. (Intr. by D. Winkelmann).

The structure of mouse polyoma virus capsids has been determined to 22.5 Å resolution by single crystal X-ray diffraction. The virus capsids crystallize in space group I23 where $a=572$ Å, and diffract to 8 Å resolution. Data to 22.5 Å resolution were collected using the precession method. A total of 13 films were recorded giving 95% of the observable data to 22.5 Å resolution. An initial set of phases were derived by modeling the coarse surface structure observed in electron micrographs. These were refined in real space by imposing the constraints of noncrystallographic symmetry and solvent flattening. The final R factor between observed and calculated structure factors was 14.2%. The resultant electron density map shows that the virus capsid does not conform to a T7 icosahedral surface lattice which would necessitate pentamer-hexamer clustering as was thought previously. All of the 72 morphological units on the capsid surface contain five copies of the major coat protein. These observations present new problems in understanding the assembly of large macromolecular aggregates.

Supported BY NCI grants CA15468 (DLDC) and CA27260 (IR) and Medical Foundation 97 80 0274 JS (TSB).

M-AM-A9 NON-CONSERVATION OF BONDING SPECIFICITY IN PROTEIN ASSEMBLIES: QUASI-EQUIVALENCE REVISED. D.L.D. Caspar, Rosenstiel Basic Medical Sciences Research Center, Brandeis Univ., Waltham MA 02254.

The unexpected discovery by Rayment et al. (1981, *Nature* in press) that the 72 capsomeres of the polyoma virus capsid are all pentamers shows that bonding specificity is not conserved among the protein subunits in this icosahedrally symmetric assembly. It had been presumed, based on principles formulated to account for the design of simple icosahedral virus particles (Caspar & Klug, 1962, Cold Spring Harbor Symp. 27, 1), that the capsids of T=7 papova viruses should be constructed from 420 protein subunits quasi-equivalently bonded into 12 pentameric and 60 hexameric capsomeres. Quasi-equivalence, which would conserve essential bonding specificity, appeared to explain why icosahedral symmetry was selected for the design of simple isometric virus capsids. Since bonding specificity is not conserved in the polyoma capsid, the reason for its icosahedral symmetry is no longer obvious. Bonding specificity has been recognized to change in the transition from one structural state to another of many protein assemblies--eg. from oxy- to deoxyhemoglobin; from the TMV protein disc to the helix; from the extended to the contracted bacteriophage tail sheath, etc. Switching of bonding specificity within an assembly, as recognized in the polyoma capsid structure, must also occur in the self-assembly of myosin into bipolar thick filaments (Huxley, 1963, *J. Mol. Biol.* 7, 291) and of flagellin into supercoiled bacterial flagella (Asakura, 1970, *Advan. Biophys.* 1, 99). Self-controlled conformational switching can regulate the assembly of structural proteins (Caspar, 1980, *Biophys. J.* 32, 103); similar switching can lead to functional differentiation of identical protein subunits into non-equivalent conformations within a single assembly.

Supported by NIH grant CA 15468.

M-AM-A10 DYNAMIC COMPARISON OF COMPACT AND SWOLLEN STRUCTURES OF SOUTHERN BEAN MOSAIC VIRUS.

Jade Li¹, Carl Fricks, D.L.D. Caspar and Ivan Rayment. Rosenstiel Ctr., Brandeis Univ., Waltham, MA

The structures of the compact and swollen southern bean mosaic virus (SBMV) particles have been compared by X-ray diffraction and proton magnetic resonance (PMR). Small-angle X-ray scattering showed that removal of divalent cations at alkaline pH leads to an increase of particle diameter by 12% in solution, and by 9% in microcrystals, from the 289 Å in the native SBMV. The swelling is fully reversible upon the readdition of both Ca⁺⁺ and Mg⁺⁺ ions, as shown by the X-ray patterns to 6 Å resolution and the 270 Hz PMR spectrum. X-ray patterns of the compact SBMV in solution and in microcrystals are characterized at high angles ($S > 0.035 \text{ \AA}^{-1}$) by fine fringes ($\sim 1/225 \text{ \AA}$ width) extending to 6 Å resolution. Patterns from the swollen SBMV both in solution and in microcrystals display only broad fringes ($\sim 1/92 \text{ \AA}$ width) at these scattering angles. Model calculations demonstrate that the fine fringes observed from compact SBMV are a consequence of the regular packing of the protein subunits on the icosahedral surface lattice; the smearing out of fine fringes in the swollen virus pattern can be simulated by uncorrelated displacements of pentamers and hexamers of protein subunits with a standard deviation of $\sim 6 \text{ \AA}$ from their mean locations. PMR data indicate that the disorder in the swollen SBMV has a dynamic character. Whereas the PMR spectrum of compact SBMV is ill-resolved, the spectrum of swollen SBMV shows sharp resonances in the methyl proton region. The line-narrowing for a fraction of the aliphatic protons upon swelling cannot be accounted for by rotational relaxation of the virus particle of 6×10^6 MW, but must be attributed to internal motion in regions of the protein subunits in the swollen structure. (PMR spectra were kindly taken by Dr. A.G. Redfield.)

¹Dr. Li's present address is Dept. of Biochemistry, Columbia University, N.Y. 10032.

M-AM-A11 RAMAN STUDIES OF SOUTHERN BEAN MOSAIC VIRUS. L. Dombrowsky, C. Young, Physics Department; D. Caspar and I. Rayment, Rosenstiel Basic Medical Sciences Research Center, Brandeis University, Waltham, MA.

Southern Bean Mosaic Virus is an icosahedral plant virus whose coat, composed of 180 protein subunits, encapsulates one molecule of RNA. Upon removal of the stabilizing Ca⁺⁺ and Mg⁺⁺ ions reversible swelling of up to 12% occurs at pH values >7. Dynamics of the swelling process has been studied by small angle X-ray diffraction (Li et al., this proceeding).

Raman experiments are currently being carried out to determine the structural similarities and differences between the compact and swollen states and to characterize the protein and RNA configurations. We are, in addition, experimentally testing the N-terminal arm model for protein-RNA interactions, wherein the RNA binds to the N-terminal arm of the protein subunits. Preliminary results of these experiments will be presented.

Supported by NIH grant CA 15468 to D.L.D. Caspar.

M-AM-A12 TWO FORMS OF 20S TMV PROTEIN. Ragaa A. Shalaby and Max A. Lauffer. Biophysical Laboratory, Dept. of Biological Sciences, University of Pittsburgh, Pittsburgh, PA 15260

Previous observations led us to postulate two forms of 20S TMV protein, one resulting from polymerization when hydrogen ions are available from buffer or by titration, and the other formed by polymerization in the absence of abundant hydrogen ions. In one current attempt at direct demonstration, two sets of experiments were performed. In the first, at starting pH values of 6.6, 7.0 and 7.6, unbuffered TMV protein in 0.10 M KCl at 4°C was allowed to warm slowly to 22°C. Sedimentation coefficient measurements showed no 20S material at 7.6, but when the starting pH was 7.0 and 6.6 there was a small increase in pH and 20S material was found at 22°C. The number of hydrogen ions bound per protein monomer (molecular weight 17,500 daltons) was 2.8×10^{-5} at pH 7 and 1.3×10^{-4} at pH 6.6, trivial amounts. When temperature was reduced to 4°C, the protein dissociated to 100% 4S material and the original pH. In the second set, carried out at pH 6.6, pH was kept constant with HCl. At 22°C, all of the material was found in 25S and 38S forms and 0.87 moles of hydrogen ion were bound per mole of protein monomer. When the temperature was subsequently reduced to 4°C, 4S and 33S material remained, but the pH dropped to 5.9. At 12°C, equal parts of 4S and 20S material were formed and 0.86 moles of hydrogen ions were bound per mole of protein monomer polymerized. When equivalent KOH was added while lowering temperature to 4°C, 100% 4S material resulted and the pH remained at 6.6. It has thus been demonstrated that there are two different polymerization processes resulting in the formation of 20S material, one involving binding of hydrogen ion and the other not. There must be more than one form of 20S material. (Supported by NIH Grant GM 21619)

M-AM-A13 USE OF TRYPSIN TO PROBE THE STRUCTURE OF A BACTERIOPHAGE T7 PROCAPSID. Philip Serwer, Department of Biochemistry, The University of Texas Health Science Center at San Antonio, San Antonio, Texas, 78284.

In previous studies from this laboratory, sieving during electrophoresis in agarose gels has been used for determining the radius of spherical bacteriophages and their capsids; extrapolation of electrophoretic mobility (μ) to an agarose concentration of 0 and correction for electro-osmosis has been used to obtain μ in the absence of agarose, a linear function of the average electrical surface charge density (σ) of particles. The configuration of the proteins at the surface of a DNA-free bacteriophage T7 procapsid, capsid I (capsid I has a thicker, rounder envelope than the envelope of bacteriophage T7 and capsid I converts to a capsid [capsid II] with a bacteriophage-like envelope as it packages DNA "in vivo"), has been probed by digesting capsid I with trypsin. It was found using agarose gel electrophoresis that trypsin raises the magnitude of the negative σ of capsid I by 6-12% without altering the radius of capsid I. The cause of this change in σ is digestion of the major envelope protein of capsid I (and capsid II), P10, leaving P10 (molecular weight = 38,000) reduced in molecular weight by approximately 3,500. In capsid II and bacteriophage T7, P10 is not sensitive to trypsin. It is proposed that the trypsin-sensitive region of capsid I-associated molecules of P10 is a structurally disordered terminus that becomes internalized during conversion of capsid I to capsid II. After internalization, some of these termini may fold between domains in P10 to give the envelope of capsid II stability, an aspect of the structure of plant viral capsid envelopes previously demonstrated by others using x-ray diffraction. This work was supported by the National Institutes of Health (grants AI-16117 and GM-24365).

M-AM-B1 CROSS RELAXATION AND SPIN DIFFUSION EFFECTS ON THE PROTON NMR T_1 RELAXATION RATES OF MEMBRANE LIPIDS. Alan J. Deese*, Edward A. Dratz†, Lin Hymel†, Sidney Fleischer†, and Michael F. Brown*. *Chem. Dept., Univ. of Virginia, Charlottesville, VA 22901; †Chem. Dept., Univ. of Calif., Santa Cruz, CA 95064; ‡Molec. Biology Dept., Vanderbilt University, Nashville, TN 37235.

Previous observations of biexponential ^1H T_1 relaxation rates of retinal rod outer segment (ROS) disk membrane lipids were interpreted as being due to a direct protein perturbation of the high frequency motions of those lipids in contact with rhodopsin (1). We have extended this investigation to the study of the effects of residual solvent water protons on the T_1 relaxation behavior of the lipid resonances of ROS and sarcoplasmic reticulum (SR) membranes. Selective excitation-saturation transfer studies show that water protons, protein protons, and lipid protons are significantly spin coupled. Because of this, residual solvent water protons are able to induce biexponential ^1H T_1 relaxation rates in ROS and SR membrane lipid protons via cross relaxation and spin diffusion. We have carried out three types of experiments which support this interpretation.

i) Sufficient reduction of the water protons by lyophilization or selective saturation results in single exponential T_1 rates for the lipid protons. ii) Biexponential lipid T_1 relaxation can be restored in the lyophilized membranes by adding back H_2O ; iii) The addition of Cr^{+++} ions to ROS or SR membranes reduces the T_1 relaxation time of the residual solvent water protons and results in single exponential lipid proton relaxation rates. (1) Brown, M.F., Miljanich, Franklin, L.K., and Dratz, E.A. (1976) FEBS Letters, 70, 56.

M-AM-B2 DEUTERIUM NMR STUDIES OF BILE SALT-LIPID MIXED MICELLES

R. E. Stark*, J. L. Manstein*, W. C. Curatolo†, and B. Sears†

*Department of Chemistry, Amherst College, Amherst, Massachusetts 01002

†Francis Bitter National Magnet Laboratory, Massachusetts Institute of Technology, Cambridge, Massachusetts 02139

Bile salt micelles play a crucial role in the digestion of fats and in the pathogenesis of cholesterol gallstones. In order to understand the physical chemistry of bile on a molecular level, we have performed a series of deuterium (^2H) NMR measurements on phospholipids solubilized in bile salt micelles. Using 1-palmitoyl-2-oleyl-phosphatidylcholines (POPC's) which are selectively deuterated at a single acyl chain site, we have studied ^2H NMR linewidths and spin-lattice relaxation times as a function of chain position and temperature. We compare the dynamic state of lipids in these model bile systems with that of phospholipid bilayers in multilamellar dispersions and sonicated vesicles. In addition, we use the NMR results to evaluate several proposed structures for bile salt-lipid aggregates.

M-AM-B3 THE "SUBPHASE" OF DIPALMITOYL PHOSPHATIDYLCHOLINE : A RAMAN AND CALORIMETRIC

CHARACTERIZATION R. Magni and J. P. Sheridan, Biomolecular Optics Section, Code 6510, Naval Research Laboratory, Washington, D.C. 20375 USA

Raman spectroscopy and calorimetry have been used to study the metastability and structural characteristics of dipalmitoyl phosphatidylcholine (DPPC) bilayers at temperatures near 0°C . It was found by DSC that the "subtransition" temperature for DPPC varied with time of incubation at 0°C , ranging from $\sim 15^\circ\text{C}$ after one day to $\sim 25^\circ\text{C}$ after several weeks. Raman spectra of the "subphase" reveal a number of interesting structural details : (1) Quantitative analysis of the total integrated intensity of the 1130 cm^{-1} band indicates that the trans bond population of the acyl chains is close to 100%; (2) two longitudinal acoustic modes are observed at 160 cm^{-1} and 173 cm^{-1} corresponding to all-trans acyl chain lengths of fifteen and fourteen carbon atoms respectively; (3) the frequencies and intensities of the symmetric and anti-symmetric C-H stretching modes are consistent with the existence of a fairly rigid quasi-triclinic subcell; (4) the carbonyl stretching band consists of at least two components, a sharp peak at $\sim 1742\text{ cm}^{-1}$ and a much broader one at $\sim 1730\text{ cm}^{-1}$, suggestive of a partial and inequivalent dehydration of the two carbonyl groups. In contrast, Raman data on the un-incubated gel phase near 0°C indicates that this phase is considerably more disordered with respect to chain conformation and packing.

M-AM-B4 STRUCTURAL ASPECTS OF PHOSPHATIDIC ACID-DIVALENT CATION COMPLEXES, V. W. Miner and J. H. Prestegard, Chemistry Department, Yale University, New Haven, CT 06511.

Vesicle fusion upon addition of divalent cations has been demonstrated for vesicles composed of a mixture of phosphatidylcholine and phosphatidic acid (PA). Among the proposed mechanisms for fusion are 1) formation of an intermediate state involving lipids in a non-bilayer phase such as the inverted hexagonal (H_{II}) phase, and 2) creation of a structural defect at the fusion site due to segregation of lipids on binding of cations. In the latter case, a tightly bonded ionic network has been suggested to account for formation of a non-leaky junction between membranes. In an attempt to elucidate the fusion mechanism on a molecular level, we have undertaken an investigation of the structure and dynamics of PA-cation complexes. In these studies, we employ solid state nmr methods to directly probe phosphate (^{31}P) and divalent ion (^{113}Cd) environments. Comparison of ^{31}P data suggests that anionic lipid- Cd^{2+} structures are identical to anionic lipid- Ca^{2+} structures but that anionic lipid- Mg^{2+} structures differ significantly in geometry or mobility. ^{31}P and ^{113}Cd data on lipids are compared to data on crystalline model compounds to more clearly define structural characteristics which may explain differences in fusion activity for these ions.

M-AM-B5 ^{13}C AND ^2H NMR STUDY OF DPPC/DPPE AND DPPE/CHOL BILAYERS

A. Blume, D. M. Rice, R. J. Wittebort, S. K. Das Gupta and R. G. Griffin, M. I. T., Cambridge, Mass 02139

^{13}C and ^2H NMR spectra have been used to study the phase equilibria, molecular conformation, and dynamics in DPPC/DPPE and DPPE/CHOL bilayers. ^{13}C sn-2 C=O spectra and ^2H spectra of head group and chain labelled lipids permit the location of the phase boundaries and the molecular changes which occur at these boundaries. In both systems a conformational change at the sn-2 C=O yields a two component ^{13}C spectrum, indicating the existence of two long lived conformations, presumably due to two different phases. The exchange between the two conformations is slow in the DPPC/DPPE system when compared to DPPE/CHOL, and we believe this is due to the larger domain size. The ^2H spectra suggest that the chains and head group disorder simultaneously with the sn-2 C=O conformational change in DPPC/DPPE bilayers. However, in DPPE/CHOL mixtures the sn-2 conformational change occurs first and this is followed by chain and head group melting at higher temperatures. Thus, the mechanism of the phase transition appears to be different in the two systems.

M-AM-B6 SOLID STATE NMR INVESTIGATIONS OF PHASE TRANSITIONS AND PHASE EQUILIBRIA IN PHOSPHOLIPID BILAYERS

R. J. Wittebort*, A. Blume*, T. -H. Huang*, S. K. Das Gupta*, and R. G. Griffin, MIT, Cambridge, MA. 02139 (Intr. by R. Frankel).

The temperature dependence of the ^{13}C NMR spectra of DPPE and three lecithins (DMPC, DPPC, and DSPC) which have been ^{13}C labelled at the sn-2 carbonyl have been studied. In the L_β or L_β' phase an axially symmetric powder pattern of about 100 ppm breadth is observed and this transforms to an isotropic line at the main L_β (L_β') \rightarrow L_α phase transition. In the case of DPPE this transformation occurs precipitously, and, with data from ^2H spectra of ^2H chain labelled DPPE, is shown to be due to a change in conformation at the sn-2 carbonyl. In contrast the ^{13}C sn-2 spectra of lecithins exhibit a gradual transformation, beginning at temperatures below the endothermic pretransition temperature. Thus, in the intermediate P_β' phase a temperature dependent superposition of the L_β and L_α ^{13}C spectra is observed, suggesting that the P_β' phase is structurally heterogeneous and exhibits properties of both the L_β' and L_α phases. Addition of cholesterol to the four pure lipids also results in a superposition of the L_β (L_β') and L_α patterns. Similar results are observed for binary mixtures of DPPC and DPPE. Collectively the results suggest that the conformational change at the sn-2 C=O is a general property of phospholipid phase transitions.

M-AM-B7 ^1H -NMR INVESTIGATION OF THE CONFORMATION OF CHARGED AND ZWITTERIONIC α - and β -PHOSPHOLIPIDS IN SONICATED VESICLES. Andreas Plückthun, Jacqueline deBony and Edward A. Dennis, Department of Chemistry (M-001), University of California at San Diego, La Jolla, California 92093 U.S.A.

The two fatty acyl chains of α -phospholipids are conformationally distinct when the phospholipids are in aggregated structures such as micelles. These differences can also be detected in sonicated vesicles by ^1H -NMR spectroscopy (360 MHz) of the α -methylene group using resolution enhancement techniques [J. deBony and E.A. Dennis, *Biochemistry* 20, 5256-5260 (1981)]. In vesicles with anionic phospholipids or PE at high pH, the spectra of the α -methylene region can be well resolved and fully accounted for. Zwitterionic α -PC, however, shows a more complicated pattern. On the other hand, β -phospholipids such as β -PE, N-methyl- β -PE, and N,N-dimethyl- β -PE give rise to two signals in sonicated vesicles (although both acyl chains are equivalent by symmetry) but only one signal in mixed micelles with detergent. Zwitterionic β -PC, however, shows only one peak in either case. Since this behavior is paralleled by the signals of the N-methyl groups, it probably derives from inside-outside differences of the β -phospholipids in the vesicle. The unusual spectra of both α - and β -PC compared to their charged analogues will be discussed in terms of packing differences within the bilayer. (NSF 79-22839)

M-AM-B8 NATURAL ABUNDANCE CARBON-13 NMR T_1 STUDIES OF LIPID BILAYER MOLECULAR DYNAMICS: EFFECT OF ACYL CHAIN LENGTH AND UNSATURATION. M.F. Brown, G.D. Williams,* and A.A. Ribeiro,†* Dept. of Chemistry Univ. of Virginia, Charlottesville, VA 22901, and†Stanford Magn. Res. Lab., Stanford, CA 94305

Natural abundance ^{13}C T_1 measurements have been made for unilamellar vesicles in which the phospholipid acyl chain length and unsaturation have been varied in a systematic manner. At present, ^{13}C T_1 values have been obtained as a function of temperature for DLPC, DMPC, DPPC, DSPC, and DOPC bilayers, in the liquid crystalline state, at resonance frequencies of 15, 25, 45, and 90 MHz. At superconducting magnetic field strengths, the data clearly reveal a "plateau" in plots of $1/NT_1$ vs. chain position, in agreement with ^2H T_1 studies.^{1,2} A surprising feature is that $1/NT_1$ is approximately independent of acyl chain length, in spite of the vastly different phase transition temperatures. For the unsaturated DOPC bilayer, $1/NT_1$ of the CH=CH segment is almost twice that of the chain CH_2 segments. These new experimental results will be discussed in terms of theoretical models for molecular dynamics in lipid bilayers. The ^{13}C and ^2H T_1 data for the DPPC bilayer can be quantitatively described by a relaxation law of the form $1/T_1 = A\tau_f + B S_{\text{CD}}^2 \omega_0^{-1}$, where A and B are constants, S_{CD} the segmental order parameter, and ω_0 the resonance frequency. The first (A) term corresponds to thermally activated trans-gauche isomerizations of the lipid acyl chains, while the second (B) term describes collective bilayer modes (director fluctuations) which predominantly influence the relaxation frequency dependence. The value of $\tau_f \sim 10^{-11}$ sec suggests that the microviscosity of the bilayer hydrocarbon region is not appreciably different from that of simple paraffinic liquids. (Supported by NIH Grant R01 EY 03754 and by the Cystic Fibrosis Foundation).

1) M.F. Brown et al., *J. Chem. Phys.* 70, 5045 (1979), 2) M.F. Brown, *J. Magn. Res.* 35, 203 (1979).

M-AM-B9 X-RAY DIFFRACTION AND CALORIMETRIC STUDIES OF N-PALMITOYL GALACTOSYLSPHINGOSINE (NPGS) (CEREBROSIDE) AND DIPALMITOYLPHOSPHATIDYLCHOLINE MIXTURES. M.J. Ruocco*, D.M. Small, R. Skarjune, E. Oldfield and G.G. Shipley, Biophysics Institute, Boston Univ. Schl. of Med., Boston, Mass. and Schl. of Chem. Sci., Urbana, Ill.

Differential scanning calorimetry and x-ray diffraction show that up to 20 mol% NPGS can be incorporated into hydrated DPPC bilayer phases both below and above the gel \rightarrow liquid crystal transition ($T_c \sim 42^\circ\text{C}$). Transition enthalpy measurements indicate complete miscibility of DPPC and NPGS; x-ray diffraction data demonstrate only minor differences in the DPPC bilayer parameters on incorporation of up to 20 wt.% NPGS. At $> 20\%$ mol% NPGS additional high temperature transitions indicate phase separation of NPGS. For example, at NPGS:DPPC (mol ratio 1:1), the transition at $\sim 42^\circ\text{C}$ is followed by an exotherm at $\sim 50^\circ\text{C}$ and an endotherm at $\sim 82^\circ\text{C}$. At 20°C , x-ray diffraction shows two lamellar phases, hydrated DPPC-NPGS ($d \sim 64 \text{ \AA}$) and NPGS ($d \sim 55 \text{ \AA}$); further heating to $T > 82^\circ\text{C}$ melts the NPGS phase and a single NPGS-DPPC bilayer L_α phase is formed ($d \sim 54 \text{ \AA}$). The observed phase behavior suggests that at molar ratios $> 1:4$ NPGS:DPPC, NPGS-NPGS lateral hydrogen bonding promotes phase separation of the cerebroside.

M-AM-B10 STRUCTURE AND THERMOTROPIC BEHAVIOR OF PHOSPHATIDYLSELINE BILAYER MEMBRANES H. Hauser, F. Paltauf, and G.G. Shipley, Biophysics Institute, Boston Univ. Schl. of Med., Boston, Mass.; Labor. für Biochemie, ETH-Zurich, Switzerland; Inst. für Biochemie, Tech. Hochschule, Graz, Austria.

The structure and thermotropic properties of an homologous series of diacyl phosphatidylserines (PS) in the anhydrous and hydrated state have been examined using low angle x-ray diffraction and differential scanning calorimetry. In the anhydrous state at low temperature both acidic-PS and its NH_4^+ -salts exhibit lamellar bilayer crystal forms which transform to liquid-crystalline hexagonal (Type II) structures at high temperatures. The crystal liquid-crystal transition temperature increases with increasing chain length, the transition temperature of an NH_4^+ -PS being higher than that of its corresponding acidic form. In contrast, the transition enthalpies of the acidic PS are higher than those of the NH_4^+ -salts. Hydrated acidic and NH_4^+ -PS exhibit reversible lamellar gel liquid-crystal transitions. In this case the acidic form undergoes this chain length dependent transition at a higher temperature, but with a lower enthalpy change, than the NH_4^+ -PS. Both below and above the hydrocarbon chain melting transition hydrated lamellar bilayer structures are present. The temperature-composition phase diagram of the NH_4^+ -dimyristoyl PS/ H_2O system has been studied in detail. The chain melting transition decreases with increasing hydration reaching a limiting value of 39 °C. X-ray diffraction shows that both the bilayer gel structure and the bilayer liquid crystal form take up water continuously, a characteristic of lipid bilayers with a net charge. Electron density profiles of NH_4^+ -dimyristoyl PS at different hydration levels permit detailed analysis of the structural parameters of the PS bilayer.

M-AM-B11 MOLECULAR MOTION IN MEMBRANES. R. J. Pace and S. I. Chan. Caltech, Pasadena, CA 91125

The dynamics of acyl chain motion in fluid bilayers, as reflected by several classes of NMR, ESR relaxation measurements are interpreted in terms of a previously described model of the fluid membrane.¹ This assumes an average 'crank shaft' like structure for the acyl chains, consisting of alternating trans and gauche segments, with the gauche bonds aligned with the long chain axis. Fast relaxation occurs by single bond $g^\pm \rightleftharpoons t \rightleftharpoons g^\pm$ interconversion about the axially aligned bonds, a process which does not alter the average chain axis direction or gross intermolecular ordering. The model predicts reasonably both the magnitude and shape of the high frequency (54 MHz) methylene ^2H T_1 profile along DPPC chains, assuming $t \rightleftharpoons g^\pm$ isomerization rates consistent with published estimates from molecular dynamics simulations of polyethylene chains. In addition, the angular dependence of ^{13}C and ^2H T_1 relaxation is predicted to be very small, as a direct consequence of the average orientation of the C-H bond to the chain axis in the crank shaft geometry. A nematic liquid crystal description of chain axis fluctuation is shown to provide a good fit to the ^1H T_1 and $T_{1\rho}$ data over an extended frequency range (10^4 - 10^8 Hz), where relaxation rates linear in $\omega^{-1/2}$ are observed in the high ($>10^7$ Hz) and low ($<10^6$ Hz) frequency regions. It is suggested that relaxation behavior in the 10^6 - 10^7 Hz range is strongly influenced by lateral diffusion and non crank shaft intramolecular motions. The nematic model is also consistent with the amplitudes and time scales for axial fluctuation deduced from rigid spin probe (cholestane) studies. (Supported by USPHS NIH grant GM22432.)

¹R. J. Pace & S. I. Chan, *Biophys. J.* **33**, 165a (1981)

M-AM-B12 RAMAN SPECTROSCOPY AS A QUANTITATIVE PROBE OF CONFORMATIONAL ORDER IN BILAYERS CONTAINING PHOSPHATIDYLCHOLINES AND SELECTIVELY DEUTERATED DERIVATIVES J. P. Sheridan and R. Magni,

Optical Probes Branch, Code 6510, Naval Research Laboratory, Washington, D.C. 20375 USA A method has been developed for the quantitative determination of conformational order/disorder in phospholipid bilayers from Raman line intensities. The approach involves the temperature dependence of the $1130\text{cm}^{-1}/1298\text{cm}^{-1}$ and $1064\text{cm}^{-1}/1298\text{cm}^{-1}$ ratios in linear alkane fluids. These chain molecules are in an isotropic environment, so the trans or gauche bond populations can be easily calculated by the methods discussed by Flory. This allows a calibration of the Raman intensity ratios as functions of conformational structure. Using this method the trans bond populations have been determined in all four phases of dipalmitoyl phosphatidylcholine (DPPC). It is found that 100% of trans bonds exists only in the so-called "sub-phase" while the unannealed gel phase contains an increasing amount of gauche rotamers as the temperature is raised. The discontinuity at the main phase transition and the fraction of trans bonds persisting in the fluid phase agree well with data from other physical techniques and with current theoretical predictions. We have also determined that the $2850\text{cm}^{-1}/2940\text{cm}^{-1}$ ratio on the C-H stretching region is a sensitive measure of interchain segmental correlations and can be used to monitor changes in lattice packing as a function of temperature or phase. These spectral probes of chain conformation and packing are now being extended to phospholipids containing selectively deuterated chain segments. Data will be presented on DPPC in which (1) both chains are deuterated at positions C2 thru C8, and (2) both chains are deuterated at positions C9 thru C16.

M-AM-B13 CURRENT-VOLTAGE CHARACTERISTICS OF SMALL LIPID VESICLES: A DETERMINATION USING SPIN-LABELED HYDROPHOBIC IONS. David S. Cafiso and Wayne L. Hubbell Dept. of Chemistry University of Virginia, Charlottesville, Va. 22901 and Dept. of Chemistry University of California Berkeley, Ca. 94720.

Magnetic resonance has been utilized to characterize the transport of hydrophobic ions in small unilamellar vesicles. We have used a rapid mixing device adapted to an EPR spectrometer to monitor changes in the phase partitioning of spin-labeled phosphonium derivatives which occur when concentration gradients of this ion are established across small lipid vesicles. These changes, which are seen as a decrease in a motionally averaged aqueous component, result from the transmembrane migration of the ion and have been used to calculate the electrical current in this system. By measuring the current under conditions where known potentials are established across the vesicles, a non-linear current-voltage curve is obtained. The data is adequately accounted for in terms of a simple Eyring rate model of the membrane in which the barrier is not centrally located. In several respects, these results agree favorably with measurements made in planar bilayers; in addition, the ability here to directly measure the binding constants for the ion also permits an estimation of the barrier height for the hydrophobic cation. In small sonicated vesicles we observe an asymmetry for the binding of this ion such that the binding constant measured on the vesicle interior exceeds that on the exterior by approx. 50 to 20%, depending on the time since sonication.

This work was supported by NIH grant EY729 and The Jane Coffin Childs Fund for Medical Research.

M-AM-B14 DEUTERIUM NMR STUDY OF PHOSPHATIDYLCHOLINE (PC) HEADGROUP ORDER IN PC/CEREBROSIDE/CHOL-ESTEROL MODEL MEMBRANES AND IN INTACT NERVE. W. Curatolo, B. Sears, L. J. Neuringer, and F. B. Jungalwala*. MIT, Cambridge, MA, and E. K. Shriver Center for Mental Retardation, Waltham, MA.

We have used ^2H -NMR to study the effects of various cerebroside (CER) on the orientational order of the choline headgroup of N-(C^2H_5)₃-dipalmitoyl-PC (^2H -DPPC). The effects of the following CER's have been studied: bovine brain CER (BOV-CER), non-hydroxy fatty acid CER (NFA-CER), 2-OH-fatty acid CER (HFA-CER) and palmitoyl-CER (C16:0-CER). ^2H -DPPC in the liquid crystalline state exhibits a quadrupole powder pattern with a splitting ($\Delta\nu_Q$) of 900 Hz. Incorporation of 20 mol% BOV-CER, NFA-CER, or HFA-CER results in collapse of this doublet to a singlet, indicating disordering of the ^2H -DPPC headgroup. Incorporation of 20 mol% C16:0-CER has no effect on ^2H -DPPC headgroup order. We tentatively attribute this difference to the presence of long-chain fatty acids (C24:0, C24:1) in BOV-CER, NFA-CER, and HFA-CER, which may interdigitate with chains in the opposite half of the bilayer, causing sufficient disruption of packing to be sensed by the ^2H -DPPC headgroup. ^2H -NMR spectra have also been obtained of intact sciatic nerves which have been biosynthetically deuterated with N-(C^2H_5)₃-choline. Intact nerve exhibits a quadrupole powder pattern with $\Delta\nu_Q \sim 900$ Hz, indicating that phospholipid headgroup order is similar to that in liquid crystalline ^2H -DPPC. The observation of a quadrupole doublet was surprising, since intact nerve contains $\sim 20\%$ BOV-CER, and the 80/20 ^2H -DPPC/BOV-CER model system exhibited a singlet. However, addition of 10% cholesterol (CHOL) to 80/20 ^2H -DPPC/BOV-CER results in reappearance of the quadrupole doublet. This suggests that CHOL acts as a spacer which decreases PC/CER interactions, relaxing CER-induced disordering of the PC headgroup. This work supported by NIH and NSF.

M-AM-C1 CHEMICAL MODIFICATION OF AMINO GROUPS SLOWS K CHANNEL CLOSING IN MYELINATED NERVE.

P.A. Pappone and M.D. Cahalan, Dept. of Physiology & Biophysics, Univ. of Calif., Irvine, CA 92717.

Trinitrobenzene sulfonic acid (TNBS) has dramatic effects on potassium channel gating in voltage clamped frog myelinated nerve fibers. TNBS is a membrane-impermeant amino group reagent, which acts at high pH to convert titratable amino groups to neutral trinitrophenylated derivatives. 10-20 mM TNBS was applied externally at pH 9-10.5. After reaction, the modified K channels were studied in pH 7.4 isotonic K external solution. TNBS treatment slows the rate of decline of K "tail" currents up to tenfold without altering the "on" kinetics for depolarizing pulses beyond -30 mV. The tail time constants are increased by TNBS treatment by a factor of 2 to 10 for potentials from -150 to -80 mV. For voltages between -60 and -30 mV, TNBS also slows channel opening. The steady-state conductance-voltage curve measured from tails upon repolarization is not altered by TNBS. There is no change in the shape of the instantaneous I-V curve and no change in the potency of TEA block after TNBS treatment. The effects of TNBS treatment on the K channels of myelinated nerve are permanent, in contrast to the reversible effect of TNBS on Na channel inactivation we have previously reported in nodes of Ranvier. The time course of K channel tail currents after TNBS treatment depends upon the external ion composition. With 20% K, 80% Na as the external medium, tail currents are 2-3 times as fast at -110 mV as in isotonic K. The effects of TNBS are qualitatively mimicked by treating the node for 2-3 minutes with pH >11. High pH treatment produces an irreversible increase in tail current time constants. These results implicate involvement of an amino group in the rate limiting step for closing the channel. (Supported by NIH grant NS14609 and a fellowship from the American Heart Association.)

M-AM-C2 PROPERTIES OF K CURRENT FLUCTUATIONS IN FROG NERVE. F. Conti, B. Hille and W. Nonner, Dept. of Physiology and Biophysics, Univ. of Washington, Seattle, WA 98195.

Current noise from myelinated nerve has a component attributable to K channels, which is activated by depolarization, is insensitive to tetrodotoxin, is blocked by 10 mM tetraethylammonium ion, and is absent at the reversal potential of K current. We have analysed such fluctuations during transient and steady-state K currents from voltage-clamped, *R. pipiens* axons bathed in solutions with 60 mM K ion and TTX. Plots of the non-stationary variance (bandwidth 10-20 kHz, 13°C) versus the mean K current yield curves close to the parabola expected from a simple, open-close gating process. Their initial slopes correspond to single-channel conductances of 14-27 pS (mean 21 pS), independent of voltage from -50 to +70 mV. Their curvature is consistent with the presence of ca. 10,000 K channels per node. The parabola fit, however, is poor for strong depolarizations, and curves from the on- and off-phases of K current do then not superimpose. Better fits could be obtained on the assumption that there are at least two populations of K channels, differing in their rates of gating. Power spectral densities of the stationary fluctuations often show a hump at frequencies roughly equivalent to τ_n , but, spectral density keeps increasing towards frequencies below 1 Hz, and it falls less steeply than $1/f^2$ towards higher frequencies, probably expanding beyond the maximal bandwidth of the records (20 kHz). Analysing our records in terms of non-stationary covariance indicates that correlations develop with time after a voltage step. Covariance relative to a time early in a depolarization decays rapidly, whereas covariance relative to a time some hundred msec later reveals a marked slow phase of decay. This result is inconsistent with there being a single kind of K channels that have only one conductive state. Supported by NIH grants NF08174 and HR9585.

M-AM-C3 EFFECTS OF EXTERNAL Cs AND Rb ON OUTWARD K CURRENTS IN SQUID AXONS. J. R. Clay¹ and M. F. Shlesinger², ¹Lab. of Biophysics, NINCDS, MBL, Woods Hole, MA 02543; ²Inst. for Physical Sciences, Univ. of MD, College Park, MD 20702.

We have studied the effects on internally perfused squid axons of external Cs^+ and Rb^+ , both of which cause instantaneous ($< 100 \mu\text{sec}$) voltage dependent block of K conductance. Currents were measured immediately after a voltage step from the end of a depolarizing prepulse to either -20 or 0 mV; holding potential was either -100 or -80 mV. The K concentration internally (K_i) was 300 mM; externally (K_o) it was either 100, 300, or 500 mM. Blocking ion concentration was between 5 and 340 mM with 100 mM K_o ; it was either 50 or 150 mM with 300 mM K_o (Cs, Rb, and K were substituted for external Na). The control current-voltage relation (IV) was non-linear for either 100 or 500 mM K_o . The slope conductance at the reversal potential (E_r) was an increasing function of K_o with an approximate proportionality of $(K_o + K_i)$. Cs_o^+ blocked inward currents in a manner similar to the results of Adelman and French (1978; J. Physiol. 276: 13-25). Inward current was virtually abolished by 200 or 340 mM Cs_o . No change in E_r was observed. Outward current was reduced at the higher levels of Cs_o^+ ; at 0 mV the current was reduced by about 1/3 ($\text{Cs}_o=340 \text{ mM}$); this effect was relieved at positive potentials. Rb_o^+ partially blocked inward current for potentials between $E_r-50 \text{ mV}$ and E_r ; the block was relieved at more negative potentials. Increasing Rb_o with 100 mM K_o produced an increasing block for $0 \leq \text{Rb}_o \leq 50 \text{ mM}$. Further increases of Rb_o increased inward current and shifted E_r in the positive direction ($E_r \approx -5 \text{ mV}$ for 340 mM Rb_o). Outward current was suppressed by about 3/4 at +20 mV ($\text{Rb}_o=340 \text{ mM}$); this effect was relieved at more positive potentials. We conclude that Cs_o blocks inward current more effectively than Rb_o , whereas the converse relation is observed for outward current.

M-AM-C4 PERMEANT CATIONS ALTER CLOSING RATES OF K CHANNELS. D. R. Matteson and R. P. Swenson Jr. Dept. of Physiology, G-4, Univ. of Pennsylvania, Philadelphia, Pa. 19104. The influence of the addition of monovalent cations (25-200 mM) to the external solution on the closing rate of K channels was examined in squid giant axons. Using a double pulse protocol to minimize the problem of K⁺ accumulation in the restricted extracellular space, we found that Rb⁺, Cs⁺ and K⁺ markedly slowed the closing of K channels. Rb⁺ and Cs⁺ were equally effective, slowing closing by a factor of 2-3 at -70mV. K⁺ increased the closing rate 1-2 times. In contrast, at the same potential Tl⁺, and in some cases NH₄⁺, speeded the rate at which K channels close. Na⁺ and Li⁺ had no significant effect.

To determine if these changes in K channel kinetics were correlated with the K channel permeability of these ions, we estimated their relative permeabilities when added externally. The K⁺ gradient was reversed so that the K⁺ equilibrium potential (E_{rev}) was near +20 mV. The relative permeabilities were then calculated, using the Goldman-Hodgkin-Katz equation, from the measured shifts in E_{rev} following addition of the cations. The relative permeabilities agreed favorably with previous reports from other preparations: Tl⁺ > K⁺ > Rb⁺ > NH₄⁺ = Cs⁺ > Li⁺. These results imply that only measurably permeant cations can modify closing kinetics of K channels. Since no direct correlation can be drawn between the degree of permeability and the direction of the change of kinetics, some other factor must be involved. One possibility is that the length of time an ion resides at a specific site in the K channel may account for the nature of the alteration in K channel closing rate.

M-AM-C5 ACETYLCHOLINE RECEPTORS ON DEVELOPING MUSCLE CELLS DIFFUSE AS SUBMICROSCOPIC CLUSTERS: AN APPLICATION OF FLUORESCENCE CORRELATION SPECTROSCOPY. Nancy L. Thompson and Daniel Axelrod. Biophysics Research Division and Department of Physics, Univ. of Mich., Ann Arbor Mich. 48109.

Acetylcholine receptors (AChR) in developing rat muscle cells in culture are distributed both in macroscopic patches of immobile AChR and in "diffuse" areas of laterally mobile AChR. We show by fluorescence correlation spectroscopy (FCS) that many of the AChR in the diffuse areas do not move in the membrane as single molecules but rather as microclusters of 15 to 40 receptors. Membrane AChR are specifically fluorescence-labeled with tetramethylrhodamine α -bungarotoxin; their fluorescence is excited by a laser beam of Gaussian intensity profile focused to a small spot in a "diffuse" area. As AChR molecules or groups of molecules randomly enter and leave the small illuminated area ($\sim 2 \mu\text{m}^2$), the total fluorescence collected from the area spontaneously fluctuates. These fluctuations are autocorrelated on-line by minicomputer. The normalized variance of the fluctuations, measured from the amplitude of the correlation function, is equal to the reciprocal of the average number of independent mobile units N in the region of illumination. In our experiments, N ranges from 50 to 120. However, the average number of AChR molecules in the observation region (obtained by calibration of the mean fluorescence intensity) is about 2000. Therefore, many of the AChR must be aggregated in laterally mobile microclusters. (Supported by NIH grant NS14565.)

M-AM-C6 STRUCTURE AND FUNCTION OF EMBRYONIC ACETYLCHOLINE RECEPTORS IN DISPERSED FORM IN XENOPUS MUSCLE. P. C. Bridgman*, S. Nakajima, A. S. Greenberg* and Y. Nakajima* (intr. by W. L. Pak), Dept. of Biological Sciences, Purdue University, West Lafayette, IN 47907.

There are two forms of arrangement of acetylcholine receptors (ACh-R) in the membrane: aggregates composed of many receptors or diffusely distributed receptors (as seen using autoradiography). Although the structure of ACh-R aggregates has been extensively studied, diffusely distributed receptors have received little attention in this regard. Embryonic *Xenopus* muscle cells in culture at various developmental stages were tested for sensitivity to acetylcholine, and then prepared for freeze-fracture. Acetylcholine sensitivity was first observed at developmental stage 20 and gradually increased up to stage 27. Freeze-fracture replicas of muscle cells that were non-sensitive to acetylcholine revealed diffuse arrangement of P-face particles of small size. However, ACh sensitive cells contained a greater proportion of diffusely distributed large particles (median diameter, 11 nm). The size distribution of these large particles was close to, but slightly smaller than, that of aggregated particles found on hot spots. The density of these diffuse large P-face particles increased as development proceeded. In contrast, the density of small particles (less than 8 nm) did not change with development. These results suggest that a substantial part of these large diffuse particles represents ACh-R's. These particles exist mainly in solitary form, suggesting that an ACh-R can function without an interaction with other ACh receptors. (Supported by grant NS-10457.)

M-AM-C7 INTERACTION OF D-PENICILLAMINE WITH METHYLMERCURY AND MERCURIC CHLORIDE IN RELATION TO INHIBITION, PROTECTION AND REGENERATION OF BRAIN MUSCARINIC RECEPTORS. MERCURIC CHLORIDE POTENCY OF INHIBITION IN A HYDROPHOBIC MEDIUM. A-S.A. Abd-Elfattah and A.E. Shamoo, Dept. Biol.Chem., Univ. Maryland School of Medicine, Baltimore, Maryland 21201.

Methylmercury (MeHgCl) and mercuric chloride (HgCl_2) strongly inhibit the atropine-sensitive $L(^3\text{H})$ quinuclidinyl benzilate ($^3\text{H-QNB}$) binding to rat brain lysed synaptosomes. D-Penicillamine (D-PA) effectively protects, in a concentration-dependent manner, muscarinic acetylcholine receptor (mAChR) against MeHgCl and HgCl_2 . D-PA and dithiothreitol (DTT) also protect mAChR against the loss in $^3\text{H-QNB}$ -binding of the control due to auto-oxidation. D-PA regenerates mAChR binding after inhibition with either MeHgCl or HgCl_2 . D-PA alone does not have any effect on mAChR, except at a concentration higher than 10mM when incubated for 2 hrs. or more. A gradual change in the hydrophobicity of the aqueous incubation medium, by adding varying amounts of dimethyl sulfoxide (DMSO), did not show any inhibitory effects on $^3\text{H-QNB}$ -binding of the control between 0-20% DMSO. In the presence of 2.5% DMSO, the dose-response curve of HgCl_2 inhibition of mAChRs is shifted slightly to the right. DMSO apparently reduces the charge-charge interactions between Hg^{2+} and the free -SH groups in the receptor site. These observations indicate that Hg^{2+} favors the aqueous medium for maximum inhibitory effects on mAChRs. Supported by NIEHS AND DOE.

M-AM-C8 SINGLE CHANNEL PROPERTIES OF NEWLY INSERTED ACETYLCHOLINE RECEPTORS IN NON-INNervATED EMBRYONIC MUSCLE CELLS IN CULTURE. A. S. Greenberg*, S. Nakajima and Y. Nakajima*, Dept. Biological Sciences, Purdue University, West Lafayette, IN 47907.

Muscle cell cultures were prepared from *Xenopus* embryos (stage 18-19) prior to formation of synaptic contacts. Single channel currents activated by cholinergic agonists were measured by the "giga seal" patch clamp on cells maintained for 4-6 days. We found a heterogeneity of channel behavior like that reported by Clark and Adams (1981). Specifically, we have observed in the majority of patches single channel currents that were distributed between two distinct size classes, each of which appeared to have its own characteristic mean open time. The behavior of single channel events for two different cholinergic agonists, acetylcholine and suberyldicholine, showed no marked difference in channel properties. Existing acetylcholine receptors (AChRs) were blocked with α -bungarotoxin (α -BGT) and, over the next 1-6 hours, the single channel properties were measured from those receptors believed to be recently inserted. Though fewer membrane patches displayed the non-homogeneous receptor behavior typical of control records, both types of single channel events were observed. The majority of cells pretreated with α -BGT exhibited, soon after the establishment of seal, clusters of events followed by long quiescent periods. This is in contrast to the relatively maintained frequency of single channel events found in control records. The single channel behavior of pretreated cells qualitatively resembled that displayed by receptors in a desensitized state (Sakmann et al., 1980). Supported by NIH grant NS-08601.

Clark, R. B. and P. R. Adams, Soc. Neurosci. Abstr. 7:838 (1981).

Sakmann, B., J. Patlak and E. Neher, Nature, 286:71-73 (1980).

M-AM-C9 ENDPLATE ACETYLCHOLINE RECEPTOR KINETICS FROM SINGLE CHANNEL RECORDS. M.D. Leibowitz and V.E. Dionne, University of California at San Diego, La Jolla, California 92093

The temporal behavior of single channel events recorded from endplate membrane has been analyzed to estimate the kinetic rates at which channels both open and close plus the mean lifetime of the specific closed-channel state from which opening-transitions occur. Patch recording experiments were performed on the acetylcholine receptors (AChR) of garter snake (sp. *Thamnophis*) twitch fiber junctional membrane which had been enzymatically treated to remove nerve terminal and connective tissues. Although small, patches of junctional membrane should contain large numbers of AChRs; single channel activity was sustained at a low rate with 1 μM carbamylcholine ($K_D = 400\mu\text{M}$). Current-time records containing 400 to 1000 single events (together with infrequent multiple events) were examined. Brief, square current steps occurred with a uniform amplitude and variable duration. The occurrence of events was time-dependent; channels opened more frequently just after a channel closed than at other times. The distribution of event durations was exponential and provided a direct estimate of the channel closing rate, α (400-700/sec 20°C). Two additional parameters were measured; these were (1) the Probability (an opening-transition will occur in the time interval $t, t+\Delta t$) and (2) the conditional Probability (an opening-transition will occur in the time interval $t, t+\Delta t$ given that no openings occurred from 0 to t). In both, time is measured from that instant when a closing-transition occurs which leaves all channels closed. Specific probability expressions derived from the following kinetic model have provided estimates of the opening transition rate, β (500-2000/sec) and of the closed state (A_2R) lifetime (150-300 μsec). $2A+R \xrightleftharpoons[k]{\beta} (A_2R) \xrightleftharpoons[\alpha]{\beta} A_2R^*$ (open) (Supported by NIH: NS 15344 and ONR: N00014-79-C-079)

M-AM-C10 TEMPERATURE DEPENDENCE OF ENDPLATE CHANNEL CONDUCTANCE. H.M. Hoffman⁺ and V.E. Dionne (Intr. by S.E. Mayer), University of California at San Diego, La Jolla, California 92093 and ⁺University of Vermont, Burlington, Vermont 05401

The mean single channel conductance (γ) depends strongly and monotonically on temperature. Evaluation of this behavior using several permeant ions has allowed the free energy profile for ion permeation to be estimated. Experiments were performed on the acetylcholine receptors of garter snake (sp. *Thamnophis*) neuromuscular junctions. Endplate regions, identified with Nomarski optics, were voltage-clamped with two microelectrodes, and acetylcholine induced endplate current noise was analyzed to estimate γ . Measurements over the temperature range circa 0-23°C were made in normal saline (mM: NaCl 159, KCl 2.15, CaCl₂ 1, MgCl₂ 4.2; HEPEs, pH 7.2) and solutions with 50% of the Na⁺ replaced by either Li⁺, Rb⁺, or Cs⁺. Membrane potential was held close to E_K and the dominant current-carrying ions were Na⁺ and its substitutes. Temperature had no measurable effect on the reversal potential. At all temperatures a permeability sequence inversely graded with ion size was observed: $\gamma(\text{Li/Na}) < \gamma(\text{Na/Na}) < \gamma(\text{Rb/Na}) < \gamma(\text{Cs/Na})$. Regression lines fitted to Arrhenius plots of $\ln(\gamma)$ versus $1/T$ were continuous and had similar slopes (below). The simplest energy profile which

	Slope \pm SE	ΔH	$\Delta U - \Delta U_{Na}$	$\Delta S - \Delta S_{Na}$	
		(kcal/mol)		cal/mol $^\circ$ K	
Li/Na	-4228 \pm 440	8.8	0.34	-7.0	accounts for both the temperature dependence of γ and the ion selectivity consists of a single major barrier with peak transfer enthalpy (ΔH), relative transfer free energy ($\Delta U - \Delta U_{Na}$) and entropy ($\Delta S - \Delta S_{Na}$). Both channel selectivity and conductance seem to result from coupled differences of ionic transfer entropy and enthalpy.
Na/Na	-5020 \pm 504	10.4	0	0	
Rb/Na	-5120 \pm 657	10.4	-0.24	2.0	
Cs/Na	-5211 \pm 561	10.9	-0.60	4.0	

M-AM-C11 ACTIVATION OF INDIVIDUAL ACETYLCHOLINE CHANNELS BY CURARE IN EMBRYONIC RAT MUSCLE. C. E. Morris*, M. B. Jackson, H. Lecar and B. S. Wong, NINCDS, NIH, Bethesda, MD 20205, and C. N. Christian*, NICHD, NIH, Bethesda, MD 20205. (Intr. by D. Gilbert).

The classical effect of curare is to competitively block the acetylcholine (ACh) receptor of the vertebrate neuromuscular junction. In embryonic rat muscle, however, curare is known to depolarize the cell to approximately -50 mV while still competing with ACh (Ziskind & Dennis, *Nature* 276:622, 1978). We have recorded single channel currents induced by curare (d-tubocurarine chloride) in tissue-cultured rat myotubes. A simple explanation for the dual agonist/antagonist action of curare arises from the kinetics of curare-induced channel activation. At -100 mV, the mean single channel current was 4.7 \pm 0.6 pA. The reversal potential of the curare-induced events was about +6 mV. These findings are in good agreement with the carbachol-induced currents measured in a similar culture (Jackson & Lecar, *Nature* 282:863, 1979). A single exponential fit to the current jump durations gives a mean open time of 0.3 \pm 0.04 ms. Thus, the major difference between curare and a cholinergic agonist is that curare produces very short-lived channels. Dual agonist/antagonist action can be explained by a three-state kinetic scheme in which the open-close transition rates are such that a channel is open only a small fraction of the time during a relatively long drug occupancy time.

(C.E.M. was supported in part by a grant from the Scottish Rite Foundation. C.E.M.'s present address: Department of Biology, University of Ottawa, Ottawa, Ontario, Canada. M.B.J.'s present address: Department of Biology, University of California, Los Angeles.)

M-AM-C12 DURING STIMULATION OF PANCREATIC ACINAR SECRETION THE ACETYLCHOLINE-INDUCED CURRENTS CARRIED BY Na⁺ AND Ca⁺⁺ ARE INDEPENDENT. J. O'Doherty and R. J. Stark, Department Physiology, Indiana University Medical School, Indianapolis, Indiana 46223

In the exocrine pancreas, acetylcholine (ACh) released from vagal nerve terminals increases the permeability of the acinar membrane to Na⁺ and Ca⁺⁺ ions. Activation of the acinar cell in this manner causes the physiological transmission of the signal required to initiate fluid and enzyme release. Furthermore, the action of ACh on acini can be mimicked by Ionophore A23187. We compared the induced changes in intracellular ionic potentials due to ACh-stimulation of acini with those changes due to Ionophore stimulation. Stimulation with ACh concentrations varying from 10⁻⁸ to 10⁻⁵M and with A23187 concentrations of 10⁻⁶ and 10⁻⁵M caused parallel increases in cytosolic Ca⁺⁺ and Na⁺ ([Ca]_i, [Na]_i). The increases in [Ca]_i and [Na]_i observed with 10⁻⁶ A23187 were similar to those increases found with the concentration of ACh (10⁻⁷M) that produced the maximal enzyme secretion. ACh stimulation following removal of either extracellular Na⁺ or Ca⁺⁺ ions, eliminated the intracellular increases usually observed when the removed ion is present, but did not affect the increases usually observed with the other ion. These experiments demonstrate the ACh-induced current: carried by Na⁺ and Ca⁺⁺ are independent. They also suggest that the acetylcholine receptor associated with the acinar membrane may have two structural functions. As a receptor it is involved with the recognition of the neurotransmitter, as an ionophore with the selective translocation of Na⁺ and Ca⁺⁺. Supported by PHS26246.

M-AM-C13 DETERMINATION OF THE ACTIVATION KINETICS OF THE CA CURRENT AND THE ESTIMATION OF SINGLE CA CHANNEL CURRENT IN THE RAT PITUITARY TUMOR CELL LINE (GH₃). H. Ohmori and S. Hagiwara, Dept. Physiol., Ahmanson Lab. of Neurobiology, and Jerry Lewis Neuromuscular Research Center, UCLA, Los Angeles, CA 90024.

The kinetics of the current of the Ca channel were analyzed by using a suction pipette voltage clamp technique. The Na current was eliminated by TTX (10^{-6} g/ml) or by replacing the external Na with TEA, and the K current was minimized by TEA. The channel is permeable to Ca, Sr and Ba in the sequence of Ba > Sr > Ca. The activation kinetics showed the best fit with m^2 kinetics. When changes of the surface potential are taken into consideration the voltage dependence of the time constant of activation is independent of either the permeant ion species or the concentration. When the permeant ion was Ba, the K current was almost totally suppressed in TEA solution and the Ba current showed no significant inactivation. Under this condition, a steady state fluctuation was analysed by using power density spectrum. The technique of ensemble noise analysis was also applied to the activation process of the Ba-current. Both methods gave the unitary Ba-current as -0.2 pA at the membrane potential around the peak inward current (1.6 ± 6.7 mV, S.D.) in 25 mM Ba, in TEA solution. (Supported by NIH Grant NS09012 and MDA Grant).

M-AM-C14 RELAXATION DUE TO DEPLETION IN AN EGG CELL CALCIUM CURRENT. A.P. Fox and S. Krasne, Dept. of Physiology, School of Medicine, UCLA, L.A., CA, 90024.

Two voltage-activated Ca^{++} channels have been described previously for the egg cell membrane of *Neanthes a.* The currents through both channels relax with time; for one channel, Ca(I), the relaxation is due to a voltage-dependent inactivation and for the other, Ca(II), the relaxation is current dependent. We have now analyzed the current relaxation through Ca(II) to determine whether it is due to blocking or inactivation by internal Ca^{++} or to a change in driving force because of Ca^{++} depletion or accumulation phenomena. We have found that the time course of the current relaxation is a function of $1/\sqrt{I}$. In addition, the magnitude and kinetics of the relaxation has the same dependence on current when Ca^{++} is replaced by Ba^{++} or Sr^{++} . By contrast, raising external Ca but limiting current size by use of Ca-channel blockers shows that the kinetics of the relaxation process depend on the external Calcium concentration; that is the more calcium there is in the bath (with divalents kept constant using magnesium) at any given current amplitude, the slower are the kinetics of current relaxation. Thus, the current-dependent relaxation for Ca(II) appears to be due to a depletion of Ca^{++} near the channel rather than either inactivation or blocking by internal Ca^{++} . This mechanism is similar to that found for Ca^{++} currents in frog skeletal muscle membranes.

Supported by the Muscular Dystrophy Association, NIH grant (HL 20254) and MDA of Canada Fellowship (C790501).

M-AM-C15 ELECTROPHYSIOLOGY OF ACINAR GLAND CELLS: IONIC SENSITIVITY OF THE BASAL AND LUMINAL MEMBRANE SURFACES. David Senseman and Irene Horwitz, Department of Physiology and Pharmacology School of Dental Medicine, University of Pennsylvania, Philadelphia, Pennsylvania 19104

The outer membrane of an acinar gland cell can be anatomically divided into a luminal and a basal surface. Since secretion is restricted to the luminal surface, it is reasonable to assume that the membrane in this region differs from the membrane in the basal region in its biophysical characteristics. In order to identify these differences we have used the salivary gland of the snail *Helisoma* as a simple model of an exocrine gland system. Intracellular microelectrodes were used to monitor electrical activity in single acinar cells while the ionic composition of the saline solutions bathing the luminal and the basal membrane surfaces were independently varied.

We found that the acinar rest potential was dependent upon the $[\text{K}^+]$ at both the basal and the luminal surfaces. However, elevated levels of K^+ produced larger membrane depolarizations when applied to the basal than to the luminal surface. Differences in sensitivity of these membrane regions were also observed with the Ca^{2+} antagonist Cd^{2+} . Electrically evoked action potentials in these cells could be reversibly blocked by micromolar concentrations of Cd^{2+} applied to either the basal or the luminal surface. However, complete blockade required significantly higher concentrations of Cd^{2+} at the luminal surface than required at the basal surface.

We believe that these differences in ionic sensitivity of the basal and the luminal membrane regions are not due to qualitative differences in the membrane *per se*. Rather, these effects can be explained simply by the proportionally larger surface area of the basal region.

(Supported by NIH Grant DE05271-3)

M-AM-D1 EFFECTS OF NILE BLUE ON ELECTRICAL PROPERTIES OF MEMBRANES. M. Block and S. Krasne, Dept. of Physiology, Sch. of Med., UCLA, Los Angeles, Cal. 90024

We have examined the effects of Nile Blue purchased from Allied Chemical Co. on the conductances and surface potentials of planar bilayer membranes. We have used this impure, commercially available brand of dye as it appears to be the only one which produces the large spectral signals thought to be correlated with potential changes across the SR membrane of vertebrate skeletal muscle. In unbuffered, 0.1M KCl solutions (pH 5.5), the conductances of neutral (PE) and negatively charged (PE/PS) bilayers are increased negligibly by dye concentrations up to 10^{-5} M; the highest conductance change, 2×10^{-8} mho-cm⁻², was induced in PE bilayers. The membrane conductance due to valinomycin-K⁺ was decreased in both PE and PE/PS bilayers upon addition of dye, this decrease being less than a factor of 3 at 10^{-5} M dye. In a buffered, pH 7.2, "relaxing" solution, the dye-induced bilayer conductances were about 1.5 orders of magnitude higher than at pH 5.5. These data suggest that a positively charged dye adsorbs to the membrane whereas a neutral form of dye might be involved in carrying a charged form to the SR membrane (as well as through the bilayer). We are currently investigating purified sub-fractions of this dye to determine the species responsible for these electrical effects as well as (in collaboration with J. Vergara) that giving the spectral signals from the SR.

This research is supported by grants from NIH (HL20254) and Muscular Dystrophy Assoc.

M-AM-D2 STROPHANTHIDIN INDUCED INOTROPIC RESPONSE AND LOSS OF CELLULAR POTASSIUM IN VOLTAGE-CLAMPED FROG VENTRICULAR MUSCLE. L. Cleemann, Department of Physiology, School of Dental Medicine, University of Pennsylvania, Philadelphia, Pennsylvania 19104.

The single sucrose gap technique is used to voltage-clamp strips of frog ventricular muscle and to measure the isometric force. ⁴²K is used to obtain a simultaneous record of the cellular K content and the rate of net cellular K loss or uptake (Cleemann, Biophys. J. 36: 303 (1981)). The rate of cellular K uptake is measured as a function of the extracellular K⁺ concentration (K_o) in the presence and absence of $2 \cdot 10^{-5}$ M strophanthidin. The active, strophanthidin sensitive K uptake reaches half of its maximal value (ca. 3 pmole/cm²sec) when K_o is 0.6 mM. The passive K loss measured in the presence of strophanthidin continues to decrease when K_o is increased from zero to values at or above the normal level (K_o=3 mM). This suggests that small changes in K_o alters the cellular K content by altering the passive K efflux and not by changing the rate of active K uptake. The inotropic action of strophanthidin, rapid beating and low K_o is compared to the simultaneous loss of cellular K. A 4 fold increase in the twitch force is accompanied by a 3-10 mM decrease in the intracellular K concentration. During and following repeated treatments with strophanthidin a one to one relationship is found to exist between the inotropic response and the net loss of cellular K. Strophanthidin gives rise to no additional inotropic response when active K transport is already blocked by the absence of K. The steady state tension-voltage relation is moved toward more negative membrane potentials when the cellular K content is decreased. These findings support a direct relationship between the inotropic action of strophanthidin and its inhibitory affect on active K transport. (HL 24667)

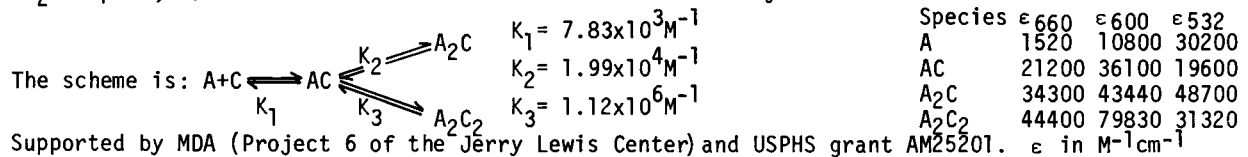
M-AM-D3 CAFFEINE CONTRACTURES IN FATIGUED TWITCH MUSCLE FIBERS. Garcia, Maria del Carmen* and Gonzalez-Serratos, H., Dept. of Biophysics, University of Maryland, Baltimore, Maryland.

We have reported previously that during fatigue, a) the T.C. Ca content is above normal, (Proc. Nat. Acad. of Sci.(US) 75, 1329, 1978), b) the duration of the active state increases (Proc. Int. Union Physiol. Sci. XIX, 440, 1980) and, c) that some myofibrils or groups of them, were either less activated or not activated at all (Biophys. J. 33, 224a, 1981). These led us to suppose that caffeine applied after the development of fatigue should release the TC Ca from the SR associated with all the myofibrils and add it to the one already present in the myoplasm, responsible to the increase of the active state, should produce contractures larger than the control ones.

We have investigated this possibility in isolated twitch muscle fibers by giving them repetitive (300 msec stimulation period repeated every 3 sec) tetanic stimulation (40 Hz) until fatigue developed. Immediately after the last stimulation the cell was exposed to caffeine. The corresponding contracture was compared to a control one done previously in the same fiber. Different caffeine concentrations were used (1.4-5 mM). Since caffeine at high concentrations produces irreversible damage, the degree of reversibility achieved after different concentration of caffeine was determined first. Within the range in which caffeine exposure is reversible the contractures after fatigue were always around 40% larger than the control contractures. When, for example, 1.4 mM control caffeine exposure produced no contracture, after fatigue the same concentration is capable of producing a contracture. Tension development was of approximately 40% of an 80 Hz control tetanus. Another feature is that within these concentrations the relaxation of caffeine contracture is 2 - 10 times slower than the control one. In conclusion a) this confirms the above proposition, b) that metabolic exhaustion during fatigue plays a minor role, and c) that Ca²⁺ reuptake by the S.R. is slowed down during fatigue. (Supported by NIH: NS 13420-05 and MDA and CONACYT for GMC* on leave of absence from Centr. Invest., Mexico, D.F.).

M-AM-D4 MULTIPLE COMPLEX FORMATION BETWEEN ARSENAZO III AND CALCIUM. P. Palade & J. Vergara, Dept. of Physiology, School of Medicine, UCLA, Los Angeles, CA 90024.

Titration of arsenazo III(A) with calcium (C) have been performed in 100 mM KCl, 20 mM KMOPS, pH 6.88, with pH held constant and magnesium absent. Absorbance changes were recorded at 660, 600, and 532 nm using cuvettes of path length 0.01-10.0 cm over a 10,000-fold range of dye concentration, free calcium being measured with a calcium electrode in some instances. At high dye concentrations (5.75 mM) a complex is formed which results in a larger ΔA_{660} than ΔA_{600} . Computer analysis indicates that one complex alone cannot satisfactorily explain the data, but suggests that the complex most often encountered is of the form A_2C_2 . However, the fittings are improved by allowing for AC formation at very low [dye] and significantly improved by allowing for A_2C formation at high [dye]. Extinction coefficients determined from the fittings suggest that formation of A_2C from 2A would be accompanied by a $\Delta A_{660} > \Delta A_{600}$, as seen in calcium transients from muscle fibers injected with arsenazo III. Final fittings of spectrophotometric data accurately predict the free calcium ion concentrations measured experimentally, in a manner that no other scheme, even those including an A_2C complex, can match. Kinetic variations of this scheme yield identical fits.



M-AM-D5 THE TIME COURSE OF FREE MYOPLASMIC CALCIUM IN SKELETAL FIBERS AS MONITORED AND MODIFIED BY THE DYE ANTIPYRYLAZO III. E. Ríos and M.F. Schneider, Dept. of Physiology, Rochester, NY 14642.

The change ΔA in light absorbance associated with fiber depolarization was monitored in voltage-clamped cut frog skeletal muscle fibers containing the dye antipyrilazo III. The transient change $\Delta[Ca](t)$ in myoplasmic $[Ca^{2+}]$ at time t was calculated from $\Delta A(t)$ using results of cuvette calibrations (E. Ríos and M.F. Schneider, *Biophys. J.* **36**, 1981) and the value of [dye] determined from the fiber's resting absorbance. Since the Ca:dye reaction is very fast and the observed $[Ca^{2+}]$ are essentially in the linear (low saturation) range of the reaction, the dye acts to expand the effective myoplasmic volume for Ca. Accordingly, $\Delta[Ca]$ for a given pulse decreases with increasing [dye]. The cuvette calibrations allow calculation of the effective extra volume ("volume expansion") contributed by the presence of the dye. Due to the 1:2 Ca:Dye stoichiometry (ref. above), the "volume expansion" increases approximately as the second power of [dye], e.g. 0.1 and 1.0 mM dye contribute volume expansions of approximately 0.18 and 13 times the physical myoplasmic volume. As expected, $\Delta[Ca](t)$ at a given early time t during a pulse but at different [dye] was seen to be inversely proportional to the "volume expansion". From the straight line fit to the plot of $1/\Delta[Ca](t)$ vs. "volume expansion", an effective intrinsic fiber volume could be derived.

The time course of the $\Delta[Ca]$ records was also altered by increased [dye]. During the pulse the change was consistent with a three compartmental model in which the only modification due to increasing [dye] was a volume expansion of the myoplasmic compartment. After a pulse the decay of $\Delta[Ca]$ was slowed with increasing [dye], also as expected for an increase in effective myoplasmic volume. Supported by NIH (R01-NS13842) and MDA. We thank Dr. W. Melzer for his participation.

M-AM-D6 CORRELATION OF MOVEMENT WITH CALCIUM SIGNALS IN MUSCLE USING CALCIUM-SENSITIVE DYES. M. Delay, B. Ribalet* and J. Vergara, Dept. of Physiology, UCLA, Los Angeles, CA 90024.

The calcium-binding metallochromic dyes antipyrilazo III (Ap) and arsenazo III (Ar) can report fast changes in calcium concentration in contracting muscle. The dye signals may also include wavelength-dependent contributions due to motion and to interaction of dye molecules with other cell constituents. The simultaneous measurement of absorbances at several wavelengths in dye-stained fibers may therefore allow the systematic extraction of the calcium level. Light collected from a muscle fiber using a 40x long working distance objective within a bright field microscope was passed into a grating spectrometer based on a Czerny-Turner design. The outgoing light, dispersed in wavelength, was focussed on a number of individual low-noise photodiodes, each of which could be moved to intercept light at a wavelength of interest. Optical aberrations were small, the dispersion was 7 nm/mm and photodiode acceptance was 10 nm. Single skeletal muscle fibers were voltage clamped in a vaseline gap chamber, and absorbance signals with Ar (injected into the fiber under pressure) or with Ap (diffused in through the cut ends) were recorded at several wavelengths. Motion-induced changes in light scattering, measured before dye introduction, were found independent of wavelength when scaled by the specific resting light intensities. The presence of Ap does not alter scaling of the motion signal, which can then be subtracted from the Ap response, leaving only the calcium release signal. However, 500 μM Ar significantly delayed the motion signal and altered the motion contribution at other wavelengths, consistent with dye binding to moving cell constituents. Supported by USPHS (AM 25201 and fellowship to M.D.), MDA (Project 6 of the JLNRC), AHA(GLAA) fellowship to B.R.

M-AM-D7 CALCIUM DEPENDENT ELECTRICAL ACTIVITY IN FAST AND SLOW TWITCH FIBERS OF RAT SKELETAL MUSCLE. D.J. Chiarandini and E. Stefani, Departments of Ophthalmology and Physiology and Biophysics, New York University Medical Center, New York, N.Y. 10016 and Department of Physiology, I.P.N., Mexico DF 14, Mexico.

Extensor digitorum longus (EDL) and soleus muscles were exposed to a saline containing (mM): TEA methanesulphonate (MeSO_3), 136; CaMeSO_3 , 10; KMeSO_3 , 5; MgSO_4 , 1.2; and 3,4-diaminopyridine, 5; (pH 7.3) to eliminate g_{Na} and g_{Cl} and block voltage dependent g_{K} 's. Muscle fibers were current clamped with the standard 2 microelectrode technique, using 1-2 sec. pulses. Membrane potential was held at -80 mV. In EDL muscle depolarizing pulses of increasing amplitude elicited a response that had a threshold of ca. -20 mV and reached a peak amplitude of 50-60 mV in 150-200 msec. The response was essentially sustained during the duration of the pulse. It was blocked by 3-6 μM nifedipine, 1 mM Cd, 5 mM Co or by replacement of Ca by Mg. In contrast, in soleus muscle fibers the response was absent, probably because of a remaining, shunting g_{K} . To reduce this g_{K} , muscles were incubated (ca. 18 hrs, 4°C) in (mM): CsCl, 70.5; TEACl, 70.5; CaCl_2 , 2; and MgSO_4 , 1.2; (pH 7.1). With this treatment about 80% of the internal K was lost. Thereafter, muscles were tested in: (mM): TEAMeSO_3 , 141; CaMeSO_3 , 10; and MgSO_4 , 1.2. The muscles displayed Ca responses with rising phases similar to those of EDL. However, the responses were not sustained and exhibited an undershoot which disappeared when Ca was replaced by Ba, suggesting that it was due to a Ca-activated K conductance. A g_{Ca} of about 1 mS/cm² was calculated for both muscles. Supported by NSF grant INT 7920212 and CONACyT PCCBNAL 790022 and PCAIEUA 790057.

M-AM-D8 MEASUREMENT OF MEMBRANE CHARGE MOVEMENT AND INTRACELLULAR Ca^{2+} RELEASE IN FROG SKELETAL MUSCLE FIBERS. R.F. Rakowski and P.M. Best, Departments of Physiology and Biophysics, Washington University School of Medicine, St. Louis, MO 63110, and University of Illinois, Urbana, IL 63801.

Membrane charge movement and the release of intracellular Ca^{2+} have been measured in cutaneous pectoris muscle fibers of the frog, Rana temporaria. Membrane charge was measured using the three microelectrode voltage clamp technique as described by Chandler, et al. (J. Physiol. 254: 245, 1976) and by Adrian & Rakowski (J. Physiol. 278: 533, 1978). The experimental solution was identical to that described by Rakowski (J. Physiol. 317: 129, 1981) except that 350 mM sucrose was used. The Ca^{2+} indicator dye arsenazo III was iontophoretically injected into the muscle fibers. Light from a 100W tungsten-halogen lamp was focused to a 50 μm diameter spot adjacent to the point of voltage control. The absorbance change produced by Ca^{2+} release was measured using a three-beam microscope photometer at 572, 632 and 653 nm. Suprathreshold depolarizations produced no optical response at the isosbestic point (572 nm). The signals obtained at 653 and 632 nm were identical in time course when scaled to the same peak magnitude. The absorbance increase at 653 nm had a single exponential time course after an initial delay. At high dye concentrations (>1mM) the dye acts as an intracellular Ca^{2+} sink so that the optical signal measures the time course of Ca^{2+} release rather than the change in free $[\text{Ca}^{2+}]$. The initial rate of Ca^{2+} release is a linear function of membrane potential for suprathreshold voltages. The delay and initial rate of Ca^{2+} release are not consistent with a simple mechanical model in which membrane charge movement is directly linked to Ca^{2+} release. Additional intervening steps are required. Supported by NIH grant NS-14856 and by the Muscular Dystrophy Association.

M-AM-D9 MAMMALIAN SKINNED MUSCLE FIBERS: EVIDENCE OF AN OUABAIN-SENSITIVE COMPONENT OF Cl^- -STIMULATED Ca^{2+} RELEASE. Sue K. Donaldson, Department of Physiology and Department of Medical Nursing, Rush University, Chicago, IL 60612.

Abrupt substitution of Cl^- , a membrane permeant anion, for an impermeant anion, such as propionate, in the bathing solutions stimulates Ca^{2+} release in skinned (sarcolemma removed) skeletal fibers. This Cl^- substitution might "depolarize" any sealed off membrane system within the skinned fiber, such as transverse tubules (TT's) or sarcoplasmic reticulum (SR). In order to evaluate the possible stimulation of sealed off, polarized TT's in the Cl^- -stimulated Ca^{2+} release, we studied halves of single skinned rabbit skeletal fibers (soleus, adductor magnus), stimulating the fibers by substituting Na^+ and Cl^- for K^+ and propionate ($\text{K}^+ \times \text{Cl}^- = \text{constant}$) and recording the Ca^{2+} -activated isometric tension transient. Each fiber was cut transversely and one half was skinned in a low Ca^{2+} relaxing solution while the other half was soaked for 2-3 hours at 0°C in the same solution containing $50 \times 10^{-6}\text{M}$ ouabain prior to skinning. The halves of each fiber were studied using the same force transducer and bathing solutions. The fiber halves not exposed to ouabain prior to skinning released Ca^{2+} in response to both Cl^- and caffeine stimulation. The ouabain pre-treated halves always responded like the untreated ones to caffeine, demonstrating normal SR, but not to Cl^- . In some fibers the entire Cl^- response was eliminated by the ouabain pre-treatment. This suggests the possibility that the Cl^- stimulus was acting on sealed off polarized TT's within the mammalian skinned fibers. Supported by grants from Muscular Dystrophy Association of America and NIH (HL 23128).

M-AM-D10 OPTICAL RECORDINGS OF SURFACE AND T-SYSTEM TRANSMEMBRANE POTENTIAL CHANGES IN SKELETAL MUSCLE. J.A. Heiny and J. Vergara, Dept. of Physiology, UCLA School of Medicine, Los Angeles, CA.

Absorbance signals were recorded from voltage-clamped cut single muscle fibers stained with the non-penetrating potentiometric dye NK2367. The fibers were mounted in a three vaseline gap chamber and illuminated in the A-pool with either unpolarized or linearly polarized light. The absorbance signal recorded with unpolarized illumination has both fast and slow signal components which can be distinguished on the basis of wavelength. At 720nm, the signal is symmetric in response to hyperpolarizing and depolarizing steps. It has predominantly a fast component which follows the speed of the potential step imposed across the surface membrane and is linearly related to potential over at least a +100mV range. At 670nm, the signal is slower and shows a large asymmetry for the same potential steps. In the depolarizing direction it has a sodium-dependent peak; in the hyperpolarizing direction it rises monotonically to a steady-state level within 10ms at 10°C. These characteristics of the 670nm signal are similar to those reported for the dye WW781 (Vergara & Bezanilla, 1981), suggesting that this signal arises from the t-system membranes in which the potential is not well controlled by the voltage clamp. In records from glycerol treated fibers, the amplitude of the 670nm signal is greatly reduced but that of the 720nm signal is essentially unchanged. The absorbance signals recorded with dye NK2367 using linearly polarized light show a similar wavelength dependent separation of signal components at 670 and 720nm, but the relative contribution of fast and slow components to the total optical change is dependent on the plane of polarization; a better separation of these components is obtained using light polarized parallel to the fiber axis. (Supported by USPHS grant AM 25201, MDA grant 6-JLNRC, and an MDA postdoctoral fellowship to J. Heiny.)

M-AM-D11 KINETICS OF VOLTAGE-DEPENDENT CHARGE MOVEMENT IN MAMMALIAN SKELETAL MUSCLE. Bruce Simon and Kurt G. Beam, Dept. of Physiology and Biophysics, University of Iowa, Iowa City, IA 52242

Charge movements were studied in rat skeletal muscle at 7 to 25°C using the three microelectrode voltage clamp technique. Sucrose (400mM) was used to block contraction; TTX and TEA were used to minimize ionic currents; Ca was raised to 10 mM to improve electrode sealing. The control pulses were from -130 to -90 mV. The test pulses (31 msec duration) depolarized the cell from -90 mV to potentials ranging from -60 to +50 mV. Q_{off} was equal to Q_{on} for depolarizations ≤ 10 mV but was larger than Q_{on} for $V \geq 10$ mV. This difference was reduced by the addition of 0.5 mM Cd. Q_{on} vs. V could be fit by $Q = Q_{max}/(1 + \exp(-(V - \bar{V})/k))$ with $\bar{V} = -30$ mV, $k = 12$ mV and $Q_{max} = 25-30$ nC/ μ F. The kinetics of Q_{on} movement are well described by a model developed for frog muscle by Horowicz and Schnegler (J. Physiol. 314:595-633) but the Q_{off} movements are not. According to the model $Q = K(u + Ru^3)$ where R is a constant, K is determined for each fiber from Q_{max} and u is a first-order voltage-dependent parameter derived from the steady-state Q vs. V curve. By varying the single parameter τ_u it was possible to achieve a good fit of Q_{on} movement for all test pulses. Q_{off} could be fit by a single exponential whose time constant (τ_{off}) was independent of the test voltages. In a typical fiber at 15°C, τ_u was 1.5, 1.9, 2.4, 3.8 and 2.7 msec at 30, 10, -10, -30, and -50 mV respectively, and τ_{off} (at -90 mV) was 3.2 msec. Using an average Q_{10} of 1.54 determined from measurements at 7, 15 and 25°C, the magnitude and voltage dependence of τ_u in rat are consistent with those in frog at 1-4°C. The temperature-dependence of τ_{off} was similar to that of τ_u . Supported by research grants from MDA and NIH (NS 14901).

M-AM-D12 ACTIVATION AND INACTIVATION PROPERTIES OF TWO CHARGE SPECIES IN FROG SKELETAL MUSCLE. Chiu Shuen Hui, Dept. Biol. Sci., Purdue Univ., West Lafayette, IN 47907, U.S.A.

Charge movements in sartorius muscle fibers of *Rana temporaria* were studied using the three-microelectrode voltage clamp technique. In a moderately hypertonic solution containing 350 mM sucrose, Q_{on} shows two components, Q_B and Q_Y . Based on the fact that (i) the two components have different kinetics (ii) Q_Y can be suppressed by tetracaine, dantrolene sodium and higher hypertonicity (467 mM sucrose), it is assumed that Q_B and Q_Y are two distinct species of charge arising from different origins. This assumption is further supported by different properties of the two species with regard to voltage-dependence of activation and inactivation.

Q_{on} was dissected mathematically by assuming that Q_B decays with a single exponential and Q_Y is roughly bell-shaped. The activation of Q_B and Q_Y can be individually fitted by a two-state model: $Q(V) = Q_{max}\{1 + \exp(-(V - \bar{V})/k)\}^{-1}$. The average values of k and Q_{max} are: for Q_B , 8.2 mV and 19.2 nC/ μ F; for Q_Y , 3.6 mV and 5.1 nC/ μ F (6 experiments). The steep k -factor of Q_Y correlates well with that of the rise in myoplasmic calcium concentration as monitored by arsenazo III (Baylor, Chandler and Marshall, J. Physiol. 287: 23P, 1979). Steady-state inactivation of Q_B and Q_Y were studied by changing the holding potential to various levels. After equilibration, charge movements were elicited by a constant test pulse. The inactivation curve of Q_Y drops more steeply with increasing voltage than that of Q_B . Each inactivation curve of Q_B and Q_Y forms a mirror image with the respective activation curve. The pair of curves for Q_Y correlates well with the pair for tension. It is speculated that Q_Y is more closely associated with calcium release and tension generation than Q_B . (Supported by grants: NIH15375, AHA 79634 and MDA 31557).

M-AM-E1 A NEW FLUORESCENT ASSAY MONITORS VESICLE FUSION AND LYSIS. D.A. Kendall and R.C. MacDonald, Northwestern University, Evanston, Illinois 60201 U.S.A.

A new fluorescent assay based on the compound, 2',7'[(bis[carboxymethyl]-amino)-methyl]-fluorescein (calcien), has been developed to investigate vesicle fusion and lysis. This assay involves encapsulating the nonfluorescent Co^{2+} complex of calcien in one set of vesicles and EDTA in a second set. If fusion occurs, EDTA chelates Co^{2+} , releasing calcien which may be assayed by means of its intense fluorescence. Leakage of calcien and the calcien/ Co^{2+} complex can be directly quantitated by titrating the external medium with Co^{2+} and EDTA respectively. This permits the concurrent analysis of vesicle fusion and lysis. In addition, calcien is stable and highly fluorescent upon excitation with visible light. Quantitative analysis can therefore be verified with fluorescence microscopy. The assay has been used to study the consequences of calcium ion interaction with small, phosphatidylserine vesicles. In this system, we observe immediate and extensive leakage of the encapsulated contents and no vesicle fusion is detected from the onset of Ca^{2+} addition. These results and other applications of the calcien assay will be presented. Supported by NIH grant #GM 28404.

M-AM-E2 PHOSPHOLIPID VESICLE FUSION MONITORED BY RAPID-FREEZING AND BY MIXING OF AQUEOUS CONTENTS N. Düzgüneş, E. Bearer and D. Papahadjopoulos. Cancer Research Institute and Department of Pathology University of California, San Francisco, California 94142

The morphology of phosphatidylserine/phosphatidylethanolamine or cardiolipin/phosphatidylcholine vesicles undergoing Ca^{++} -induced fusion was investigated by rapid-freezing freeze-fracture electron microscopy. Large unilamellar vesicles (100-200 nm diameter) were stimulated for 1-2 sec and frozen on a copper block cooled by liquid helium. Freeze-fracture replicas revealed vesicles larger than 200 nm as well as vesicles in the process of membrane fusion. Lipidic particles or the hexagonal H_{II} phase, which have been proposed to be intermediate structures in membrane fusion, were not observed at the sites of fusion. After long-term incubation of cardiolipin/phosphatidylcholine vesicles with Ca^{++} (2h, 25 C) lipidic particles were evident in less than 10% of the vesicles, and the addition of glycerol produced more vesicles displaying these particles. We suggest, therefore, that lipidic particles are structures obtained at equilibrium and not necessary intermediates for fusion. Fusion of these vesicles on a time scale of seconds was confirmed by a fluorescence assay for the intermixing of internal aqueous contents (Wilschut et al., Biochemistry 19:6011, 1980). This assay also revealed that Mg^{++} triggered the fusion of phosphatidylserine/phosphatidylethanolamine vesicles, although it does not favor the formation of the H_{II} phase in these liposomes. We suggest that divalent cations cause fusion by forming dehydrated complexes with phospholipids and local packing defects within the bilayer which act as nucleation points for membrane intermixing.

M-AM-E3 MASS ACTION KINETICS OF PHOSPHOLIPID VESICLE FUSION AND AGGREGATION. J. Bentz^a, S. Nir^a and J. Wilschut^c. ^aRoswell Park Memorial Institute, Buffalo, N.Y., 14263. ^bHebrew University, Rehovot, Israel. ^cUniversity of Groningen, The Netherlands.

The kinetics of vesicle fusion has been examined both theoretically and experimentally with Ca^{2+} induced fusion of both large and small PS vesicles. Using the Tb/DPA assay, (J. Wilschut and D. Papahadjopoulos, Nature 281, 690 (1979), the kinetics of vesicle aggregation (J. Bentz and S. Nir, J. Chem. Soc. Faraday Trans. 1 77, 1249 (1981) can be separated from the kinetics of vesicle fusion by varying the initial concentration of vesicles. We are able to measure both the rate constant for vesicle dimerization and the rate constant for vesicle fusion by this analysis. The kinetics of leakage, following the fusion event, is also examined. The theoretical analysis can be easily adapted to other fusion assays and, as such, provides a unique opportunity for determining the effects of other parameters, e.g. temperature and bilayer mixing, on the fusion event, per se. The effect of aggregation reversibility on the fusion kinetics is considered and shown to be negligible. Overall, it is shown that the Ca^{++} induced fusion of PS vesicles can be a very rapid process wherein the vesicles can aggregate and fuse in seconds and the initial leakage associated with the fusion event, per se, is essentially zero for the large vesicles and is less than 7% for the small vesicles. Supported by NIH Grants GM-23850 and CA-16056 and by the Netherlands Organization for the Advancement of Pure Research (Z.W.O.).

M-AM-E4 A MECHANISM OF DIVALENT ION-INDUCED PHOSPHATIDYL SERINE MEMBRANE FUSION. S. Ohki, Dept. of Biophysical Sciences, SUNY at Buffalo, Buffalo, New York 14214.

A mechanism for the divalent cation-induced membrane fusion of phosphatidylserine membranes is proposed. Fusion was followed by the Tb/DPA assay monitoring the fluorescent intensity for mixing of internal aqueous contents of unilamellar lipid vesicles, and the threshold concentrations for various divalent cations to induce membrane fusion were determined from the fluorescence spectrum of the lipid vesicle suspension with respect to various concentrations of divalent ions. Also, the surface tension of monolayers made of the same lipids used in the fusion experiments was measured with respect to the variation of divalent cation concentrations. The surface tension increase in the monolayer induced by changing divalent ion concentrations from zero to a concentration which corresponded to its threshold concentration to induce vesicle membrane fusion was the same (~ 8 dynes/cm) for all divalent ions used. From these experimental data and the ion binding theory to the membrane, it is deduced that the main cause of divalent cation-induced membrane fusion of acidic phospholipid membranes is due to the degree of increased hydrophobicity of the membrane surface, which results from the binding of cations to acidic phospholipid membrane surfaces.

M-AM-E5 THE NATURE OF THE REGION OF CONTACT BETWEEN FUSING MEMBRANES. F.S. Cohen, and M.H. Akabas. Departments of Physiology, Rush Medical College, Chicago, Illinois 60612 and Albert Einstein College of Medicine, Bronx, NY 10461, Intr. by C.L. Schauf.

Over the past few years we have studied the fusion of phospholipid vesicles to planar bilayer membranes. To determine the properties of the region of contact between the planar membrane and vesicles we have prepared vesicles from lipids with well-known phase transition properties. With vesicles prepared from a single lipid, the rate of fusion is small for temperatures below a transition temperature (T_f) which is close to the phase transition temperature (T_c) of the lipid, and is high for temperatures above the T_f . The rate of fusion increases in a step function manner at T_f . The fusion transition temperatures are 23°C for DMPC and DMPG, 37°C for DPPC and DPPG, and 46°C for DSPC and DSPG. When mixtures of miscible lipids are used, the transition temperature for fusion is the mole fraction ratio of the T_f 's of the individual lipids. It has been shown by others that for miscible lipids, the phase transition temperature of the vesicle is the mole fraction ratio of the individual T_c 's. For mixtures of immiscible neutral lipids, the rate of fusion increases in a step function manner as each component becomes fluid. As fusion occurs with only a fraction of the vesicle in a fluid state, we conclude that at least a portion of the region of contact between vesicle and planar membrane must be fluid for fusion to proceed. When immiscible mixtures of neutral (PC) and charged (PG) lipids are used, fusion proceeds only if the charged lipid is fluid, irrespective of the state of the neutral lipid. This implies that the region of contact is rich in negative lipids. (Supported by Grants USPHS GM27367, 5T32GM7288 and NS14246.)

M-AM-E6 INTERACTION OF MONOVALENT AND DIVALENT CATIONS WITH PHOSPHATIDYL SERINE BILAYER MEMBRANES. H. Hauser and G.G. Shipley, Biophysics Institute, Boston Univ. Schl. of Med., Boston, Mass.; Labor. fur Biochemie, ETH-Zurich, Switzerland.

Utilizing differential scanning calorimetry and x-ray diffraction, 1,2 dimyristoyl-L-glycero-3-phospho-L-serine (DMPS) was shown to form hydrated bilayer membrane structures exhibiting a gel \rightarrow liquid crystalline transition at 39°C ($\Delta H = 7.2$ Kcal/mol). Addition of up to molar concentrations of the alkali halides NaCl, KCl, RbCl and CsCl, produced relatively minor changes in DMPS bilayer structure or stability. For example, in the presence of 0.5 M NaCl the transition temperature increases slightly ($T_c = 42^\circ\text{C}$) and the transition enthalpy ($\Delta H = 7.0$ Kcal/mol) is essentially unchanged. X-ray diffraction of 50 wt. % dispersions of NH_4^+ -DMPS gave a lamellar bilayer repeat distance, $d = 107$ Å, and a sharp reflection at $1/4.2$ (\AA^{-1}) characteristic of the "hexagonal gel" hydrocarbon chain packing. At 0.5 M NaCl, Na^+ shield the negatively charged bilayer surface and the lamellar periodicity reduced from 107 to 62 Å. No change occurs to the $1/4.2$ (\AA^{-1}) reflection showing that no significant change occurs in the hydrocarbon chain packing as NaCl is added. In contrast addition of LiCl results in "crystallization" of the DMPS bilayer membrane structure as indicated by additional diffraction lines in the wide angle region. At 0.5 M LiCl, the crystalline DMPS exhibits a bilayer gel \rightarrow liquid crystal transition at 89°C accompanied by a high enthalpy change, $\Delta H = 16.0$ Kcal/mole. Thus, Li^+ induces an isothermal crystallization of DMPS bilayers, the hydrocarbon chains adopting a more ordered packing mode than the "hexagonal" arrangement of the gel state. The structural changes produced by Li^+ will be compared with similar changes produced by Mg^{2+} , Ca^{2+} and other divalent metal ions.

M-AM-E7 LIGHT SCATTERING MEASUREMENTS OF THE TEMPERATURE DEPENDENCE OF PHOSPHOLIPID VESICLES
Eddie L. Chang, James P. Sheridan, and Bruce P. Gaber, Naval Research Laboratory,
Washington, D. C.

The temperature dependence of a highly uniform suspension of small unilamellar DPPC vesicles was measured by photon correlation spectroscopy (PCS), 90° light-scattering, and Raman Spectroscopy. We found the hydrodynamic diameters of the vesicles to be sensitive to the fluidity of the phospho-lipids with the diameter decreasing by $6.7\% \pm 0.1\%$ on the cooling curve and increasing by $7.6\% \pm 0.7\%$ on the heating curve. The initial polydispersity of the vesicle suspension was comparable to a standard suspension of polystyrene spheres and the polydispersity remained two to four times lower than all previously reported measurements by PCS. The vesicle diameter was $270\text{\AA} \pm 4\text{\AA}$ above and $252\text{\AA} \pm 4\text{\AA}$ below the transition zone respectively.

Fusion of the vesicles was allowed to proceed at 18°C for 96 hours in order to achieve a size and polydispersity range close to other reported works. Upon heating slowly, the vesicles aggregated on a massive scale followed by precipitation. This process was shown to be a reversible step when the sample was recooled and pre-heating values for the apparent diameter and scattered light intensity were obtained.

The Raman and PCS data showed that the vesicle lipids do not fully reach their gel state conformations when below the transition region. The implications for current models of vesicles are discussed in light of these results.

M-AM-E8 STIMULATION OF FLUORESCENCE IN A SMALL CONTACT REGION BETWEEN RAT BASOPHIL LEUKEMIA CELLS AND PLANAR MEMBRANE TARGETS BY COHERENT EVANESCENT RADIATION. Robert M. Weis*, Krishna Balakrishnan*, Barton A. Smith**, and Harden M. McConnell*; *Department of Chemistry, Stanford University, Stanford, Ca. 94305, and **IBM Research Laboratory, Department K42, San Jose, Ca. 95193.

We have included dinitrophenyl (Dnp) lipid hapten in dipalmitoylphosphatidylcholine monolayers supported on alkylated quartz microscope slides to serve as specific target membranes for rat basophil leukemia (RBL) cells that have been incubated with anti-Dnp-fluorescein-5-isothiocyanate conjugated IgE (α -Dnp-FITC-IgE). These RBL cells bind strongly to the hapten-containing membranes in the presence of Ca^{++} and/or Mg^{++} , but only weakly in the absence of hapten. Coherent evanescent radiation produced by a focused laser beam (488 nm) totally internally reflecting at the quartz-cell buffer interface excites fluorescence of the α -Dnp-FITC-IgE only within ~ 100 nm of the membrane-membrane interface. Fluorescent molecules far from the monolayer membrane are not observed due to the rapid decay of the evanescent wave intensity normal to the interface (decay distance = 120 nm). The pattern of fluorescence excited in the manner described above is highly punctate, unlike conventional epifluorescence observation that shows essentially uniform fluorescence of the FITC-IgE molecules. An interference pattern produced by two coherent intersecting beams insures that all the observed fluorescence is due to evanescent exciting radiation, and not scattered exciting radiation. The interference pattern can also be used for photobleaching, to measure the diffusion of α -Dnp-FITC-IgE bound to the monolayer membrane in the absence of RBL cells. Our experimental results will be discussed in terms of current theories of the molecular basis of cell triggering by Fc receptor clusters. Support: NIH 5 R01 AI13587.

M-AM-E9 INTERACTIONS BETWEEN CLATHRIN-COATED VESICLES AND LYSOSOMES. L.D. Altstiel, K. Giedd and D. Branton. The Biological Laboratories, Cellular and Developmental Biology, Harvard University, Cambridge, Massachusetts 02138.

Factors that influence fusion between clathrin-coated vesicles (CV) and lysosomes *in vitro* were assayed by fluorescence. CV were isolated from bovine brain and purified to homogeneity by equilibrium density and sedimentation velocity centrifugation. Clathrin-depleted vesicles (DV) were prepared by elution of clathrin from CV in 1.0 mM tris, pH 8.2 buffer. Both CV and DV were loaded with the non-fluorescent dye 6-carboxyfluorescein (diAc-CF) and washed to remove label not incorporated in the interior of the vesicles. Upon fusion of vesicles with purified lysosomes isolated from bovine kidney, the non-fluorescent diAc-CF mixes with lysosomal esterases which catalyze hydrolysis of acetate groups on the label and convert it to the fluorescent 6-carboxyfluorescein. The rate of fusion was determined by measuring the increase either in absorbance at the excitation wavelength at 490 nm or in fluorescence at 520 nm. CV showed a low rate of fusion with a half life of approximately 250 sec, whereas DV showed a more rapid rate of fusion with half lives ranging from 25-115 sec. depending upon incubation conditions. These results suggest that clathrin may inhibit fusion of coated vesicles with lysosomes. In control experiments, when either CV or DV were incubated with lysosomes disrupted by sonication, the rate of fluorescence increase was negligible. The control experiments suggest that the observed increase in fluorescence is due neither to leakage of label out of the vesicles nor to leakage of lysosomal contents into the vesicle.

M-AM-E10 CLATHRIN COAT INTERACTIONS WITH LIPID VESICLES Jane Robinson*, Yves Engelborghs* & Evelyn Ralston, *Labo. Chem. Biol. Dynamics, Katholieke Universiteit te Leuven, B-3030 Heverlee & Chimie Biologique, Université Libre de Bruxelles, B-1640 Rhode-St-Genèse, Belgium.

The dynamic role of clathrin-coated pits and vesicles may be regulated by interaction between cellular membranes and coat proteins, the major constituent of which is clathrin. We have studied the interaction of isolated clathrin coats with sonicated phospholipid vesicles of dipalmitoyl-phosphatidylcholine. Coated vesicles were prepared from pig brain by a modification of the method of Pearse, and coats devoid of membrane were isolated by treatment with 2 M urea. Clathrin coats, added intact or dissociated by urea, induced leakage from carboxyfluorescein-loaded vesicles, at as little as 1 to 10 protein monomers per vesicle. The leakage was faster at pH 6.5 than at pH 7.4, independent of the buffer salt, and was accelerated by heating through the lipid phase transition. Smaller vesicles interacted more readily than did large vesicles. Vesicle size was monitored by dynamic light scattering. Formation of a stable protein-phospholipid complex was shown by KBr density gradient centrifugation. Incubation of [¹²⁵I]-labelled protein with [¹⁴C]-labelled vesicles at pH 6.5, but not at pH 7.4, resulted in the appearance of a new doubly-labelled band. Our results show direct interaction between clathrin coat proteins and phospholipid membranes. The pH-dependence of the interaction may reflect changes in the protein structure, known to occur in this pH range. Stability of the complex in high KBr salt concentration shows that electrostatic interactions are not required to maintain the association. Vesicle size- and pH-dependence suggest possible means of regulating the interaction between clathrin coats and cellular membranes.

M-AM-E11 INTRODUCTION OF HUMAN HISTOCOMPATIBILITY ANTIGENS INTO MOUSE LYMPHOID CELL MEMBRANES BY CELL-LIPOSOME FUSION. Maria C. Correa-Friere and Victor H. Engelhard, University of Virginia, Charlottesville.

Conditions have been defined for optimal surface binding, by mouse lymphoblastoid cell lines, of liposomes containing purified human histocompatibility antigens. Purified HLA-A,B antigens were reconstituted into phospholipid vesicles by detergent dialysis, and incubated with the acceptor cell lines. After washing, the amount of HLA antigens expressed on the surface was quantitated by a double antibody radioimmunoassay. Uptake and surface expression was shown to be strongly dependent upon vesicle phospholipid composition, vesicle/cell ratio, acceptor cell lines, and stage of cell growth. These studies indicate that, under optimum conditions, using vesicles composed of 50% PE/50% PS, it is possible to introduce about 70ng HLA/10⁶ mouse EL4 cells, which is 70% of the amount expressed on the human lymphoblastoid line JY. The amount of antigen expressed on the surface is stable for several hours, and appears to be incorporated into the cell membrane. These cells are capable of eliciting a specific secondary cytotoxic T lymphocyte response against appropriate human cells, but are incapable of being recognized and killed by cytotoxic effector cells. Possible explanations for this dichotomy will be discussed.

This work was supported by USPHS Grant AI 16808. M.C.-F. is a USPHS Postdoctoral fellow.

M-AM-E12 IRREVERSIBLE COUPLING OF IMMUNOGLOBULIN FRAGMENTS TO LARGE UNILAMELLAR LIPOSOMES: An Improved Method for Liposome Targeting. F. Martin and D. Papahadjopoulos, Cancer Research Inst., UCSF, San Francisco, California 94143.

Rabbit Fab' antibody fragments were covalently coupled to preformed large unilamellar vesicles using a new sulfhydryl-reactive phospholipid derivative N-(4-(p-maleimidophenyl)butyryl)phosphatidyl-ethanolamine (MPB-PE). A highly efficient reaction between the sulfhydryl group on each Fab' fragment and the maleimide moiety of MPB-PE molecules incorporated at a low concentration in vesicle bilayers led to the formation of a highly stable Fab'-vesicle linkage. Coupling ratios in excess of 250 ug of Fab' per umol of vesicle phospholipid were reproducibly obtained without vesicle aggregation. Bound Fab' fragments did not elute from vesicles in serum or in the presence of reducing agents (mercaptoethanol or dithiothreitol). Vesicles bearing Fab' fragments raised against specific human erythrocyte surface determinants bound selectively to human erythrocytes under physiological conditions (isotonic medium containing 50% human serum, pH 7.4) with minimal leakage of vesicle contents. Advantages of the present coupling method are discussed in relationship to our efforts to optimize the properties of liposomes as a carrier system.

M-AM-E13 MAPPING THE IONIC DOUBLE LAYER AT THE SURFACE OF MODEL AND BIOLOGICAL MEMBRANES.
L.D. Altstiel* and F.R. Landsberger. The Rockefeller University, New York, New York.

Spin label electron spin resonance (ESR) techniques were used to measure properties associated with the ionic double layer at the surface of model and biological membranes. Phospholipid spin labels containing a nitroxide group, separated from the lipid phosphate ester moiety by spacer groups of differing length, were inserted into sonicated unilamellar liposomes containing either 100% phosphatidyl choline (PC) or 10% phosphatidic acid (PA) and 90% PC. The electric field associated with the double layer at the surface of the charged liposomes is reflected by the isotropic hyperfine coupling constant, A_{iso} , of the spin labels. A_{iso} was measured as a function of distance from the surface of the lipid bilayer. The results indicate that the local electric field varies in a manner predicted by the Chapman-Gouy theory. Nuclear magnetic resonance measurements of the width of the choline methyl proton line in the presence of the probes suggest that the probes are extended normal to the surface of the liposomes.

*Present address, The Biological Laboratories and the Department of Cellular and Developmental Biology, Harvard University, Cambridge, Massachusetts.

M-AM-F1 AN INTERSPERSED REPEATED SEQUENCE OF MOUSE. D. L. Vizard, J. A. Yarsa and A. T. Ansevin. The University of Texas System Cancer Center and Graduate School of Biomedical Sciences, Houston, Texas 77030.

In scanning the mouse genome with numerous restriction enzymes, many distinct length classes (discrete fragments) can be identified as tandemly repeated DNA sequences by virtue of the multimeric length arrays that may be resolved by electrophoresis after restriction fragmentation. However, some fragments are not associated with multimeric arrays, and are therefore identified as interspersed repeated DNA sequences. Studies of others (Cheng and Schildkraut, *NAR* 8,4075 (1980); Manuelidis, *NAR* 8, 3247 (1980); and Krayev et al., *NAR* 8, 1201 (1980)) have identified a few interspersed repeated sequences in the mouse. We have identified a different interspersed repeated sequence (400 bp in length) that can be generated by Hind III fragmentation of the mouse genome. Thermal denaturation and reassociation data suggest extreme sequence heterogeneity within this length class; however, both Hinf I and Hae III sites can be mapped within this sequence. A most interesting feature of this interspersed repeated sequence is that in liver nuclei its internucleosomal regions are relatively resistant to nuclease activity when compared to other repeated sequences, and the adjacent unique sequences. This work was supported by GM-23067 from the National Institutes of Health and BRSG #RR5511-19.

M-AM-F2 THE NON-SENESCENT MITOCHONDRIAL GENOME OF *PODOSPORA ANSERINA*. Richard M. Wright and Donald J. Cummings. University of Colorado Health Sciences Center, Denver, Co.

The ascomycete *Podospora anserina* is characterized by the strain specific timing of cellular death (senescence). Mitochondria from senescent mycelia have been shown to be the genetic elements responsible for the inheritance of the development of senescence. Mitochondrial DNA (mtDNA) derived from senescent mycelia has undergone an excision-amplification process resulting in senescent mtDNA which is composed of circularized repeats of monomeric subunits from the non-senescent mtDNA (Cummings et al., 1979; *Molec. Gen. Genet.*, 171:239; Jamet-Vierny et al., 1980; *Cell* 21:189). Our objective is to study the relationship between senescent specific mtDNA and the development of senescence. For this reason we have begun to characterize the non-senescent mitochondrial genome. In the present study, a mitochondrial DNA clone bank has been developed for the 94 kilobase pair (kbp), circular, non-senescent genome. Restriction maps of mtDNA have been constructed for the enzymes Sal I, XhoI, Bam HI, ECOR I, Bgl II, and HAE III. The ribosomal RNA genes have been localized by Southern and Northern blot analysis. The physical structure and organization of the ribosomal RNA genes has been determined by R-loop analysis. The large rRNA gene is very unusual for a ribosomal RNA gene. The large rRNA is 3.8 kb long, and it is coded by a gene 8.2 kbp long. The gene possesses two intervening sequences of 1.6 and 2.7 kbp yielding three exons of 0.3, 1.3, and 2.1 kbp. The small rRNA is 2.0 kb long, the gene possesses no intervening sequences and lies approximately 8 kbp away from the large. These data combined with similar data for the other identifiable genes on *Podospora* mtDNA will provide the basis for a molecular biological description of the role of mtDNA in the development of senescence.

M-AM-F3 PATTERN RECOGNITION IN THE REGULATION OF GENE EXPRESSION. D.G. George and M.O. Dayhoff, National Biomedical Research Fdn., Georgetown University Medical Center, Washington, D.C. 20007

The advent of a rapid nucleic acid sequencing technology has allowed gene control elements to be studied in detail. The experimental data indicate the existence of specific sequence patterns in the DNA that serve as signals for the transcriptional and translational regulation of gene expression in prokaryotes. Recently, there has been considerable interest in the study of similar patterns in eukaryotes. From a purely statistical point of view, in order to avoid a high frequency of aberrant transcriptional or translational events these control signals must satisfy two criteria: 1) they must faithfully occur in the control regions in question and 2) they must not occur with a high frequency elsewhere in the genome. We maintain a computerized nucleic acid sequence database, which currently contains over 560,000 nucleotides in more than 500 entries. The data are readily accessible through a computer retrieval system. In addition to rapid sequence retrieval the system also allows for the manipulation and comparison of sequence data. Utilizing this data and a computer program developed for pattern recognition and analysis, a tabulation of various signal sequence patterns has been compiled. This tabulation will be presented and the patterns will be analyzed statistically. This work is the result of research aimed at improving the computer retrieval system. Techniques developed in this study will soon be implemented in the retrieval system.

Partially supported by NIH grant GM08710 and NASA contract NASW3317.

M-AM-F4 ENZYMATIC ENHANCEMENT OF ULTRASTRUCTURAL CHROMOSOMAL DAMAGE INDUCED BY RADIATION AND

DRUGS. Arthur Cole, Ruthann Langley and Margaret Hall. The University of Texas System Cancer Center, Houston, Texas 77030.

We have previously reported that mammalian chromosomes appear to contain a side-by-side array of eight circular DNA duplex molecules (Cole et al., *J. Cell Biol* 87:44a(1980)). The DNA strands, condensed as nucleohistone fibrils, loop outward from a chromosome backbone ribbon structure which, in interphase cells, is associated with the nuclear envelope (Cole, *Biophysical J.* 33:197a (1981)). Damage to both the nucleohistone loops and the backbone ribbons, induced by moderate doses of radiation (500 to 1500 rads) or drugs, can be assayed by electron microscopy as ultrastructural aberrations in partly dehistonized chromosomes and nuclei (Cole, *Radiation Res.* 87:492, (1981)). Expression of the damage is greatly amplified by exposure of the chromosomes to exogenous or endogenous proteases and nucleases. Chromosomes from cells irradiated in growth medium and lysed in the presence of nuclease and protease inhibitors show no significant damage unless the lysed sample is subsequently exposed to very weak protease (50 ng/ml proteinase K) or nuclease (1 ng/ml micrococcal nuclease) treatments which have little or no effect on unirradiated chromosomes. Enhancement of the induced damage is also observed when cell lysis is carried out in the presence of nuclease inhibitors but in the absence of protease inhibitors. Thus, endogenous cell protease activity appears to lead to a similar expression of the initial damage. These results support the proposal that biological damage results from cellular enzymatic amplification of local chromosomal lesions (Cole, *Radiation Res.* 83:445 (1980)). The studies will be illustrated by stereo electron microscopic projections. Supported in part by DOE Contract DE-AS05-76-EVO-2832.

M-AM-F5 CONSISTENT KINETIC MODEL FOR SUPEROXIDE DISMUTASE INACTIVATION, A. Petkau, C.A. Chuaqui* and W.S. Chelack*, Medical Biophysics Branch, Whiteshell Nuclear Research Establishment, Atomic Energy of Canada Research Company, Pinawa, Manitoba, Canada R0E 1L0.

Nitrous oxide-saturated, aqueous solutions of dimeric and tetrameric superoxide dismutases were Co^{60} -gamma irradiated to study inactivation of the enzymes by hydroxyl radicals. With both enzymes, the dose response was linearized by plotting the reciprocal of the % Enzyme Activity remaining against the radiation dose, thus indicating a bimolecular reaction for the inactivation process. These results are accounted for by a kinetic model which assumes that hydroxyl radical damage of the enzymes is transferred from one subunit to another. With dimeric Cu,Zn-superoxide dismutase and tetrameric Mn-superoxide dismutase, this transfer process involves monomer and dimer exchange, respectively. The subunit exchange processes, while extending the damage to more than one enzyme molecule, also allow for the formation of inactivated enzyme molecules in which both subunits have lost their activity. This latter feature, together with the faster reaction rate of hydroxyl radicals toward the inactivated subunits, accounts for the sparing effect on enzyme activity, seen at high radiation doses. The biological inactivation of superoxide dismutase in red blood cell membranes (Petkau et al., *BBA* 645 (1981) 71), which follows first order kinetics is also accounted for by this model, assuming a monomeric state for the enzyme.

M-AM-F6 REPAIR OF DNA DAMAGE INDUCED BY X-IRRADIATION AND THE RADIOSENSITIZER MISONIDAZOLE.

Stuart Berger and Branko Palcic. B.C. Cancer Research Centre, Medical Biophysics Unit, Vancouver B.C.

The unwinding method has been shown to be a particularly sensitive and reliable method for assaying DNA strand breaks. The incorporation of an internal control¹ further enhances its sensitivity so that damages from doses of radiation as low as 0.1 Gy can be routinely detected. This method has been used to study the kinetics of repair of x-ray induced lesions in the DNA of Chinese hamster cells (CH2B₂ line) over the dose range of 1 to 5 Gy. At least two distinct repair regions can be resolved: the first with a half-life of 8 minutes and a second with a half-life of 4 hours.

It has been shown that the radiosensitizer misonidazole induces lesions in the cellular DNA even under conditions where no cytotoxicity can be demonstrated. The repair of these lesions will be discussed and the repair kinetics will be compared to the repair kinetics of x-ray damage.

¹Rydberg, B. Detection of induced DNA strand breaks with improved sensitivity in human cells. *Radiat. Res.* 81: 492-495 (1981).

M-AM-F7 WEIGLE-REACTIVATION AND WEIGLE-MUTAGENESIS OF X-RAY-DAMAGED PHAGE LAMBDA IN UV-INDUCED *E. COLI* AB1157. D. J. Fluke and E. C. Pollard, Department of Zoology, Duke University, Durham, NC 27706.

In extension of earlier work (Rad. Res. 74, 576, 1978) we have examined W-reactivation and now W-mutagenesis for X-ray damage in phage lambda in *E. coli* AB1157 cells induced by 265-nm UV exposure. Phage inductates at ca 3×10^{10} pfu/ml were prepared in a casamino acids (2 g/l) + glucose (5 g/l) + minimal salts medium, clarified of cell debris. Cultures of *E. coli* AB1157 for repair induction were grown to ca 3×10^8 cfu/ml in a medium similar except for maltose as carbon source. They were transferred into adsorption buffer (0.01 M $MgSO_4$ in 0.01 M Tris-HCl) for UV irradiation, for attachment of phage by 15' at 37°C, and were appropriately diluted and plated for plaques. Clear-plaque observations were at total-plaque levels around 5×10^4 . X-ray exposures were at ca 9 krad/min, stir-aerated, by 50-kvp X-rays filtered by 50 mg Al/cm². Direct action on the phage was established by irradiation in concentrated nutrient broth (35-40 g/l) as earlier, but indirect action was at 100-fold rather than at 10-fold dilution of the lambda inductate in the adsorption buffer as X-irradiation medium. Plaque-survival D_0 values were about 100 krad (broth-protected) and about 2.5 krad (least-protected). About 6% of direct-action damage to the phage was W-reactivable, as found earlier. W-mutagenesis increases of 3-5X over background were associated with this repair at maximal induction. At the greater degree of indirect action now tested ($D_0 = 2.5$ vs 22 krad earlier) neither W-reactivation or W-mutagenesis was observed. Technical assistance of Mr. S. M. Nolte and Mr. C. E. Bronner is acknowledged. The work is supported by U. S. Department of Energy Contract No. DE-AS05-76EV03631.

M-AM-F8 THE INDUCTION OF λ -PROPHAGE BY X-RAYS AND UV AS MEASURED BY ENDOLYSIN ACTIVITY.

E.C. Pollard and D.J. Fluke, Zoology Department, Duke University, Durham, N.C.

A method for observing the induction of prophage in the *lac*⁻ AB strain of *E. coli* K12 has been worked out. Cells are induced for β -galactosidase by IPTG and are then tested for endolysin activity by adding ONPG to the cells and holding at 34°C for 15 minutes. Yellow color develops only if the cell wall has been lysed by the phage endolysin. Dose-effect relationships for X-ray and UV (254nm) have been observed. X-rays produce a sharp yield of prophage induced at low doses, followed by a marked diminution at high doses. A lower yield, requiring more dose is observed in *recB*⁻ cells. The effect of UV is more sigmoidal: low doses are relatively ineffective. The drop at high doses is less marked and *recB*⁻ cells are not appreciably different. *uvr*⁻ cells are induced at much lower doses than *uvr*⁺ and they show a marked drop at high doses. We suggest that for X-rays the unwinding and degradation of DNA leads to the presence of activating agents that are not repaired. For UV the presence of daughter strand gaps which are repairable leads to a different activating process, taking more dose and different in character.

We acknowledge good technical assistance from Cynthia White. We were aided by the D.O.E. contract number DE AS05 76 EVO 3631.

M-AM-F9 THERMAL STUDIES ON THE PROFLAVINE-NUCLEOSOME COMPLEX, Mei Lu, Kenneth S. Schmitz, and Jennifer Gauntt, Department of Chemistry, University of Missouri-Kansas City, Kansas City, Missouri 64110.

Proflavine was used as a probe to examine the thermal stability of mono- and poly nucleosomes in 30 mM cacodylate buffer (pH 7.3). Optical absorbance methods using a two-state model were employed to construct Scatchard plots, which were then characterized by modification of the Ramanathan-Schmitz model (Biopolymers, 17(1978)2171),

$$r/c_f = (B/\sigma)(r^2/r-\phi)\{(\alpha - r\phi - \phi)/\alpha - r\phi\}^q \quad (\text{cf. text for definitions})$$

The results of these studies tend to suggest that: 1) the initial binding process is limited to a fraction (α/q) of the total number of base pairs; 2) the initial binding process is highly cooperative ($\sigma < 1$); 3) additional proflavine binding to secondary sites results in a conformational change in the nucleosome unit; 4) the external lysine rich histones protect a small portion of the primary binding sites; 5) the enthalpy of association of proflavine at the primary sites is ≈ -8 Kcal/mole proflavine; and 6) (α/q) and σ are relatively insensitive to T over the range $10^\circ\text{C} < T < 40^\circ\text{C}$. These studies, coupled with sedimentation velocity and enzyme digestion experiments suggest the core particle structure is "more fluid" at temperatures above 30°C .

This research was supported by grants from NSF and ACS.

M-AM-F10 LOW DOSE PARAMAGNETIC SIGNALS PRODUCED BY IONIZING RADIATION IN CALCIFIED TISSUES. M.J. McCreery, C.E. Swenberg and J.J. Conklin, Radiation Sciences Department, Armed Forces Radiobiology Research Institute, Bethesda, MD 20814

Ionizing radiation is known to produce several paramagnetic defects in calcified tissues. At least one of these centers is known to be stable for at least 10^4 years and has been quantitatively utilized for the archeological dating of fossil bones. Using the technique of electron paramagnetic resonance (EPR), we have observed these radiation induced defects in a variety of calcified tissues including human and rat teeth and bovine and rat bone. Both stable and unstable signals were recorded with the central line occurring at $g = 2.002$. Measurement of the intensity of these lines from tissues irradiated in air with a 130,000 Ci ^{60}Co gamma source or electrons from a Varian linear accelerator yielded a linear dose-response relationship at doses from 10^2 to 10^6 rads. Signal averaging techniques were necessary for accurate quantitation at exposures less than 500 rads and allowed detection of doses as low as 13 rads. The dose-signal intensity relationship at low doses appeared to be hyperbolic with saturation occurring at about 100 rads. The linear and non-linear behavior of the high and low dose domains, respectively, suggests at least two types of stable paramagnetic centers are generated by ionizing radiation. The molecular nature of these defects are still unclear. The temperature dependence of the stability of these radical defects will also be reported.

M-AM-F11 A NEW DOUBLE-HELICAL MODEL FOR DNA, Robert C. Hopkins, Ph.D., Division of Chemistry, The University of Houston at Clear Lake City, Houston, Texas, 77058. Introduced by: R.J. Shalek

For nearly three decades, the elegant Watson-Crick double-helical model for DNA, with its specific base pairing, has served as the foundation for the enormous advances in molecular biology. However, there is growing evidence that various properties of native DNA are not consistent with the family of models based on the Watson-Crick structure. A new family of double-helical models has been proposed (*Sci.* 211, 289, 1981) which retains the confirmed properties of the traditional model family, yet exhibits features consistent with the known biological characteristics of DNA. Although the new model structures (configuration II) are double-helical, they have deoxyribosephosphate chain directions opposite to those of the Watson-Crick family of models (configuration I).

Models from the configuration II family supercoil easily, exhibit great flexibility, are more compact than configuration I models, accept intercalating drugs readily, have the known binding site of the carcinogen 2-acetylaminofluorene (C8 on guanine) exposed, and can be interconverted between right- and left-handed forms by an axial twisting motion. Other aspects of this new family of models will be described.

M-AM-F12 EFFECTS OF PHOSPHOPEPTIDES ISOLATED FROM CALF THYMUS DNA ON THE PROLIFERATION OF NORMAL AND TUMOR CELLS. R.S. Welsh, W. Dohmen and K. Vyska. Institute for Medicine, Nuclear Research Center Jülich, Fed. Rep. Germany.

The present study analyses the effects of the peptides (PPs) released from purified calf thymus DNA during its cleavage on Walker Carcinoma, Ca. 256 (WC), L1210-cells (LC) and mouse bone marrow cells (BMC). These PPs were determined to be phosphorylated and to have a molecular weight of about 1,500 daltons. Suspensions of 0.5 mil cells/ml TCM199 were subdivided into 3 portions: one was the control, to the second 1 $\mu\text{g/ml}$ adriamycin (ADM), and to the third 0.8 $\mu\text{l/ml}$ PPs were added. After two hours of incubation, 2.5 μCi of ^3H -TdR was added and the incubation continued for one hour. Subsequently, aliquots were placed on paper discs, the non-incorporated ^3H -TdR extracted with TCA, the residual substance washed, and the activity determined. The analysis of the data demonstrated that in the PP- and ADM-treated aliquots of WC the incorporation of ^3H -TdR was reduced to 49 % and 39 % respectively. In the PP- and ADM-treated LC the incorporation of ^3H -TdR was reduced to 72 % and 49 % respectively. No significant reduction of ^3H -TdR incorporation (99 %) could be observed in the PP-treated BMC. In the case of ADM-treated BMC the ^3H -TdR incorporation was reduced to 72 %. The impulse cytophotometric analysis of the PP-treated WC demonstrated that the PPs inhibit the cell cycle in early S- and/or in the G_2 -phase. The data suggest that the PPs interfere with the tumor cell cycle. They inhibit significantly tumor cell proliferation. No significant effects were observed in normal cells.

M-AM-Po1 STUDIES ON THE PRIMARY STRUCTURE OF CARDIAC MYOSIN S-1: ISOLATION OF THE 21K, 25K AND 51K TRYPTIC FRAGMENTS AND COMPARISON OF THE PARTIAL SEQUENCE OF 21K WITH A SIMILAR PEPTIDE FROM RABBIT SKELETAL MYOSIN. Irwin L. Flink and Eugene Morkin, Departments of Internal Medicine and Pharmacology, University of Arizona Health Sciences Center, Tucson, Arizona 85724.

Very little is known about the primary structure of cardiac myosin subfragment-1 (S-1). Accordingly, we have prepared S-1 from bovine left ventricular myosin using papain and are in the process of determining the sequence of the heavy chain fragment. A limited tryptic digest of S-1 was prepared and shown to produce three subfragments with molecular weights of 51K, 25K and 21K. These fragments were purified by chromatography on CL-Sepharose 6B and SP-Sephadex. Heavy chain S-1 was found to contain about 25%, 16%, and 59% acidic, basic, and non-polar residues, respectively. 51K, 25K and 21K each contained approximately the same proportions of acidic, basic, and non-polar residues, suggesting that these residues are distributed fairly uniformly throughout cardiac S-1. Two residues of N- ϵ -trimethyllysine were found in S-1; 51K and 25K each contained about 1 mole of this unusual amino acid per mole. The 21K fragment was cleaved with CNBr and trypsin and the resulting peptides were sequenced by automated Edman degradation. Comparison of a nearly complete sequence of this fragment with the published sequence of skeletal 21K (Gallagher, et al., Fed.Proc. 39:2168, 1980) showed considerable homology. About one-fourth of the cardiac sequence differed from the skeletal sequence. The NH₂-terminal region near the SH₁-SH₂ thiols was conserved. However, there were a fairly large number of replacements in the COOH-terminal region. The latter region is near the S-1/S-2 hinge and may be a variable domain in different myosin isoenzymes.

M-AM-Po2 ARTHROPOD THICK FILAMENT STRUCTURE. Robert W. Kensler, Rhea J. C. Levine, Mary Reedy* and Waltraud Hoffmann.* Dept. of Anatomy, The Medical College of Pennsylvania, Phila., PA, 19129 and Dept. of Anatomy, Duke University, Medical Center, Durham, N.C. 27710.

We have previously shown that the thick filaments of *Limulus* telson muscle are highly periodic with 4 myosin cross-bridges/crown (Kensler and Levine, Biophys. J. 33:242a, '81; J. Cell Biol., In Press; Stewart, Kensler and Levine, J. Mol. Biol., In Press). Using similar procedures, we have examined thick filaments isolated from other chelicerate arthropod species (tarantula and scorpion) and non-chelicerate arthropods (grasshopper and praying mantis). In negatively stained images the thick filaments of the chelicerate muscles appear highly periodic with a cross-bridge helical arrangement very similar to that of *Limulus* filaments. Optical diffraction patterns of images of these filaments, like those of *Limulus*, are detailed, with meridional reflections at 14.5nm⁻¹ and 7.2nm⁻¹ and strong off-meridional layer lines at orders of a 43.5nm⁻¹ repeat. The images of platinum-carbon shadowed chelicerate filaments clearly show a right-handed helical arrangement of myosin cross-bridges with a pattern similar to that seen on shadowed *Limulus* filaments. In contrast to the chelicerate thick filaments, those isolated from the non-chelicerate arthropods showed less signs of order, consistent with the X-ray results of Wray et al. (Nature 257:561, '75; Nature 277:37, 79) on lobster muscle. Thus, filament structure may be, at least in part, phylogenetically determined.

Supported by USPHS Grants: NRSA GM 07475, AM 14317 and HL 15835 to the Pennsylvania Muscle Institute.

M-AM-Po3 CALCIUM-ACTIVATED NEUTRAL PROTEASE IN NERVE, AND CARDIAC AND SKELETAL MUSCLE IS ACTIVE AT PHYSIOLOGIC Ca²⁺ LEVELS AND IS INHIBITED BY PHENYTOIN AND VALPROATE. T.M. Nosek, M. Brasher-Crosland, and R.E. Godt, Dept. of Physiology, Medical College of Georgia, Augusta, GA 30912.

A calcium-activated neutral protease (CANP) has been isolated by others from a number of cell types and shown to metabolize contractile regulatory proteins, Z- and M-line proteins, and proteins of the cytoskeleton. We compared the Ca²⁺ requirements for activation of CANP from guinea pig ventricular myocardium, frog sartorius, rabbit psoas and soleus, and crayfish nerve fibers. Crude homogenates of these tissues were analyzed for Ca²⁺-dependent proteolytic activity using the assay of Kar and Pearson (Clinica Chimica Acta 73:293, 1976) based on the proteolysis of casein yellow. Care was taken to control the Ca²⁺ concentration of all incubation media with EGTA and to maintain the ionic strength of all solutions at 0.15 M with KCl. All tissues studied were similar in that their CANP activity monotonically increased as pCa decreased from 8 to 3, with significant activity being measured at a pCa of 6-7, i.e. Ca²⁺ levels normally observed intracellularly in resting cells. The anticonvulsant and antiarrhythmic agents phenytoin (PHT) and valproate (VPA) were tested for their effects on CANP activity in nerve and muscle. PHT (0.11 mM) and VPA (4 mM) were found to decrease peak CANP activity between 25 and 80% in all tissues assayed. These results demonstrate that CANP activity can be modulated by changes in intracellular Ca²⁺ within the physiologic range and by a structurally different pharmacologic agents. They also suggest that CANP activity may be a significant factor in the maintenance of normal cell function. (This work was supported by NIH Grant #1-NS-6-2340 and by a grant from the Georgia Heart Association to T.M.N.)

M-AM-Po4 AN ^1H -NMR STUDY OF THE STRUCTURE AND INTERACTIONS OF THE HIGH AFFINITY REGIONS OF TROPONIN C. P. C. Leavis¹, Z. Grabarek¹, J. Gergely¹ and B. A. Levine². 1. Dept. Muscle Research, Boston Biomedical Research Institute and Harvard Medical School, Boston, MA 02114 2. Dept. Inorganic Chemistry, Oxford University, Oxford, U. K.

The C-terminal half of the TnC molecule, containing the Ca^{2+} - Mg^{2+} binding sites III and IV is known to undergo a large ($\sim 100\%$) increase in α -helical structure upon binding of Ca^{2+} . The induced helices have been shown to be at the N-terminal flank of site III (III_N) and the C-terminal flank of site IV (IV_C, Nagy and Gergely, 1979, J. Biol. Chem. 254;12732). ^1H -NMR studies of TR₂C, a tryptic fragment of TnC comprising the C-terminal half, indicate that Ca^{2+} -binding also induces a tertiary fold stabilized by hydrophobic contacts between Phe residues located in the newly formed helices III_N (Phe 99) and IV_C (Phe 148, 151). These contacts are indicated by ring current-induced upfield shifts in the resonance energies of Phe 99 and 148, assigned on the basis of lanthanide effects, signal broadening by a spin label on Cys 98 of TnC and nuclear overhauser experiments. These changes are also evident in the ^1H -NMR spectra of intact TnC indicating that the structure of the TR₂C fragment reflects that of the corresponding region in the parent molecule. Binding between TnC and TnI was studied using TnC spin-labelled at Cys 98, located within a known site of interaction with TnI. A shift in the resonance energies of TnI Phe residues 100 and 106 upon complex formation reflects the proximity of these residues to Cys 98 and is consistent with observations indicating that a region of TnI comprising residues 96-117 binds to TnC (Syska et al, 1976 Biochem. J. 153;375). This work was supported by NIH, NSF, MDA, AHA, MRC.

M-AM-Po5 PHOSPHORESCENCE ANISOTROPY OF EOSIN-LABELED CONTRACTILE PROTEINS

Thomas M. Eads, Brian P. Citak & David D. Thomas. Dept. of Biochemistry, University of Minnesota Medical School, Minneapolis, MN 55455

We report the use of time-resolved phosphorescence to measure macromolecular motion in the tens of microseconds to millisecond time range. The method is well suited to probe slow motion in the contractile proteins. We have measured phosphorescence anisotropy of eosin derivatives covalently bound to myosin and Sl. Evidence is presented which indicates that labeling is somewhat specific for the reactive sulfhydryl (SH1). Polarized excitation near the absorbance maximum of the dye (520 nm) is provided by a pulsed nitrogen laser-pumped tunable dye laser. Polarized emission near the phosphorescence emission maximum (680 nm) is isolated with a narrow bandpass interference filter. Phosphorescence decay is measured to 1 μs resolution. Phosphorescence anisotropy $(I_{\parallel} - I_{\perp}) / (I_{\parallel} + 2I_{\perp})$ of probe attached to Sl and monomeric myosin is zero in the μs range. This is expected since these particles have rotational correlation times in the range of hundreds of ns. In contrast, anisotropy of actomyosin (myosin labeled) is finite; it has one component of decay in the tens of μs , and another in the ms range. This indicates that probe motion is highly anisotropic and is limited by slow macromolecular fluctuations. Several models are proposed. The results are consistent with combined rapid, restricted plus slow, large-amplitude fluctuations. The method complements the results from saturation transfer electron paramagnetic resonance experiments by providing time resolution, and it extends the range of observable correlation times to the ms range.

M-AM-Po6 THE EFFECTS OF LC2 PHOSPHORYLATION ON THE AGGREGATION CHARACTERISTICS OF RABBIT SKELETAL MYOSIN WITH AND WITHOUT C-PROTEIN AT PH 7.0 Jane F. Koretz, Anne M. Bertasso, and Thomas H. Crouch*, Dept. of Biology, Rensselaer Polytechnic Institute, Troy, N.Y. 12181 and Miles Laboratories, Ames Division, Elkhart, IN 46515 (Intr. by Joseph V. Landau)

The population characteristics of column-purified rabbit skeletal myosin aggregates were investigated as a function of degree of phosphorylation (80%, 50% and 20% as determined on urea gels), presence or absence of C-protein, and concentration of divalent cations at pH 7.0 and 0.10M KCl, 10 mM imidazole. All filaments formed in the presence of C-protein in a molar ratio to myosin of 1:3.3 are shorter on the average and exhibit a narrower length distribution than any population in its absence irrespective of divalent cation concentration or degree of phosphorylation. Whether C-protein is present or not, filament populations demonstrate increasing average length with increasing degree of phosphorylation in the absence of added Ca^{++} ; in the presence of EGTA (2 mM) or high Ca^{++} (.1 mM), there is again a gradient of average length, but in the opposite direction. The same Ca^{++} variation in the presence of Mg^{++} (1 mM) gives less clear-cut results. Without added Ca^{++} , filament length increases with increasing degree of phosphorylation, while with EGTA it decreases. However, in the presence of both Mg^{++} and Ca^{++} , length increases with increasing phosphorylation.

Supported in part by NIH grant NS/GM 14377.

M-AM-Po7 CHARACTERIZATION OF RABBIT MASSETER FIBERS. K. Mabuchi, K. Pinter, J. Gergely and F.A. Sreter, Department of Muscle Res. Boston Biomedical Res. Inst., Dept. of Neurology, Mass. Gen. Hosp. and Harvard Medical School, Boston, MA 02114.

Rabbit masseter fibers exhibiting acid labile (pH 4.3) ATPase can be subdivided into two groups on the basis of their CaMg-ATPase activity: 10-20% show little staining, as do the slow fibers of soleus muscle, while the majority stain moderately. Myosin extracted from masseter shows 4 bands on electrophoresis in non-denaturing PP_i-gels. Electrophoresis on SDS-gels shows the presence of both slow and fast type light chains. Analysis of masseter single fibers indicates that slow-type light chains, identified by their mobility on SDS-gels, are associated with the slowest isozyme on PP_i-gels, which moves somewhat faster than the typical slow (soleus) isozyme. The 3 myosin isozymes found in 2B fibers of masseter have a somewhat lower mobility than those in m. adductor magnus. The middle band corresponding to the LC₁+LC₃ heterodimer is weaker than the two flanking bands - LC₁ and LC₃ homodimers - whose intensities are about equal. This is in contrast to the 2B fibers of adductor magnus where the middle band is the strongest. Masseter 2A fibers exhibit an isozyme pattern consistent with the low LC₃ content and a non-preferential distribution of light chains. The relative intensities of the masseter isozyme bands suggest preferential formation of homodimers. In medium-to-small-size masseter fibers, slow and fast type light chains coexist. On the basis of PP_i-gels studies on a limited number of these fibers it appears that the LC₂ type plays a role in determining the difference between slow and fast type isozymes. (Supported by NIH grants AG-02103, HL-23967, HL-5949, NSF and the Musc. Dystroph. Assoc. Inc.)

M-AM-Po8 DIFFERENTIAL CHANGES IN MYOSIN LIGHT CHAIN AND PHOSPHORYLASE PHOSPHORYLATION DURING CONTRACTION OF TRACHEAL SMOOTH MUSCLE. P.J. Silver and J.T. Stull, Dept. of Pharmacology, Univ. of Texas Health Science Center, Dallas, Tx. 75235.

Since activation of phosphorylase (Ps) kinase and myosin light chain kinase involves Ca²⁺ binding to calmodulin (CM), we examined temporal and agonist concentration dependent changes in Ps a formation and phosphorylation of the phosphorylatable light chain (P-LC) of myosin during changes in isometric tension (I.T.) in intact strips of bovine tracheal smooth muscle. Maximal increases in I.T., during incubation with 1 μM carbachol (carb.), were maintained for up to 30'. After 1', the phosphate content (PC) of the P-LC increased from a resting value of 0.13 mol P/mol P-LC to 0.75, and subsequently declined to values of 0.41 after 10', and 0.26 after 30'. Ps a formation (ratio of activity measured -AMP/+AMP) increased from a resting value of 0.15 to 0.61 after 1', remained elevated up to 10' (0.54), then declined to a ratio of 0.27 after 30'. As with 1 μM carb., incubation with a submaximal contractile dose of carb. (30 nM) produced initial increases in PC of the P-LC after 1' (0.10 to 0.38) and subsequent declines at later time intervals. In further experiments, pretreatment with isoproterenol inhibited the initial carb. (1 μM) mediated increases in I.T. development and P-LC phosphorylation, yet increased Ps a formation. K⁺-induced responses were compared with carb.-mediated responses at concentrations of the agents which produced comparable increases in I.T. After 1' of incubation, differential increases in Ps a levels were apparent as K⁺ stimulation increased Ps a formation to a greater extent than did carb. stimulation. These results suggest that phosphorylation of Ps and the P-LC is not directly related to absolute levels of I.T. in smooth muscle. Moreover, the intracellular regulation of these two Ca²⁺/CM dependent processes may differ. (Supported by NIH grants HL26043 and HL06359).

M-AM-Po9 CHARACTERIZATION OF A PARAMYOSIN PHOSPHOKINASE. Lynn Radlick and W. H. Johnson, Dept. of Biology, Rensselaer Polytechnic Institute and the Muscle Biology Group, College of Agriculture, The University of Arizona, Tucson, AZ 85721

Cooley et al. reported that paramyosin contained up to four covalently bound phosphate groups per molecule. We have isolated a paramyosin kinase from adductor muscles of *Mercenaria mercenaria* which is carried with paramyosin through the initial preparative washes. The kinase remains in the supernatant when paramyosin and other contractile proteins are precipitated at pH 6.2 and 0.1 M KCl and can be further purified by batch treatment with DEAE-Sephadex and fractionation on a Sephacel 300 column. We have found that commercially available *Staph. aureus* protease hydrolyses α-paramyosin, giving 2 to 3 bands on SDS acrylamide gradient gels in the region of β-paramyosin, along with a small peptide. This is similar to changes reported by Stafford and Yphantis during isolation of β-paramyosin in the absence of agents which inhibit bacterial growth. β-paramyosin is not phosphorylated by the kinase described above. Commonly used protein substrates, such as casein, histone 2A, phosvitin are also not phosphorylated, while phosphorylase B is phosphorylated to a small extent. It thus appears that the kinase is specific for the small peptide located at the c-terminal end of paramyosin which is responsible for its unique solubility properties. Supported by NIH senior fellowship 1 F33 AM06688-01 to WHJ.

M-AM-Po10 THE TWO CONFORMATIONAL STATES OF TROPOMYOSIN. A SPIN LABEL STUDY. Philip Graceffa and Sherwin Lehrer, Dept. of Muscle Res., Boston Biomed. Res. Inst., Boston, MA 02114.

Several studies have shown that tropomyosin (Tm) is more unstable in the C-terminal half of the molecule, which contains cysteine-190, than in the N-terminal half. We have shown that this is due to a temperature-dependent dynamic equilibrium between two conformational states with the higher temperature state being more unfolded in the cysteine-190 region (Graceffa and Lehrer (1980) JBC 255, 11296; Lehrer et al. (1981) Ann. N.Y. Acad. Sci. 366, 285). The lower temperature state is known to be highly alpha-helical. Spin-labeled Tm has given further evidence for this two-state equilibrium and has allowed for the determination of thermodynamic differences between these states. Tm labeled at cysteine-190 with a maleimide spin label shows esr spectral components corresponding to strongly-immobilized and weakly-immobilized labels. The concentration ratio, R, of the two types of labels varies as a function of salt and temperature with $R = 1.0$ at 1M NaCl, pH 7.5, and 37 degrees. At 1M NaCl, pH 7.5, log R is a linear function of $1/T$ over the temperature range of 15-40 degrees, which is below the main unfolding transition of Tm, indicating that the native molecule is in thermal equilibrium between two conformational states, represented by two different spin label mobilities. From these data one calculates enthalpy and entropy differences between these states to be approximately 26 kcal/mol and 84 cal/deg-mol, respectively. This large entropy change indicates that the two states of Tm differ greatly in their structural organization with the higher temperature state being highly disordered and thus flexible in the region of the molecule which includes cysteine-190. (Supported by NIH HL 22461 and MDAA.)

M-AM-Po11 SITE-SPECIFIC PHOTOAFFINITY CROSS-LINKING STUDIES ON MUSCLE PROTEINS USING BENZOPHENONE-4-MALEIMIDE. M. Lamkin and T. Tao, Department of Muscle Research, Boston Biomedical Research Institute, 20 Staniford St., Boston, MA 02114.

We have used benzophenone-4-maleimide (BP-Mal) to cross-link several muscle proteins from rabbit skeletal muscle. BP-Mal is a sulfhydryl specific reagent by virtue of its maleimide ring; in addition, the benzophenone moiety can be excited by UV radiation to form a diradical triplet state which can photoreact nonspecifically. Benzophenone is a highly efficient cross-linking reagent because its photoreactivity towards C-H bonds is much greater than that towards water; so that if the triplet fails to produce a photocross-link, it will decay to the ground state and can be regenerated by re-excitation. We have used BP-Mal to photocross-link two complexes: 1) BP-tropomyosin (BP-Tm, labelled specifically at cys-190) to troponin (Tn) and 2) BP-troponin-C (BP-TnC, labelled specifically at cys-98) to TnI. In the case of BP-Tm.Tn, cross-linked species were identified on SDS gels corresponding to Tm monomer cross-linked to each of TnT, TnI and TnC as well as to the other Tm monomer. These results indicate that all three Tn subunits are within 10 Å of cys-190 of Tm. In the case of BP-TnC.TnI, cross-linked products had different mobilities on SDS gels depending upon whether the photolysis was done in the presence or the absence of calcium. The observation that different cross-linked species are formed is consistent with calcium inducing a conformational change in the TnC.TnI binary complex. (Supported by NIH AM-21673)

M-AM-Po12 TROPONIN T-TROPOMYOSIN INTERACTION. P.C.S. Chong and R.S. Hodges, Department of Biochemistry and Medical Research Council Group in Protein Structure and Function, University of Alberta, Edmonton, Alberta, Canada T6G 2H7.

Recently three different studies have indirectly indicated that troponin T (TnT) is in the vicinity of cysteine 190 or 1/3 of the distance from the COOH-terminal end of α -tropomyosin (Tm). In order to locate the actual region of TnT in the close proximity to Tm, under physiological conditions (the presence and absence of Ca^{2+}), the binding of S-carboxamidomethylated skeletal troponin (CM-Tn) was photochemically crosslinked to α -Tm which was labelled with a heterobifunctional photoaffinity probe, N-(4-azidobenzoyl- 3H -glycyl)-S-(2-thiopyridyl)-cysteine (AGTC) at cysteine 190. The covalently linked complex (CM-Tn-AGC-Tm) was isolated by hydroxylapatite chromatography in the absence of reducing agent. The radiolabelled CM-Tn was isolated from this complex by hydroxylapatite chromatography in the presence of reducing agent which cleaved the disulfide bond between AGC-Tm and CM-Tn. The radiolabelled CM-Tn was separated into its individual components by DEAE-Sephadex chromatography in 6 M urea, EGTA and DTT. Radioactive measurements indicated that only TnT was labelled. Chymotryptic digestion of radiolabelled CM-Tn indicated that the C-terminal fragment of TnT (T₂, residues 159-259) was the only component radiolabelled. These results suggest that in the presence and absence of Ca^{2+} TnT binds to Tm in such a way that the C-terminal region (residues 159-259) is within 14 Å of Cys 190 in Tm. These results are in agreement with fragment binding and fluorescence studies. (Supported by MRC).

M-AM-Po13 STRUCTURAL STUDIES OF ISOLATED NATIVE THICK FILAMENTS FROM RABBIT PSOAS MUSCLE USING AMP DEAMINASE AS A STRUCTURAL PROBE Jane F. Koretz, Dept. of Biology, Rensselaer Polytechnic Institute Troy, N.Y. 12181

AMP deaminase, a tetrameric enzyme of approximately 320,000 molecular weight, has been shown to bind specifically to the subfragment-2 region of myosin both in vitro and in situ by Frieden and coworkers (1977, 1979). More recent studies of deaminase specificity (Koretz and Frieden, 1980) demonstrate that it will bind to synthetic myosin filaments with the underlying structure of these filaments; optical diffraction of the decorated structures exhibit enhanced reflection intensity without changes in periodicity. Similar decoration experiments have been undertaken with isolated native thick filaments from rabbit psoas muscle. AMP deaminase binds most densely in the banded region of the filament, with less dense decoration in the outer zones; a single band near the beginning of the crossbridge region on either side of the bare zone is also apparent. Analysis of the pattern of deaminase binding, including optical diffraction, indicates that neither a strict three-fold nor a strict two-fold model of crossbridge arrangement is consistent with the apparent S-2 periodicity in the banded region. Instead, the data suggest either a four-fold or distorted two-fold structure.

Supported by NIH grant NS/GM 14377.

M-AM-Po14 NUCLEOTIDE AND METAL EFFECTS ON THE STRUCTURE OF MYOSIN SUBFRAGMENT-1. G. Mocz*, R.C. Lu and J. Gergely. Dept. of Muscle Res., Boston Biomed. Res. Inst.; Dept. of Neurology, Mass. Gen. Hosp.; and Dept. of Biol. Chem., Harvard Med. Sch., Boston, MA.

We and others (Szilagyi et al; Kassab et al; Muhlrads and Hozumi, pers. commun.) have recently found that the kinetics of the fragmentation of S-1 by trypsin change in the presence of MgATP, MgADP, MgAMPPNP and MgPP_i. At 25° the breakdown of the 75K fragment, formed in the 90K 75K + 20K step into 50K + 25K is slowed down, while the breakdown of the 50K to 47K and the 25K to 22K is accelerated (Kassab et al; Szilagyi et al). In agreement with Hozumi and Muhlrads, we found that MgATP suppressed the formation of a 27K fragment they suggested (Biochemistry 20, 2945, 1981) is an intermediate in an alternate path of the 75K 50K + 25K step. The effect of nucleotides do not depend on the presence of a Me²⁺. In the absence of nucleotides Ca²⁺ or Mg²⁺ accelerates the breakdown of 75K but does not affect the formation of 27K. The 27K fragment, being on an alternate pathway - rather than an intermediate in a single pathway of 75K breakdown - is supported by the observation that ATP does not accelerate the breakdown into 25K of the 27K fragment formed in the absence of ATP. At 37° S-1 becomes more susceptible to trypsin; 25K and 50K are rapidly degraded to smaller fragments, but the 20K fragment remained stable. Nevertheless, in the presence of Mg-ATP or Mg-ADP the 25K and 50K fragments were protected from being further digested. The presence of a nucleotide during digestion preserves the K⁺, Ca²⁺, or Mg²⁺-activated ATPase activity of S-1. These results are consistent with various pieces of evidence suggesting that the N-terminal 25K segment contains nucleotide interaction site(s) and also indicating conformational changes extending to the 50K region as a result of nucleotide binding. (Supp.: NIH, NSF and MDAA)

M-AM-Po15 LABILE PROPERTIES OF THE CHICKEN GIZZARD MYOSIN ATPase. R.F. Siemankowski, Department of Biochemistry, University of Arizona, Tucson, Arizona 85721.

Gizzard myosin ATPase is susceptible to modification merely by storage for 7+3 days at 0° in 0.5 M KCl, 2mM MOPS, pH7, 0.2mM DTT and/or by limited exposure to a trypsin-like serine protease from rat intestinal muscle or pancreas (details in press, Biochem. J., John Kay, et. al.).

ATPase Activity (S⁻¹; normalized per site)

Condition of Myosin	Mg ²⁺ - ATPase				Ca ²⁺ - ATPase			
	Myosin + Ca ²⁺	Acto-Myosin + Ca ²⁺	AM plus CTm + Ca ²⁺	AM plus CTm + EGTA	no K ⁺	25mM KCl Ca ²⁺ /ATP=1	=3	0.5M KCl K ⁺ -ATPase in EDTA
F	.009	.035	0.94	.012	0.77	0.074	.48	1.06
A	.037	.045	0.51	.035	1.37	0.140	.52	0.98
A + P	.037	.068	0.28	.094	----	-----	---	----
FP	.027	.070	0.30	.043	----	-----	---	----

All activities measured at 25° in presence of 0.2mM DTT and 25mM Tris, pH 7.5. Mg²⁺-ATPase measured in 33mM KCl, 1mM Mg²⁺-ATP, 3mM MgCl₂ and 0.025mM CaCl₂ or 1mM EGTA in presence (or absence) of 2mg/ml actin and crude tropomyosin (CTm). Ca²⁺-ATPase measured in KCl as desired (or 0.25M Tris, if no KCl), 3.33mM Ca²⁺-ATP. K⁺/EDTA-ATPase measured in 0.5M KCl, 3.33mM ATP, 3.33mM EDTA. Abbreviations: F, fresh; A, aged, A + P, aged and proteolysed; FP, fresh but proteolysed.

Some of the current controversies regarding Ca²⁺-regulation of smooth muscle ATPase may reflect unrecognized use of data obtained from aged or degraded myosin preparations.

M-AM-Po16 SCALLOP REGULATORY AND ESSENTIAL LIGHT CHAINS COMPLEX WITH THE SAME S-1 HEAVY CHAIN PEP-TIDE FRAGMENT. E. M. Szentkiralyi (introd. by A. G. Szent-Györgyi) from the Department of Biology, Brandeis University, Waltham, Massachusetts 02254.

Calcium regulation of scallop myosin requires the presence of both regulatory (RLC) and essential (SH-LC) light chains. RLC and SH-LC can be cross linked and probably lie side by side (Wallimann, T., Hardwicke, P.M.D. and Szent-Györgyi, A.G., J. Mol. Biol. in press). During trypsin digestion of scallop S-1 the two LC-s remain intact while the heavy chain (HC) degrades. The actin activated ATP-ase activity disappears as soon as the 95K HC is first split into a 24K and a 70K component; the high calcium and magnesium activated ATPase persist in spite of further digestion of the HC. In this respect scallop S-1 is similar to rabbit S-1 (Mornet, D., Pantel, P., Audemard, E. and Kassab, R., 1979, BBRC 89, 925) suggesting that accessibility to trypsin reflects similar features in shape and actin binding site. When a late tryptic digest of S-1 is electrophoresed under non dissociating conditions an intense band appears migrating slower than either of the purified LC-s. SDS slab electrophoresis in the second dimension shows that this band consists of a 14K peptide in association of both LC-s. The binding of the RLC to the rest of the complex is divalent cation dependent. EDTA in the sample and native gel leads to dissociation of RLC; in the presence of 1mM calcium in the running buffer the complex is fully associated, magnesium is partially effective in holding the complex together. This behavior of LC-s and peptide mimics that of the intact myosin molecule. The complex can be isolated by Sephadex gel chromatography.

(Supported by NIH AM-15963 grant).

M-AM-Po17 KINETICS OF THE BEEF HEART ACTO-S1 Mg^{2+} -ATPase. R.F. Siemankowski and H. White (Intr. by G. Tollin), Department of Biochemistry, University of Arizona, Tucson, Arizona 85721.

The beef heart S1 preparation used here comprises 72% (w/w) of a species having pI of ca. 7.6 and the 27 kd light chain and the remainder having pI of 7.1 and the 18 kd light chain. S1-A1 from rabbit skeletal muscle has pI of ca. 6.5. All ATPase parameters were measured at 15° in 10mM KCl, 2mM $MgCl_2$, 5mM MOPS, pH 7.0, 0.2mM DTT. Taking into account differences in experimental conditions, the present studies (also see previous studies: S. Marston and E. Taylor, '80; R. Taylor and A. Weeds, '76) indicate that S1's from heart (H) and rabbit skeletal muscle (RSM) bind and hydrolyse ATP at the same rate (measuring enhancement of tryptophan fluorescence). However, under the same ionic conditions, the observed second order constant for the fluorescence enhancement for RSM-S1 is subject to strong enhancement by actin, whereas H-S1 is not. The rate of dissociation of acto-S1 by ATP (measuring light scattering intensity) is also very similar for H and RSM. The kinetics of the dissociation of ADP from acto-S1 (measuring decrease in light scattering upon displacement by ATP) displays V_{max} of $70s^{-1}$ for H and K_D of $10^{-5}M$. For RSM, no saturation in rate is observed ($k > 500s^{-1}$) and K_D is $2 \times 10^{-4}M$. However, the dissociation of ADP seems not rate limiting for H since the steady state ATPase is only ca. $6s^{-1}$. Previous studies have determined V_{max} for ADP dissociation from H-S1 to be ca. $0.4s^{-1}$. Therefore, despite the much higher affinity of H-S1 for ADP, actin causes a ca. 200-fold increase in rate of release of ADP from S1. Preliminary studies of the rate of increase of light scattering intensity during single turnovers of ATP by H-acto-S1 are consistent with the notion that the rate of recombination of S1·Pr with actin determines the steady state ATPase, as was previously shown for several species of S1 from chicken. (HL20984-05)

M-AM-Po18 HYDRODYNAMIC STUDIES ON BOVINE CARDIAC TROPONIN SUBUNITS ALONE AND IN BINARY COMPLEXES. David M. Byers and Cyril M. Kay. MRC Group in Protein Structure and Function, Department of Biochemistry, University of Alberta, Edmonton, Alberta, Canada, T6G 2H7.

The structures and interactions of troponin subunits must be known in order to understand how troponin regulates muscle contraction on the thin filament. Thus, hydrodynamic techniques have been used to study bovine cardiac troponin subunits in solution both individually and in 1:1 molar combinations. Gel filtration, sedimentation and viscosity experiments have indicated that troponin-C (TN-C) is a moderately asymmetric protein in the absence of Ca^{++} (frictional ratio = 1.5) which undergoes a conformational change to a more compact structure when Ca^{++} is added. Troponin-I (TN-I) and troponin-T (TN-T) both undergo self-association in solution, although TN-I is monomeric at low concentration (frictional ratio = 1.5) whereas TN-T appears to form larger, very asymmetric aggregates. TN-C and TN-T do not appear to interact strongly in 0.5 M NaCl, 2 mM Ca^{++} (pH 7.2) since both gel filtration and sedimentation velocity profiles are bimodal. On the other hand, TN-C does seem to form a strong complex with TN-I ($\pm Ca^{++}$) since the apparent molecular weight of this mixture in the ultracentrifuge is about 40,000 and single, symmetrical profiles are observed using transport methods of analysis. Moreover, the sedimentation coefficient (3 S) and the Stokes radius from gel filtration on Sephacryl S-300 (35 Å) are both larger for the TN-IC complex than for either TN-C or TN-I alone. The present data therefore suggest that the TN-IC complex is not more asymmetric than the individual subunits. (Supported by MRC of Canada and AHFMR).

M-AM-Po19 MONOCLONAL ANTIBODIES INHIBIT THE ACTIN ACTIVATED Mg^{++} -ATPASE OF *ACANTHAMOEBA* MYOSIN II. D.P. Kiehart, D.A. Kaiser, and T.D. Pollard. Dept. of Cell Biology and Anatomy, Johns Hopkins University School of Medicine, Baltimore, MD. 21205.

Monoclonal antibodies against *Acanthamoeba* myosin II provide probes of myosin II structure and function. Twenty-six out of approximately 200 anti-myosin II hybridomas were randomly selected for cloning and subsequent analysis. A variety of different Ig isotypes verify that these monoclonals were the result of different fusion events. All bind solely and specifically to myosin II heavy chain as demonstrated by antibody overlay of SDS gel blots of either whole amoeba extract or purified myosin II. None of these myosin II antibodies cross react with myosin I, but both polyclonal (rabbit) and monoclonal antibodies directed against myosin I cross react with myosin II. The anti-myosin II monoclonal antibodies are directed against at least 7 different antigenic determinants, as demonstrated by competitive binding analysis and by antibody overlays of limited proteolytic digests of myosin II heavy chain. These different analyses of antigenic site specificity concur: antibodies which recognize the same constellation of proteolytic fragments compete for binding to whole myosin II. Eleven of these 26 monoclonals have been harvested from ascites fluid in sufficient quantities to assay their effect on myosin II function. Three partially inhibit the Ca^{++} -ATPase. One of these and one other monoclonal completely inhibit the actin-activated Mg^{++} -ATPase of myosin II. Three other monoclonals partially inhibit this ATPase activity. The two that strongly inhibit actin activated ATPase are directed against distinct yet similar constellations of proteolytic fragments of myosin II. Supported by NIH grants GM 26338 and GM 26132 and a Muscular Dystrophy Postdoctoral Fellowship to D.P.K.

M-AM-Po20 TROPONIN-LIKE COMPONENTS IN MOLLUSCAN MUSCLES. William Lehman, Dept. of Physiology, Boston Univ. School of Medicine, Boston, MA 02118

Thin filaments isolated from a variety of molluscan muscles confer Ca^{2+} -dependence on rabbit myosin and, in addition to actin and tropomyosin, contain components which may represent troponin subunits. A troponin-I-like protein has been isolated from the bay scallop, *Aequipecten irradians*. Antibodies developed against this protein stain I-bands of washed myofibrils and precipitate isolated thin filaments. Electron microscopy of antibody induced thin filament aggregates reveals transverse striations with a periodicity of $377 \pm 12 \text{ \AA}$, a value characteristic of troponin's distribution on vertebrate and invertebrate thin filaments. The thin filaments of *Aequipecten* I-segments also aggregate when treated with the anti-troponin-I antibody and show the same repeat period.

Of the thirteen molluscan muscles examined only the striated muscles of the scallops, *Placopecten magellanicus* and *Chlamys icelandica* do not appear to show troponin-like subunits on SDS-polyacrylamide gels; however our antibody to *Aequipecten* troponin-I crossreacts with *Chlamys* and *Placopecten* myofibrils and indirect immunofluorescence microscopy of these myofibrils shows staining of all I-bands observed. Moreover, electron microscopy of *Placopecten* thin filaments, precipitated with the anti-troponin-I antibody, show 380 \AA periods, indicating the possible presence of troponin in these species as well. (Supported by NIH grant AM 17062).

M-AM-Po21 EXAMINATION OF ACTIN SPECIES IN EQUILIBRIUM WITH FILAMENTS BY NANOSECOND FLUORESCENCE RELAXATION ANISOTROPY. J.D. Pardee, J. Reidler, L. Stryer, and J.A. Spudich. Department of Structural Biology, Stanford University School of Medicine, Stanford, CA 94305.

After complete actin assembly, a small amount of non-filamentous actin called the critical actin concentration (C_A) remains in equilibrium with filaments. We have analysed the critical concentration by nanosecond fluorescence relaxation anisotropy to determine the size of the C_A actin species. Highly purified skeletal muscle actin covalently labeled with the fluorescent probe IAENS (5-(iodoacetamidoethyl)aminonaphthalene-1-sulfonic acid) was assembled to equilibrium by addition of either 0.1M KCl, 0.1M KCl + 1mM $MgCl_2$, or 0.1M KCl + 1mM $CaCl_2$. All samples demonstrated normal assembly properties compared to unlabeled actin. A mode-locked cavity-dumped argon ion laser was used to obtain nanosecond relaxation correlation times (ϕ_1, ϕ_2) on solutions of monomeric actin, filamentous actin, and C_A actin separated from filaments by centrifugation. Correlation times of 18-20 nsec were obtained for monomeric actin compared to >400 nsec for filaments assembled under all ionic conditions examined. However, relaxation times for C_A actin were highly dependent on the ionic species used to initiate polymerization. Values of ϕ_2 were 21 nsec when actin was assembled with 0.1M KCl + 1mM $CaCl_2$, 41 nsec for assembly by KCl alone, and 90 nsec for assembly by 0.1M KCl + 1mM $MgCl_2$. In each case, the kinetics of anisotropy decay appeared linear suggesting that the C_A is composed of a homogenous population or narrow distribution of molecular weight actin species. Moreover, the critical concentration species appears to be larger than monomer when assembly is carried out in 0.1M KCl or 0.1M KCl + 1mM $MgCl_2$. NIH GM-25240 to J.A.S.; NIH Fellowship to J.D.P.; NIH GM-24032 to L.S.

M-AM-Po22 A POSSIBLE RELATIONSHIP OF THE 27 Kd PEPTIDE FROM S1 HEAVY CHAIN AND LIGHT CHAIN 2 IN CHICKEN PECTORALIS MYOSIN. T. Shimizu, F. Reinach, T. Masaki and D.A. Fischman. Dept. of Anatomy and Cell Biology, SUNY-Downstate Medical Center, Brooklyn, N.Y. 11203.

A monoclonal antibody against chicken pectoralis myosin (MF18) was used to study structural relations within the myosin head. By indirect solid phase RIA, this antibody reacted strongly with chymotryptic S1 lacking LC2 but no significant binding was observed to chymotryptic rod, alkaline-released LC's, DTNB-released LC2 or S2 prepared from rod. Immunoblots from SDS-PAGE of S1A1 and S1A2 showed that this antibody binds exclusively to the 96 Kd heavy chain of S1. When S1A1 or S1A2 were digested with trypsin and the products analyzed by immunoblots from SDS-PAGE, it was observed that MF18 binds only to the 27 Kd fragment and not to the 20 Kd or 50 Kd fragments. Therefore, its binding site is in the N-terminal region of the heavy chain (Mornet, D. et al, Biochemistry, 20:2110, 1981). Immunofluorescent studies of acetone or formaldehyde-acetone fixed myofibrils showed specific staining of the A-band, but no staining was observed with unfixed myofibrils. Native myofibrils could be stained only if pretreated with DTNB-EDTA but not if preincubated in either DTT or EDTA alone. In liquid phase RIA it was shown that divalent cations (Mg^{2+} or Ca^{2+}), ATP or actin, did not compete with MF18 for binding to monomeric myosin or synthetic thick filaments. We conclude that in native myofibrils, the 27 Kd peptide is masked and not accessible to the antibody. The fact that this masking effect can be overcome by treatment with DTNB suggests that LC2 may be involved in the process. (Supported by grants from MDA, NIH, American Heart Association and CNPq).

M-AM-Po23 EVIDENCE FOR SELF-ASSOCIATION OF HEAVY MEROMYOSIN. Michael E. Rodgers, and William F. Harrington, Dept. of Biology, Johns Hopkins University, Baltimore, MD 21218.

Sutoh et al., *J. Mol. Biol.* 126, 1 (1978) have demonstrated that long S-2 produced by brief chymotryptic digestion of HMM is able to undergo self-association, whereas short S-2 prepared by tryptic digestion of long S-2 has lost the ability to associate. We have extended this study to heavy meromyosin (HMM) in order to determine whether the myosin heads are able to modulate the S-2 interaction. Long HMM was prepared from rabbit myosin by the method of Weeds and Pope *J. Mol. Biol.* 111, 129 (1977). Short HMM has been prepared by tryptic digestion of long HMM in the presence of actin (to protect the 54K site (Lovell and Harrington *J. Mol. Biol.* 149, 659 (1981))). The molecular weights of these particles are $345 \pm 10 \times 10^3$ and $300 \pm 10 \times 10^3$ respectively. The average tail lengths of the particles have been found by electron microscopy to be 90 ± 15 nm (long HMM) and 50 ± 7 nm (short HMM), thus accounting for the difference in molecular weights. In a solvent comprising 0.1 M NaCl, 20 mM Imidazole, and 1 mM EGTA, pH 7.0 at 5°C, sedimentation equilibrium studies show that long HMM is able to self-associate. Assuming an isodesmic model (as was done for S-2), $K_{eq} = 1.2 \times 10^4 M^{-1}$. Pyrophosphate (> 15 mM) is able to suppress the association completely. Light scattering studies at HMM concentrations up to 27 mg/ml and chemical cross-linking studies also indicate self-association. The light scattering data is currently being analyzed to determine the mode of association. Cross-linking studies suggest that the interaction involves the S-2 portion of HMM. The geometry of the associated species is under investigation. Surprisingly, short HMM, unlike short S-2, exhibits some self-association. This interaction is also suppressed by the addition of pyrophosphate. Neither MgATP (0.5 mM) nor MgADP-Pi (0.5 mM) have any effect on the association. Our results may be relevant to the interaction responsible for locking HMM to the thick filament core. This work was supported by NIH grant #AM04349.

M-AM-Po24 TWO MAJOR ALLELES FOR MYOSIN LIGHT CHAIN-1 IN NORMAL AND DYSTROPHIC CHICKENS. Julie Ivory Rushbrook, Anna I Yuan and Alfred Stracher, SUNY-Downstate Medical Center, Brooklyn, N.Y. 11203.

Two major alleles for myosin light chain-1 of the fast white fibers of domestic chickens have been detected by sodium dodecyl sulfate/polyacrylamide gel electrophoresis and peptide mapping of the gene products. One allele predominates in commercially available White Leghorn birds, while the other is the major form in birds of New Hampshire Red origin including dystrophic line 413, its normal control, line 412, and commercially available New Hampshire Red birds. Heterozygotes were detected in White Leghorn and line 413 birds. The Connecticut dystrophic line, of mixed White Leghorn and New Hampshire Red genetic origin but traditionally having White Leghorn birds as controls in the study of avian muscular dystrophy, expressed the allele predominating in New Hampshire Red birds. No genetic variability was found in myosin light chains-2 or -3.

The distribution of the two alleles in the dystrophic birds and their traditional controls emphasizes the genetic heterogeneity of the dystrophic lines and requires a re-evaluation of the choice of control birds in studies of avian dystrophy.

M-AM-Po25 SUSCEPTIBILITY OF CARDIAC MYOSIN TO A MYOFIBRILLAR PROTEASE FROM MYOPATHIC HAMSTERS.

S.S. Margossian, A. Malhotra & T. Calderon. Dept. of Biochem. and Med. A. Einstein College of Med. & Montefiore Hospital and Med. Ctr. Bronx, NY10467.

Removal of LC2 from cardiac myosin has been possible by the use of a neutral protease from a genetic strain of myopathic hamsters. It was shown that this protease selectively attacked LC2, but that heavy chains appeared to be intact on SDS gels (Malhotra, *et al.*, *Biochem.* 18, 461 (1979)). In skeletal muscle myosin, in addition to digesting the DTNB light chains (LC2), heavy chains were also cleaved (Margossian, *et al.*, *Fed. Proc.* 39, 2309a (1980)). We have reinvestigated the specificity of this protease with respect to rabbit cardiac myosin in order to establish if indeed only LC2 was degraded. Cardiac myosin was incubated with the protease (weight ratio 30:1) and dialyzed overnight against 0.45M KCl, 0.01M imidazole (pH7.0), 2mM EDTA and 1mM DTT. The reaction was stopped with 0.1mM PMSF and soybean trypsin inhibitor and the mixture was further dialysed against a low μ buffer. The precipitated myosin was separated by centrifugation and redissolved in high salt. To monitor the products of digestion both precipitate and supernatant were analyzed by SDS gels and analytical ultracentrifugation. The LC2 was digested away, and an additional band corresponding to myosin rod had also appeared. When the precipitate was further checked by analytical ultracentrifugation, a slow-moving boundary corresponding to the rod, was clearly discernible. Moreover, the gels revealed that the supernatant contained S1. The results demonstrate that in rabbit cardiac myosin this protease, in addition to digesting LC2, also attacked the heavy chains, although the extent of heavy chain breakdown has not yet been quantitated. (Supported by Grants from NYHA, MDA and NHLBI - Grant HL-26569 to SSM).

M-AM-Po26 DEPENDENCE ON ACTIN OF HETEROGENEITY IN ^{18}O -OXYGEN EXCHANGE OF ACTO-MYOSIN (HMM). David D. Hackney, Department of Biological Sciences, Carnegie-Mellon University, Pittsburgh, PA 15213.

Hydrolysis of highly $[\gamma\text{-}^{18}\text{O}]\text{ATP}$ in unlabeled water by acto-HMM at low actin concentration was found to be heterogeneous with significant formation of both P^{18}O_0 and P^{18}O_3 species in agreement with the results of Shukla *et al.* (*J. Biol. Chem.* 255: 11344 (1980)) and Midelfort (*Proc. Natl. Acad. Sci. USA* 78: 2067 (1981)) and in contrast to the homogeneous pattern observed with acto-S1A1 by Sleep *et al.* (*J. Biol. Chem.* 255: 4094 (1980)). Detailed quantitative comparison with theoretical distributions over a wide range of actin concentrations, however, indicates that the low extent of exchange pathway only makes a significant contribution at low actin concentration and does not represent a major fraction of the total hydrolysis seen at saturating levels of actin. This result is consistent with a model in which the low exchange component represents a subpopulation of molecules whose ATPase is maximally stimulated at low actin concentrations, but which accounts for only a small fraction (< 2%) of the total V_{max} ATPase. The bulk of the HMM behaves in a manner consistent with the pattern observed previously for acto-S1A1 in that the extent of exchange is high at low actin concentration producing mainly P^{18}O_0 with a shift in the extent of exchange to lower values in a homogeneous manner as the actin concentrations is increased. (Supported by NIH grant AM25980)

M-AM-Po27 KINETIC STUDIES OF SMOOTH MUSCLE HMM AND ACTO-HMM ATPase. S. S. Rosenfeld and E.W. Taylor, Department of Biophysics and Theoretical Biology, University of Chicago, Chicago, IL 60637.

The binding of ATP to gizzard heavy meromyosin (HMM) gave a 15% enhancement of tryptophan fluorescence. The apparent second order rate constant for ATP binding was similar to that of subfragment 1 (SF-1) (S.B. Marston and E.W. Taylor, *J. Mol. Biol.* (1980) 139, 573-600) but the maximum first order rate constant was two to three times larger (14 sec^{-1} and 95 sec^{-1} for HMM at 4° and 20° respectively, compared to 4 sec^{-1} and 50 sec^{-1} for SF-1 at the two temperatures). Phosphorylated HMM, which showed a 20-fold activation by actin gave the same values for the rate constants. The rapid ATP hydrolysis step ("phosphate burst") gave essentially the same first order rate constant as the fluorescence signal for HMM and an amplitude of up to 0.8 moles per site. The rate and amplitude was not affected by phosphorylation. The rate of the hydrolysis step for acto-HMM at high actin concentrations ($40 \mu\text{M}$ actin in 5 mM PIPES buffer, pH 7.0, 20°) was reduced, relative to HMM, by at least two-fold with little change in amplitude and was not altered by phosphorylation. Under the same conditions, the amplitude of the phosphate burst of rabbit skeletal acto SF-1 was less than 0.05 moles per mole site. The evidence can be interpreted by a simple four-state model.

M-AM-Po28 THE ROLE OF ACTIN IN MODULATING Ca^{2+} BINDING TO TROPONIN. James D. Potter and Henry G. Zot, Section of Contractile Proteins, Department of Pharmacology and Cell Biophysics, University of Cincinnati College of Medicine, Cincinnati, Ohio 45267.

Much is known about the Ca^{2+} -binding properties of skeletal troponin (Tn) *in vitro* and it has been assumed that these Ca^{2+} -binding parameters reflect those of Tn in the thin filament. Several reports have suggested, however, that this may not be the case (e.g., Fuchs, F., *Biophys. J.* **21**, 273). We have recently undertaken studies to determine the effect, if any, actin has on Ca^{2+} binding to Tn using direct equilibrium dialysis techniques in combination with metal buffers to regulate the free Ca^{2+} concentration. Using this technique, Ca^{2+} binding to reconstituted thin filaments (7 mol F-actin: mol Tn: mol Tm) was measured. In the presence of Mg^{2+} , the thin filament complex exhibited a monophasic binding curve with a binding constant of $K = 5 \times 10^5 \text{ M}^{-1}$. The association constants for either Tn alone, or when complexed with Tm (Tm·Tn) were not significantly different from each other, $K = 4 \times 10^6 \text{ M}^{-1}$, but were significantly higher than in the Tn·Tm·Actin complex. A shift in Ca^{2+} affinity was also observed for Ca^{2+} binding to thin filaments in the absence of Mg^{2+} . In this case, the affinity constant for the Ca^{2+} -specific sites was lowered by an order of magnitude in the Tn·Tm·Actin complex. We conclude that the interaction of actin with Tm·Tn alters the Ca^{2+} -binding properties of the Ca^{2+} -specific regulatory sites of Tn such that there is an approximate 10 fold decrease in their affinity for Ca^{2+} . Thus, actin clearly alters the affinity of Tn for Ca^{2+} and since Tn is bound to the thin filament via Tm, actin probably alters the structure of Tm, which in turn, alters the structure of Tn (resulting in the lower Ca^{2+} affinity of Tn). It is probable that the reverse is also true, that Ca^{2+} binding to Tn alters the structure of actin through Tm. (Supported by grants from the American Heart Association (#78-1167) and NIH(HL 22619 3A, 3E)).

M-AM-Po29 MICROCALORIMETRIC STUDY OF ATP HYDROLYSIS AND ADP BINDING BY RABBIT SKELETAL MYOFIBRILS. Robert E. Johnson and Patricia Adams, Dept. of Biochemistry, University of Arizona, Tucson, Arizona 35721.

Suspensions of rabbit skeletal myofibrils were mixed with ADP in 80 mM KCl, 2 mM EGTA, 5 mM MgCl_2 , 2 mM NaN_3 , 5 mM KPO_4 (pH 7.0) at 25 °C in a batch microcalorimeter. The observed heat was only a small fraction of the large exothermic heat of binding of ADP to free myosin that has been reported in the literature. This implies that there are large differences between the energetics of the actomyosin ATPase reaction and the myosin ATPase reaction (Yamada et al, *Biochem.* **20**, 4484 (1981)) which may be related to the two interconverting conformations of myosin described by Shriver and Sykes (*Biophys. J.* **33**, 233a (1981)).

When one to six myosin-head equivalents of ATP were mixed with myofibril suspensions (without EGTA, with $10^{-5} \text{ M Ca}^{++}$) the heat released by the hydrolysis of the first equivalent of ATP was less than one half of that released by the hydrolysis of the second and subsequent equivalents of ATP. (Supported by a Grant-In-Aid from the American Heart Association, Arizona Affiliate).

M-AM-Po30 Ca^{++} DEPENDENT SPECTROSCOPIC CHANGES OF HUMAN TROPONIN-C. J. A. Schauerte, H. Mizukami, and A. E. Romero-Herrera, Department of Biological Sciences, and Department of Anatomy, Wayne State University, Detroit, Michigan 48202

The sequence of the major component of human skeletal muscle troponin C has pro(112) while rabbit skeletal muscle troponin C has ala at the same site. This substitution occurs near the $\text{Ca}^{++}/\text{Mg}^{++}$ binding site III, a site having high Ca^{++} binding affinity in rabbit skeletal muscle troponin C. Using UV-difference spectroscopy we have investigated the effect of this substitution to Ca^{++} binding of human troponin C.

Human skeletal muscle troponin C was obtained according to the method described by Romero-Herrera et al. (*J. Mol. Evol.* **8**, 251-270;1976). Computer assisted UV-difference spectroscopy (Cary 118C interfaced with MicroNova) was performed using 1mg/ml troponin C in buffer containing 50mM KCl and 10mM Hepes at pH 7.4 by addition of incremental CaCl_2 . Difference spectra generated by Ca^{++} binding to the high affinity sites produced peaks characteristic of phenylalanine red shift (248, 254, 265 and 269nm) and additional difference spectrum peaks (278 and 285nm) arising from tyrosine. Although the spectra resemble those observed in rabbit skeletal muscle, the reduction at the tyrosine region may be attributed to the local perturbation due to the proline substitution. (Supported by NIH grant, AM 25579)

M-AM-Po31 REFRACTIVE INDEX OF A-BANDS IS ~30% HIGHER THAN PREDICTED FROM FILAMENT PROTEIN CONCENTRATION. M. K. Reedy and Carmen Lucaveche. Anatomy, Duke University, Durham, N. C. 27710.

Both insect flight (IFM) and vertebrate skeletal muscle (VSM) fibrils show this discrepancy. Thick filament spacing is 58 nm in waterbug IFM, and 45.6 nm (sarcomere length = 2.9 μ m) to 47.2 nm (SL = 2.3 μ m) in rabbit psoas VSM, by our X-ray diffraction of fibrils. Mass/length of isolated filaments by electron scattering (J. Mol. Biol. 122, 55; J. Musc. Res. & Cell. Mot. 2, 45) is ~146 kilodaltons/nm for bug thick filaments (fitting 4 myosins and 1 paramyosin per crown), ~102 kd/nm for rabbit thick (fitting 3 myosins and 0.7 C- or other proteins per crown), and 23 (measured, VSM) to 25 (estimated, IFM) kd/nm for thin filaments. These values predict a filament protein concentration in A-band filament overlap zones (AO-bands) of 12.6% w/v (for IFM) or 13.8% (for VSM of SL = 2.3 μ m). This is only ~75% of actual [protein] in AO-bands of washed fibrils, as measured previously for IFM by quantitative microscopy (interference and EM; Cold Spr Harb Quant Biol 37, 423), but now estimated more simply and rapidly in both IFM and VSM by immersion refractometry. Refractive index matching was performed under the phase contrast microscope, using Percoll or Limulus hemocyanin solutions to minimize contrast of AO-bands, H-bands and I-bands. These compact megadalton solutes (20+ nm) are excluded from 14 nm interfilament interstices (checked by EM). X-ray diffraction shows little (5% by Hc) or no (by Percoll) lattice volume squeezing by A-band-matching concentrations, as expected from the low colloid osmotic pressure (2-9 mm Hg). AO-band RI match occurs with solutions whose RI is equivalent to 16.5% protein (IFM) or 18% protein (VSM), taking RI increase as .0018 for each 1% of protein. [Protein] differences of $\pm 0.5\%$ are resolvable. [Protein] in H- and I-bands of VSM (SL = 2.9 μ m) is respectively 14% and 5%, versus 9.6% and 4.2% expected. Thus, microscopic refractometry indicates at least 30% more mass localized in both insect and vertebrate A-bands than appears in isolated filaments. If filament mass/length values stand, present sarcomere maps of proteins appear quite incomplete. Support: NIH Grant AM-14317.

M-AM-Po32 IONIC MODULATION OF MYOSIN ASSEMBLY. D. Applegate, P. Cheung*, and E. Reisler, Department of Chemistry and the Molecular Biology Institute, UCLA, Los Angeles, CA 90024

Dialysis of myosin from vertebrate skeletal muscle into 10mM citrate-tris buffer (pH 8.0 at 50°C) containing no other salts results in formation of minifilaments (short filaments ~0.3 μ m long). Addition of 0.1M KCl to solutions of minifilaments induces their growth into regular-size synthetic myosin filaments. To gain insight into the process of filament growth we have explored the effect of various salts on the minifilament-filament system. The addition of 0.1M of each of KF, KCH₃COO, KBr to myosin minifilaments resulted in filament assembly as evidenced by light scattering experiments. The addition of 0.1M of each of KI, KSCN, and KClO₄, however, resulted in dissociation of the minifilament structures. The various anions tested follow the lyotropic series in their order as promoters of filament growth or minifilament dissociation. The monovalent cations differ only slightly from each other in their effect on filament growth. It was further shown that at appropriate concentrations of KI and protein (70 mM KI, 3mg/ml myosin) an apparent equilibrium exists between the myosin minifilaments and an intermediate-size species which are larger than the dissociated (monomer-dimer) myosin. These results demonstrate that the myosin association reaction is more sensitive to the ionic composition than to the ionic strength of the medium. The partial dissociation of the minifilaments by KI suggests that the above described effects may be particularly useful in studies of myosin assembly. This research was supported by grants from MDAA and USPHS (AM 22031).

M-AM-Po33 PHOSPHORYLATION OF MYOSIN LIGHT CHAIN BY PROTEASE ACTIVATED KINASE I. Polygena T. Tuazon, James T. Stull, and Jolinda A. Traugh, University of California, Riverside, CA 92521 and University of Texas Health Science Center, Dallas, TX 75235.

Myosin light chain from skeletal and cardiac muscle has been shown to be phosphorylated by two different protein kinases; the Ca²⁺, calmodulin-dependent myosin light chain kinase and a Ca²⁺-independent enzyme activated by limited digestion with trypsin. The protease activated kinase has been partially purified from rabbit reticulocytes and skeletal muscle and is not activated by Ca²⁺ and phospholipids or calmodulin. The apparent K_m value for myosin light chain with the protease activated kinase was 20 μ M. Protease activated kinase I incorporated two moles of phosphate per mole of myosin light chain, whereas only one mole was incorporated by myosin light chain kinase. The chymotryptic phosphopeptides hydrolyzed after phosphorylation by protease activated kinase I were different from those phosphorylated by myosin light chain kinase as shown by two-dimensional peptide mapping. When actomyosin from chicken gizzard was used as substrate, myosin light chain was phosphorylated by the protease activated kinase. The extent of phosphorylation was not affected by addition of Ca²⁺ or EGTA.

M-AM-Po34 SMOOTH MUSCLE ACTIN-ACTIVATED MYOSIN ATPase SHOWS BOTH COOPERATIVE AND NON-COOPERATIVE PHOSPHORYLATION DEPENDENCIES. A. Persechini and D.J. Hartshorne. Muscle Biology Group College of Agriculture, The University of Arizona, Tucson, AZ 85721.

It is widely accepted that the smooth muscle actomyosin ATPase is dependent on light chain phosphorylation. As we have previously reported [Science 213: 1383-1385 (1981)], little activation occurs until both myosin heads have been phosphorylated. In addition myosin phosphorylation is an ordered process. These properties suggest that cooperative interactions exist between the two myosin heads. Further work has confirmed and extended this model of the myosin molecule. We have studied 10-minute time courses of myosin phosphorylation and accompanying actin-activated ATPase. The bulk of the ATPase (ATPase II) shows a cooperative dependence on phosphorylation as expected. However, early in the time course (0 - 2 min.) ATPase is linearly dependent on phosphorylation showing no evidence for cooperativity in the activation process (ATPase I). It is not clear what causes the transition from ATPase I to ATPase II, although it is not likely to be thick filament assembly nor does it appear to be an effect of ADP or P_i . Studies show that only ATPase II induces "superprecipitation". This suggests that ATPase II is linked in vivo to muscle contraction.

M-AM-Po35 PURIFICATION AND PROPERTIES OF RABBIT SKELETAL MUSCLE M-LINE. Peggy J. Arps and William F. Harrington, Department of Biology, Johns Hopkins University, Baltimore, Maryland 21218.

Proteins thought to be components of rabbit striated muscle M-line have been isolated and characterized utilizing either high or low ionic strength extraction procedures. These procedures extract two proteins that appear to be specific to the M-line, a 165,000 dalton protein (M-protein) and creatine phosphokinase (CPK). Other proteins, such as glycogen phosphorylase, are also removed in the process of extraction, but none of these has yet been shown to be part of the M-line structure. Of the total muscle CPK, about 4% is bound to thick filaments. The molar ratio of bound CPK to thick filament is 24 ± 5 , which agrees with the theoretical value of 30 as proposed in the M-line model of Eppenberger and coworkers (in "Proteins of Contractile Systems", E.N.A. Biro, ed., Vol. 31, 119; 1975). Approximately 80% of the M-line CPK extracted from washed myofibrils is capable of rebinding. Isolated native filaments have bound CPK that can be removed by low ionic strength extraction; approximately 25-30% of this extracted CPK was found to rebind. However, binding studies with synthetically-formed thick filaments and CPK, using preparative centrifugation and subsequent assays of CPK activity, show no interaction between these proteins in 0.12 M KCl, 10 mM bis-Tris, 2 mM $MgCl_2$, 0.1 mM EDTA, 1 mM 2-mercaptoethanol, pH 7.2. (Supported by NIH Grant AM 4349).

M-AM-Po36 TITIN: A CANDIDATE AS A PROTEIN COMPONENT OF A NEW TYPE OF LONGITUDINAL FILAMENT IN THE SARCOMERE OF STRIATED MUSCLES. Kuan Wang and Ruben Ramirez-Mitchell*. Clayton Foundation Biochemical Institute and Department of Chemistry, Cell Research Institute, University of Texas at Austin, Texas 78712.

Titin is a pair of extremely large ($M_r \sim 10^6$) major myofibrillar proteins found in a wide range of vertebrate and invertebrate striated muscle. Its detailed structural arrangement in the sarcomere remains to be established. Our immunofluorescent localization studies indicated that titin appears to attach near the ends of thick filaments (PNAS 76 3698 (1979)). Selective extraction studies of myofibrils indicated that titin is not a thin or thick filament-associated regulatory protein. We have speculated that titin may be a component of a new type of filament distinct from thin and thick filaments in the sarcomere (J. Cell Biol. 83 389a (1979)). To test this idea, we have investigated the morphology and assembly properties of purified rabbit titin by rotary shadow and negative staining techniques of electron microscopy. Purified titin, sprayed onto mica and rotary shadowed, appeared as long, unbranched, flexible molecules (from 150 nm to 900 nm, mean ~ 400 nm). Titin aggregates easily into an elastic gel under a variety of conditions. Microscopic examinations of the gel revealed massive aggregates of very thin (2-8 nm) filaments of various lengths. Similar filaments are also found in the KI-extracted "skeleton" of myofibrils. These observations support our proposal that titin may be a component of the putative longitudinal filaments of the sarcomere. [Supported in part by NIH AM 20270 and American Heart Association, Texas Affiliate, Inc.]

M-AM-Po37 PROTEIN PHOSPHORYLATION IN GLYCERINATED LIMULUS MUSCLE. B. D. Gaylinn, W. T. Jackman, M. M. Dewey. Department of Anatomical Sciences, SUNY at Stony Brook, Long Island, NY 11794.

Glycerinated *Limulus* muscle retains a complex enzymatic system for phosphorylation and dephosphorylation of several proteins as revealed by labelling with γ - ^{32}P ATP. Both Ca^{++} -activated and Ca^{++} -inhibited kinase activities are demonstrated as well as Ca^{++} - and "history"-dependent phosphatase activities. Myosin light chain phosphorylation corresponds to conditions of myosin activation as has been shown in vertebrate smooth muscle and more recently reported for isolated *Limulus* proteins (Sellers, J. Biol. Chem., 256:9274, 1981). Paramyosin phosphorylation, which has been suggested in molluscan catch muscle, is not seen in *Limulus*. One hypothesis suggested by the data is that a 32K-dalton protein is involved in the regulation of thick filament shortening. This minor protein is phosphorylated when the muscle is relaxed (100mM KCl, 5mM MgCl, 5mM Tris, 2mM EGTA, 2mM ATP, pH 7.2) and dephosphorylated when the muscle is allowed to shorten (4mM EGTA, 8mM Ca^{++} added). However, if the muscle is pretreated to maximally shorten thick filaments (K^+ activation of live muscle held isometric before and during glycerination), then, when the muscle shortens, thick filament shortening has already occurred and the 32K-dalton protein is not dephosphorylated. We are currently examining the effects of phenothiazine derivatives that inhibit calmodulin-dependent enzymes and thiophosphorylation that inhibits some phosphatases in an effort to further test this hypothesis.

M-AM-Po38 CHEMICAL SIGNAL OF MYOSIN ATPASE AND ITS FLUCTUATIONS. Toshio Ando, Joseph A. Duke, Yuji Tonomura and Manuel F. Morales. CVRI, Univ. of Calif., San Francisco CA 94143

Concentration fluctuations (detected by fluorescence signal) in some species of a steady state reaction system allows us to determine rate constants of steps in which the species are involved. For the study of ATPase kinetics *in vivo* wherein perturbations are hard to apply, fluctuation analysis of the chemical signal is a powerful alternative. To use the fluctuation technique we have to provide a signal which shows large changes in response to the chemical events. It was found that ϵ -ATP can be made to give a very large signal by quenching the fluorescence of bulk ϵ -ATP by acrylamide, with negligible effect on myosin ATPase. The Stern-Volmer constants of myosin-bound and free ϵ -ATP were 7.3 and 57.86 M^{-1} , respectively. Then in the presence of 0.2 M acrylamide the fluorescence intensity of ϵ -ATP increases about 5 times.

Firstly we utilized this fluorescence change to measure the formation rate of the ES complex by stopped-flow. It was found that before formation of the ES complex resistant to quenching there is a previous ES complex in which ϵ -ATP is well exposed. Next we measured fluctuations in concentration of the quench-resistant ES complex. The decay rate of the autocorrelation function obtained in the presence of acrylamide was larger than that in the absence of acrylamide. The later autocorrelation function contains only information about myosin diffusion, while the former one contains informations concerning myosin-diffusion and myosin-reaction.

T.A. is MDAA Fellow. Y.T. is AHA Vis. Sci. Research supported by HL-16683 and PCM 75-22698.

M-AM-Po39 CONFORMATIONAL CHANGES INDUCED BY PHOSPHORYLATION OF THE MYOSIN P-LIGHT CHAIN.

S.P. Scordilis, M.H. Cole and L.A. Bemben, Dept. Biol. Sci., Smith College, Northampton, MA 01063

A new technique has been developed to detect conformational changes in protein secondary, tertiary and quaternary structures. By modification of the urea gradient polyacrylamide gel electrophoresis system of Creighton (J. Mol. Biol., 129:235-264, 1979) the changes in conformation of bovine serum albumin, β -lactoglobulin, unmodified and carboxymethylated ribonuclease A and tropomyosin as they unfold have been monitored and assigned to changes in their secondary, tertiary and quaternary structures. With this calibrated system native myosin and isolated myosin light chains from rabbit fast skeletal, cardiac and uterine muscle myosins were subjected to the same analysis and their behaviors studied in two ways. First, changes in the conformations of the P-light chains upon phosphorylation were detected and analyzed. These results have been interpreted to indicate a greater resistance to denaturation conferred to the P-light chain by phosphorylation. Mechanistically, this may imply a greater stability or rigidity due to the phosphorylation. Second, the change in the equilibrium between the increasing urea concentrations and the native myosin yielded information about the relative binding strengths of the phosphorylated and unphosphorylated P-light chain to the heavy chains. Phosphorylation appears to strengthen the binding of the P-light chain to the heavy chain. These studies are consistent with the idea that phosphorylation relieves the inhibition of the unphosphorylated P-light chain in the actin/myosin interaction.

This work is supported by grants to S.P.S. from the Muscular Dystrophy Association of America and the Blakeslee Fund for Genetics Research to Smith College.

M-AM-Po40 STERIC MODEL AND DIGESTED TROPOMYOSIN (TM), C.E. Trueblood, T.P. Walsh & A. Weber, Dept. of Biochem & Biophys, Univ. of Pennsylvania. Grant support, HL15692 and HL15835.

We have continued our experiments designed to test the validity of the steric model of regulation. On Ca^{2+} addition to a regulated actin filament TM moves from the periphery to the groove and acto-S-1 ATPase increases about 10 fold. When actin is in 100 fold excess over S-1 a comparison of the ATPase activity activated by pure and by regulated actin ($+\text{Ca}^{2+}$) shows that the V_{max} for infinite actin is the same for both actins while more regulated actin is needed to reach $1/2 V_{\text{max}}$. (Murray *et al.*, 1980 FEBS LETT. 114, 169), i.e. potentiation does not occur. The increase in ATPase can be explained by partial removal of sterically blocking TM. Nevertheless, ATPase rises with increasing calcium in a much more cooperative way than explained by simultaneous binding of 2 calcium/troponin (TN). Recently T.L. Hill analysed this type of cooperative transition in terms of a model where it is energetically unfavorable when one of two neighboring TM segments is at the groove and the other at the periphery compared to having both either in the groove or periphery. In terms of a single TM strand and the steric model this means crossing-over of the strand from the periphery to the groove is unfavorable (e.g. resistance against bending). In those terms the recent experiments by Wegner & Walsh (Biochem 20, 5633) also show that crossing is minimized. If the steric model is valid replacing the TM strand by separate molecules should reduce the cooperativity of the ATPase increase. After carboxypeptidase A treatment (digestion) and removal of any undigested TM, TM no longer polymerizes according to viscosity and actin binding. However, prior digestion of TM did not reduce the cooperativity of the ATPase increase. This finding is not yet in contradiction to the steric model until it has been shown that the added TN(TN-T) does not connect the C- and N- terminal ends of 2 TM molecules.

M-AM-Po41 DIGESTION OF CHICKEN GIZZARD MYOSIN WITH PAPAIN. N.Nath, T.S.Chandra, H.Suzuki, A. Carlos and J.C.Seidel, Dept. Muscle Res., Boston Biomed. Res. Inst., Boston, MA 02114.

Papain cleaves the heavy chain of gizzard myosin into five major proteolytic fragments having approximate molecular weights of 133, 110, 90, 67 and 23K, as indicated by gel electrophoresis (PAGE) in SDS. All five peptides are found in a fraction which binds F-actin and only the 110K peptide is found in the fraction which does not. The 133, 110 and 67K fragments precipitate in solutions of low ionic strength containing 10mM MgCl_2 , while the 90, 67 and 23K fragments remain in the soluble fraction. The former are present in the void volume and the latter in the retarded peak from a Sepharose 4B column. Papain cleaves the heavy chain at two major sites, A and B, which are 67 and 90K daltons from the N terminus, respectively. Cleavage at A produces a head held together by non covalent bonds, while cleavage at B forms subfragment-1 (S1), single-headed myosin and myosin rod. Unphosphorylated S1 (US1) and phosphorylated S1 (PS1), with some or all of the 20K light chain intact, can be formed from unphosphorylated and phosphorylated myosins, respectively, but their ATPase activities are fully activated by actin without light chain kinase (MLCK) or Ca^{2+} . PAGE in 8 M urea indicates that PS1 can be dephosphorylated by light chain phosphatase and subsequently rephosphorylated by MLCK but neither treatment alters the actin stimulated ATPase. At all stages of the digestion, the insoluble fraction, which contains myosin and single-headed myosin, has ATPase activity which is activated by actin only when both Ca^{2+} and MLCK are present. The actin activated ATPase of single-headed myosin appears to require phosphorylation, while S1 can be phosphorylated and dephosphorylated without change in this activity.

M-AM-Po42 POTASSIUM ACTIVITY DISTRIBUTION IN MECHANICALLY SKINNED FROG MUSCLE FIBERS IS INFLUENCED BY ATP. R.E. Godt and C.M. Baumgarten. Depts. of Physiology; Medical College of Georgia; Augusta GA 30912, and Medical College of Virginia; Richmond VA 23298.

At pH 7 and 5, we measured distribution potential (E_d) across the fiber boundary using conventional KCl-filled microelectrodes, and K^+ activity using K^+ ion-selective microelectrodes (KISE) made using Corning 477317 liquid ion-exchanger. Solutions at room temperature were buffered with Tris maleate and had 0.15M ionic strength. Those with ATP had (mM): 1 Mg^{2+} , 1 MgATP , 1 EGTA ($\text{pCa} \approx 8$). In addition, at pH 7 they had 118 KCl; those at pH 5 had 110 KCl. ATP-free solutions were similar but had 124 KCl at pH 7 and 5. In ATP solutions at pH 7, penetration of fibers with KISE showed no potential change, indicating that the K^+ equilibrium potential across the fiber boundary closely approximated E_d (E_d : -2 to -20 mV). At pH 5 however, the KISE potential was positive, indicating that K^+ was not in equilibrium with E_d (E_d : 2 to 18 mV), a result unexpected if E_d is a purely Donnan potential. In ATP-free solution, however, no potential was observed with KISE. Thus, in the absence of ATP, K^+ was in equilibrium with E_d . Skinned fibers in ATP media may not be in equilibrium because ATPase reactions are occurring and might well affect the observed E_d . For enzymic reactions in a fixed-charge milieu, differences in mobility of charged substrate and products can lead to perturbations of the equilibrium double layer. These perturbations would be accentuated when diffusing ions bear charge opposite to that of the fixed charges, as is the case at pH 5. Since substrate and products are anionic, coupling to counter-ions (primarily K^+) is required for macroscopic electroneutrality. This coupling may be the origin of the non-equilibrium K^+ distribution in the presence of ATP. (Supported by the GA Heart Assoc. and U.S.P.H.S.:AM25851 & HL24847).

M-AM-Po43 DEPENDENCE OF ACTIN ACTIVATED ATPase OF PHOSPHORYLATED GIZZARD MYOSIN ON THE CONCENTRATIONS OF Ca^{2+} AND Mg^{2+} . Sumitra Nag, Remy Nazareno and John C. Seidel, Dept. of Muscle Research, Boston Biomed. Res. Inst., Boston, MA 02114.

F-actins from chicken gizzard (Strzelecka-Golaszewska et al., *Europ. J. Biochem.*, 104, 41, 1980) or rabbit skeletal muscle activate the ATPase activities of myosins from either muscle without additional proteins or Ca^{2+} . Activation of ATPase activity of gizzard myosin measured with 10mM MgCl_2 occurs only when the myosin is phosphorylated. Neither actin increases the activity of unphosphorylated gizzard myosin if residual myosin light chain kinase has been removed. Skeletal actin stimulates the activity of skeletal myosin more effectively than does gizzard actin, while no consistent difference between the two actins is observed with phosphorylated gizzard myosin (PGM). The maximal velocity at infinite actin concentration, and K_m are the same for both actins. Gizzard tropomyosin (TM) further enhanced the actin activated ATPase activities of PGM or skeletal myosin, the activation being unaffected by Ca^{2+} . With 1 to 2mM MgCl_2 and 2mM ATP, gizzard actin does not enhance the ATPase activity of PGM unless both TM and Ca^{2+} are present, about 2uM Ca^{2+} being required to produce half maximal activation. No activation has been observed with UGM. When PGM is incubated in the ATPase medium in the absence of Ca^{2+} , subsequent gel electrophoresis in 8 M urea shows no unphosphorylated L₂₀, suggesting that the loss of activity in the absence of Ca^{2+} does not involve dephosphorylation of the myosin.

M-AM-Po44 ACRYLAMIDE QUENCHING OF TRYPTOPHAN FLUORESCENCE FROM SOLUTIONS OF MYOSIN SUBFRAGMENT-1 (S1) and F-ACTO-1. Stefan Highsmith and Anthony R. Bari, Department of Biochemistry, U. of the Pacific, San Francisco, CA 94115.

A Stern-Volmer plot for the acrylamide quenching of S1 tryptophan fluorescence at 25°C, pH 7.0 in 0.1 M KCl, 10 mM MOPS was biphasic. At low [acrylamide], the data were fit by a straight line with a slope (K_Q) of 3.8 M⁻¹. Above 0.2 M acrylamide, the slope was 2.4 M⁻¹. It appears that with regard to quenching by acrylamide, the 7 tryptophans of S1 are divided into two groups. The more accessible group was investigated in more detail. K_Q was independent of protein concentration (0.3 to 1.5 μM) and KCl (0.1 to 0.5 M). The dependence of normalized K_Q on (temperature) × (viscosity)⁻¹ indicated that the quenching mechanism is predominantly collisional. 7M guanidinium increased K_Q in the 0-0.2 M region only slightly, indicating these tryptophans are indeed accessible. Comparison to quenching of N-acetyl-tryptophanamide ($K_Q = 21 \text{ M}^{-1}$) suggested that the accessible protein tryptophans are near but not on the surface.

Quenching of the tryptophans in F-actin by acrylamide also gave a linear Stern-Volmer plot, which coincidentally had $K_Q = 3.9 \text{ M}^{-1}$. The equality of the slopes for S1 and F-actin allows one to monitor any loss in tryptophan accessibility due to binding as a decrease in K_Q . However, K_Q was unchanged for solutions of F-acto-S1 with (actin)/(S1) ranging from 0 to 3. These preliminary results suggest that the most accessible tryptophans in S1 and F-actin are not made less accessible when the proteins bind.

Support: NSF Grant CDP-7923045, NIH Grant AM25177 and an NIH Research Career Development Award.

M-AM-Po45 THE EFFECT OF SOLVENT HISTORY ON PARAMYOSIN SOLUBILITY AT DIFFERENT pHs. Nancy Munson and Sonja Krause, Dept. of Chemistry, Rensselaer Polytechnic Institute, Troy, New York 12181.

Acid-R-paramyosin from MERCENARIA MERCENARIA adductor muscle was shown by Cooley, et. al. [*JBC* 254, (1979)] to contain ~3 removable phosphates/molecule. Continued investigation has shown that these phosphates are adsorbed. If the acid-R-paramyosin is purified using a hydroxylapatite column (sample A) it absorbs ~10 phosphates/molecule. Dialysis of the column purified paramyosin against 0.01 M HEPES, 0.59M KCl, 0.5mM DTT, pH 7 for ~48 hrs (sample B) results in the loss of all but ~0.7 phosphates/molecule. Solubility studies using equilibrium dialysis have been carried out on 1mg/ml samples of samples A and B in phosphate and non-phosphate buffers at pH 8-10. Ionic strengths were changed by addition of KCl. At pH 8 in Bicine, samples A and B exhibited approximately the same behavior, while at pH 8 in phosphate buffer sample B was slightly more soluble at intermediate ionic strengths. These solubility curves exhibited the expected high solubility at both ends of the ionic strength range, 0.01M and 0.40M (Cooley, et al. above). At pH 9.0 in Bicine both samples again showed approximately the same behavior. All ionic strengths exhibited high solubility except at μ=0.10M where A was slightly more soluble than B. At pH 9.4 in phosphate both A and B were totally soluble over the ionic strength range studied. This was also the case when studies were carried out at pH 10.0 in CAPS. Preliminary birefringence studies were also carried out on these samples in this pH range using 1mM phosphate and non-phosphate buffers. These studies indicate differences in soluble aggregates of samples A and B.

M-AM-Po46 TROPONIN C-TROPONIN I INTERACTIONS. P.J. Cachia and R.S. Hodges. Department of Biochemistry and Medical Research Council Group in Protein Structure and Function, University of Alberta, Edmonton, Alberta, Canada, T6G 2H7.

A synthetic analogue of troponin I (TnI), [Fph¹⁰⁶]N^α-acetyl TnI 105-115 amide, incorporating p-fluorophenylalanine, has been synthesized by the solid phase method. Complex formation between troponin C (TnC) and this synthetic peptide has been demonstrated in the presence and absence of Ca²⁺ using CD, ¹⁹F NMR, and PMR studies. The maximum interaction occurs at a peptide:protein ratio of 1:1. The CD results show that the synthetic TnI peptide induces 40% of the α-helical change observed by the addition of Ca²⁺ to a Ca²⁺-free TnC sample. PMR studies of the aromatic regions in both the peptide and TnC exhibit changes in the aromatic envelopes of each species. Those changes occurring in the spectrum of TnC are again similar to changes which occur in the Phe envelope of Ca²⁺-free TnC when it is titrated with Ca²⁺. Our present results show that this region of TnI not only binds to actin-tropomyosin in the absence of Ca²⁺ but also binds to TnC in a 1:1 complex in the presence of Ca²⁺ suggesting that this region of TnI is a Ca²⁺-dependent site of interaction. Leavis and coworkers have demonstrated complex formation between intact TnI and proteolytic fragments of TnC which contain the region 89-100. This is the only region of TnC that contains both closely spaced acidic residues which can interact with the basic residues of our TnI peptide fragment and aromatic residues which would be affected by this interaction. Our results are contrary to the findings of Leavis and coworkers who suggest that region 89-100 of TnC is a Ca²⁺-independent site of interaction with TnI. (Supported by MRC).

M-AM-Po47 STRUCTURE OF THICK FILAMENTS IN SCALLOP STRIATED MUSCLE. Loriana Castellani, Roger Craig, Paul Norton, Peter Vibert and Carolyn Cohen, Rosenstiel Basic Medical Sciences Research Center, Brandeis University, Waltham, MA 02254.

The scallop thick filament is a remarkable protein assembly: the entire filament can be thrown into activity by the direct action of Ca⁺⁺ on the myosin molecules. The structure of these filaments may be readily analyzed by X-ray diffraction and electron microscopy. Some unusual features characterize a variety of scallop species. All relaxed muscles show a 485 Å helical repeat as well as the 145 Å axial separation of crossbridges. A special pairing interaction of alternate cross-bridge levels also produces a 2x145 Å = 290 Å repeat (Wray, Vibert & Cohen, *Nature* **254**, 561 (1975); Millman & Bennett, *J. Mol. Biol.* **103**, 439 (1976)). Electron microscopy of sectioned muscle shows a cortical layer of myosin surrounding a light core in various thick filaments that differ, however, in length. The location and organization of the small amount of paramyosin in the core are not yet established. Isolated thick filaments contrasted by negative staining maintain good preservation of crossbridge periodicities, and reveal the 290 Å perturbation most prominently in the region near the bare-zone. Three-dimensional reconstruction of these images is in progress (Vibert & Craig, this volume). A detailed packing model for these filaments may reveal the physical basis for the cross-bridge pairing as well as the nature of the paramyosin/myosin interaction.

Supported by grants from NIH, NSF and MDA, and by a Fellowship from MDA to LC. PV is an Established Investigator of the American Heart Association.

M-AM-Po48 CHARACTERIZATION OF THE TROPOMYOSIN-TROPONIN INTERACTION USING A FLUORESCENT PROBE.

E.P. Morris and S.S. Lehrer, Department of Muscle Research, Boston Biomed. Res Ins, Boston.

Rabbit skeletal tropomyosin (Tm) labeled at Cys-190 with the fluorescent probe N-(1-anilinonaphthyl-4) maleimide (ANM) shows a substantial enhancement in fluorescence (~100%) on binding troponin or troponin-T (Tn-T) (Morris and Lehrer, 1981 *Biophys. J.* **33** 239a). Titrations gave hyperbolic binding profiles which could be fitted to binding constants in the range 0.6-1.0 x 10⁷ M⁻¹. Comparison between N-terminal (Tn-T₁, residues 1-158) and C-terminal (Tn-T₂, residues 159-259) chymotryptic fragments of Tn-T (259 residues) showed no effect for Tn-T₁ and an enhancement of label fluorescence for Tn-T₂. Titrations using ANM-Tm bound to F-actin, which allows the binding to be monitored by sedimentation, were essentially the same as for ANM-Tm alone while sedimentation showed that each of the two fragments bound. A simple interpretation of these observations is that Tn-T is elongated (Ohtsuki (1979) *J. Biochem.* **86** 491), and its C-terminal region binds close to Cys-190 while its N-terminal region binds further away. This is consistent with Ohtsuki's and Pearlstone and Smillie's ((1981) *FEBS Lett.* **128** 119) observations that both of these fragments bind to tropomyosin. The binding profiles obtained with Tn-T₂ and ANM-Tm were linear and did not saturate over the readily attainable concentration range and the greatest fluorescence enhancement was substantially larger than the maximal change obtained with Tn-T. An explanation of this is that Tn-T₂ is capable of binding to a number of different sites on Tm and if it binds close to Cys-190 it produces a larger enhancement in ANM fluorescence than for Tn-T. Thus the intact Tn-T molecule may bind to tropomyosin in such a way that the binding site in the Tn-T₁ region restricts the Tn-T₂ region to binding close to Cys-190. (Supported by MDA and NIH).

M-AM-Po49 DUAL EFFECTS OF THE REGULATORY PROTEINS ON ACTO-S1 Mg^{2+} ATPase. S.S.Lehrer and E.P.Morris
Dept. of Muscle Research, Boston Biomedical Research Inst., Boston, Ma., 02114.

The $[S]$ dependence of the acto-S1 ATPase was studied at constant low $[actin]$ in .05M NaCl, 5mM Mg^{2+} , pH 7.9, 23°, over a range of $[S]$ where the specific activity (per S1) was constant in the absence of the regulatory proteins. In their presence, the activity increases from inhibiting values (below actin alone) to activating values (above actin alone) as the $[S]$ was increased, in each of the three cases: a, tropomyosin+tropoin+ Ca^{2+} (Tm+Tn+ Ca^{2+}); b, Tm; c, Tm+Tn- Ca^{2+} . The $[S]$ which resulted in activation increased in the order a,b,c. In all three cases, however, the inhibition increased toward 100% when the $[S] \rightarrow 0$ (Lehrer, 1981, *Biophys. J.*, 33, 147a). The curves were modeled using the formalism of Hill et al. (*Proc. Natl. Acad. Sci.*, 1980, 77, 3186), for the binding of S1-ADP to two states of regulated actin having a strong and a weak binding constant. Here, it was assumed that the ATPase rate is proportional to the steady state concentration of an actin bound S1-nucleotide species (i.e., analogous to an effective Michaelis-Menten intermediate). Thus, this general formalism is not dependent upon any one specific kinetic scheme. The principal difference observed in the three cases was in the Tm end-to-end cooperativity parameter, Y , which was >1 , and increased in the order a,b,c, indicating that the ease of activation by S1 is greater when the Tm cooperativity parameter is less. These results suggest: i, that the two Ca^{2+} dependent positions of Tm on the thin filament hinders the formation of the active S1-intermediate at low $[S]$; ii, that Tm occupies a third noninhibitory position in the active state at high $[S]$; iii, that Ca^{2+} facilitates the cooperative binding of S1 by decreasing the difference in the end-to-end interactions of Tm between the inhibited and activated states; (also shown by Hill et al., 1980, for S1-ADP).

M-AM-Po50 COMPARISON OF THE EFFECT OF TROPOMYOSIN AND TROPONIN-TROPOMYOSIN ON ACTO-S-1 BINDING. D.L. Williams, Jr. and L.E. Greene (Intr. by J.H. Collins), NHLBI, NIH, Beth., MD 20205

It has previously been shown that troponin-tropomyosin induces S-1-ADP to bind to F-actin in highly cooperative manner (Greene and Eisenberg, *PNAS* 77, 2616 (1980)). The binding of S-1-AMP-PNP to regulated actin shows similar cooperativity. In the present study we compared the effects of tropomyosin alone and troponin-tropomyosin on the binding of S-1-AMPPNP to F-actin, both in the presence and absence of Ca^{2+} . As expected, we found that Ca^{2+} has no effect on the cooperative action of tropomyosin alone. In the absence of Ca^{2+} , the cooperative effect of troponin-tropomyosin is much more pronounced than the cooperative effect of tropomyosin alone. When Ca^{2+} is present, the cooperative effect of troponin-tropomyosin decreases so much that it becomes (if anything) slightly less than the cooperative effect of tropomyosin alone, although the two effects are nearly identical. Troponin-tropomyosin and tropomyosin alone are also identical in their ability to strengthen the affinity of S-1-AMPPNP for actin two- to three-fold, at high levels of saturation of the actin with S-1. We conclude that the major effect of troponin on the cooperative binding of S-1-AMPPNP is to enhance this cooperativity in the absence of Ca^{2+} ; it has little effect on the cooperative action of tropomyosin in the presence of Ca^{2+} .

M-AM-Po51 PLATINUM SHADOWING OF LIMULUS THICK FILAMENTS. Rhea J. C. Levine and Robert W. Kensler. Department of Anatomy, The Medical College of Pennsylvania, Philadelphia, PA 19129.

Long thick filaments ($\sim 4.0 \mu m$) isolated from fresh, relaxed, *Limulus* muscle were adsorbed to grids, rinsed with 1% uranyl acetate (~ 30 sec.), and shadowed with either platinum or platinum-carbon. The shadowed filaments clearly reveal a right-handed helical arrangement of myosin subunits on their surface everywhere except at the bare zone. Optical diffraction patterns of images of the best shadowed filaments show meridional reflections at $14.5 nm^{-1}$ and off-meridional layer lines at 43.5 , 21.8 and $10.9 nm^{-1}$. As expected the diffraction patterns are dominated by reflections arising from only one side of the helix with the 43.5 and $10.9 nm^{-1}$ layer line reflections occurring in the same quadrants, while the $21.8 nm^{-1}$ layer line reflections occur in the opposite quadrants. These layer line spacings and the patterns are in good agreement with and support our earlier (Kensler and Levine, 1981, *Biophys. J.* 33:242a) indexing of the diffraction patterns from images of negatively-stained *Limulus* thick filaments in which reflections from both surfaces of the helix were present. Images of the shadowed filaments obtained by optical filtration of their diffraction patterns are completely consistent with the single-sided helical patterns derived from computer filtration of images of the negatively-stained filaments, and with the presence of 4 myosin cross-bridges per crown in the *Limulus* filament in its long conformation.

Supported by USPHS NRSA GM07475 (RWK) and USPHS HL 15835 to the Pennsylvania Muscle Institute (RJCL).

M-AM-Po52 KINETIC STUDIES OF CALCIUM BINDING TO CALMODULIN. Howard White, Marcia Tudor, Krishna Bose and Darlene Markley, Dept. of Biochemistry, University of Arizona, Tucson, Arizona 85721.

Removal of calcium from bovine calmodulin decreases the tyrosine fluorescence emission approximately 60 percent. The kinetics of calcium dissociation from the tyrosine sensitive site(s) were measured by the decrease in fluorescence observed upon mixing calmodulin in $\cdot\text{Ca}_4^{++}$, with excess EDTA or EGTA in a stopped-flow fluorimeter. The fluorescence decrease is very accurately fit by a single exponential decay of 8 s^{-1} and is independent of chelator and chelator concentration ($\lambda_{\text{exc}} = 280\text{ nm}$, $\lambda_{\text{emiss}} = 312\text{ nm}$, 100 mM KCl, 20 mM Bistris-propane pH 6-9, 20°C). The rate of calcium binding to the tyrosine-sensitive site(s) of calmodulin was measured from the increase in fluorescence observed upon mixing calcium free protein with CaNTA , CaEGTA and CaEDTA buffers. The kinetics of calcium binding were also very accurately fit by a single exponential over the entire range of calcium studied (0.5 to 20 μM). The observed rate constants of binding are a linear function of calcium concentration with a second order rate constant of $7.0 \pm 2.0 \times 10^6\text{ M}^{-1}\text{s}^{-1}$. Equilibrium measurements of calcium binding were determined spectrofluorimetrically using CaNTA (pH 9), CaEDTA (pH 5.7), and CaEGTA (pH 6.5) calcium buffers. The equilibrium binding data are best fit by an association constant of $8 \pm 3 \times 10^5\text{ M}^{-1}$ and a Hill coefficient of 2. The Hill coefficient indicates positive calcium binding to at least two of the four calcium binding sites in calmodulin. (Supported by grants from the Muscular Dystrophy Association and PHS AM2543-01).

M-AM-Po53 THE BINDING OF GIZZARD SMOOTH MUSCLE S-1 TO ACTIN IN THE PRESENCE AND ABSENCE OF ATP. J.R. Sellers, L.E. Greene, E. Eisenberg and R.S. Adelstein, NIH, Beth., MD 20205.

The ability of gizzard smooth muscle S-1 to bind to skeletal muscle actin was examined both in the presence and absence of ATP. In the absence of ATP, competition between gizzard S-1 and skeletal S-1 for actin binding sites showed equal strength of binding at $\mu=0.01\text{M}$ but 15-fold stronger binding of gizzard S-1 at $\mu=0.2\text{M}$. This suggests that the binding of gizzard S-1 to actin shows less salt dependence than that of skeletal S-1, as proposed by Krisanda and Murphy (JBC 255, 10771 (1980)). This was verified by measuring the binding of gizzard S-1 to skeletal muscle actin in the presence of AMP-PNP using the analytical ultracentrifuge. Over a range of ionic strength from $\mu=0.024\text{M}$ to $\mu=0.43\text{M}$ there was only ~5-fold change in the binding constant of gizzard S-1·AMPPNP to actin compared to ~200-fold change in the binding constant of skeletal muscle S-1·AMPPNP. We next investigated the binding of smooth muscle S-1 to actin in the presence of ATP. Here again, over a range of ionic strength from 0.012M to 0.112M, there was only ~4-fold change in the binding constant (K_{binding}) of gizzard S-1·ATP to actin compared to ~80-fold change with skeletal S-1·ATP. Gizzard S-1 KATPase (determined from the double reciprocal plot of ATPase vs actin) also showed less salt dependence than the skeletal S-1 KATPase and, as with skeletal muscle S-1, gizzard S-1 KATPase was stronger than gizzard S-1 K_{binding} . We conclude that, both in the presence and absence of nucleotide, the binding of gizzard S-1 shows much less dependence on ionic strength than the binding of skeletal muscle S-1, suggesting that at physiological salt, cross-bridges may bind more tightly in smooth muscle than in skeletal muscle.

M-AM-Po54 THREE-DIMENSIONAL STRUCTURE OF THE M-BAND IN FISH MUSCLE. Pradeep K. Luther, R.A. Crowther*, John M. Squire, Biopolymer Group, Imperial College, London SW7; *MRC Laboratory of Molecular Biology, Hills Road, Cambridge, England.

Previous detailed analysis of the 3-D structure of the fish M-band by Luther, Munro and Squire (J.Mol.Biol, 1981,151) involved studying micrographs of very thin (200-500Å) slightly tilted transverse sections by optical diffraction and image averaging. Because of the small tilt in the sections, the various structures observed could be assigned to appropriate axial positions (M1, M4 and M6). The present study describes the use of more direct methods using stereo microscopy and computer reconstruction. For this purpose, thicker, 500-700Å, transverse sections were used in order to include the whole M-band within the sections. In the electron microscope the sections were tilted about an axis in steps of 5° from $+60^\circ$ to -60° . Stereo views of tilted pairs e.g. 20° and 30° showed the presence of more than one level of M-bridge. For the computing an area of about 150 unit cells was chosen and the 3-D structure calculated from the tilt series using essentially the method of Henderson and Unwin (Nature, 1975,257,28). The Fourier transform data showed that the M-band and myosin filament have very strong 3-fold (and not 2 or 4-fold) rotational symmetry. This allowed 3-fold rotational averaging and the 3-D map computed using p3 symmetry showed additional 2-fold rotation axes in the plane of M1 and passing through the 3-fold axis. The 2-fold axes are parallel to the 1120 planes of the filament lattice. Fish M-band symmetry is therefore well described by the dihedral point group 32. These preliminary conclusions from 3-D reconstruction confirm the optical diffraction analysis of Luther et al.

(Research supported by the British Medical Research Council and Muscular Dystrophy Assoc.)

M-AM-Po55 THE PRIMARY STRUCTURE OF THE SUSCEPTIBLE REGION OF LONG S-2. Renné Chen Lu & Anna Wong, Department of Muscle Research, Boston Biomedical Research Institute, Boston, MA 02114

Recent studies have shown that subfragment-2(S-2) can be isolated in a longer form with a subunit chain weight of 59 kDal; the fragment contains a flexible region and the short form of S-2 with a chain weight of 37 kDal. The NH₂-terminal sequences of two forms of S-2 indicates that short S-2 arises from the NH₂-terminal region of long S-2, adjacent to S-1, and the presumptive hinge of high proteolytic susceptibility is in the COOH-terminal part of the long S-2 (Lu, PNAS 77, 2010, 1980). In order to further understand the flexible nature of the hinge region efforts were made to determine the primary structure of the susceptible region of long S-2. Since it is not feasible to isolate this region as an intact, homogenous form, the peptides derived from this region were identified by a double labeling method. The long S-2 was methylated with [¹⁴C]-HCHO + NaCNBH₃ and mixed with a small amount of short S-2 which had been methylated with [³H]-HCHO + NaCNBH₃ followed by peptide fragmentation and isolation. Thus peptides with only ¹⁴C were those derived from the susceptible region. Some of the peptides have been aligned and the following sequence obtained: M-N-K-K-R-E-A-E-F-Q-K-M-R-R-D-L-E-E-A-T-L-Q-H-E-A-T-A-A-A-L-R-K-K-H-A-D-S-V-A-E-L-G-E-Q-I-D-N-L-Q-R-V-K-Q-K-L-E-K-E-K-S-E-L-K-M-E-I-D-D-L-A-G-N-M-E-T-V-S-K-A-K-G-N-L-E-K-E. Although this segment appears to be favorable for helix formation as predicted by the method of Chou and Fasman (Biochemistry 13, 211, 1974), the presence of hydrophobic residues at positions 3 and 7 in 7-residue repeats is not apparent, nor are charged residues distributed in a manner favoring a stable coiled-coil structure, e.g. in the case of tropomyosin (ref. Parry, J.M.B. 98, 519, 1975). Supported by grants from NIH (AM 00485) and AHA (781027).

M-AM-Po56 ENERGY TRANSFER BETWEEN LANTHANIDE IONS BOUND TO TROPONIN-C. C.-L.A. Wang, T. Tao, P.C. Leavis and J. Gergely, Dept. of Muscle Res., Boston Biomedical Res. Inst., Dept. of Biol. Chem. and Neurology, Harvard Med. School, and Dept. of Neurology, Mass. Gen. Hosp., Boston, MA 02114

Trivalent lanthanide ions (Ln³⁺) are good substituents for Ca²⁺ at all four metal binding sites of skeletal troponin-C (TnC). In particular, the visible luminescence of Tb³⁺ bound at the high affinity sites of TnC is enhanced when excited through tyrosine residues. We have carried out energy transfer experiments using Tb³⁺ as the donor, and a number of Ln³⁺ as acceptors in order to measure the distance between the high affinity sites of TnC. Samples containing Tb³⁺, Ln³⁺ and TnC in a molar ratio of 1:1:1 were illuminated with a microsecond flash lamp. In the absence of acceptors, the decay of Tb³⁺ luminescence could be fitted with a single exponential with a lifetime of 1.32±0.05 msec. In the presence of certain acceptors, the decay was resolvable into two components: one had the same lifetime as Tb³⁺-TnC, the other had a shorter lifetime, presumably owing to interionic energy transfer. These results are summarized in Table I. From these lifetimes, and the published critical transfer distances (Horrocks et. al., J. Amer. Chem. Soc. 102, 3650 (1980)) we have calculated the distance between the two high affinity sites of TnC to be 9.1±0.2 Å.

TABLE I*

Donor	Acceptor	t ₀ (msec)	t (msec)	E	R ₀ (Å)	r (Å)
Tb ³⁺	-	1.32	-	-	-	-
	La ³⁺	1.31	-	-	-	-
	Dy ³⁺	1.32	-	-	5.0	-
	Er ³⁺	1.30	0.85	0.356	8.1	8.9
	Ho ³⁺	1.25	0.66	0.500	9.4	9.4
	Nd ³⁺	1.38	0.59	0.554	9.3	9.0
Average						9.1

*E is the energy transfer efficiency; R₀ is the critical transfer distance; r is the distance calculated from E and R₀.

M-AM-Po57 CALCIUM SENSITIVE INTERACTIONS OF TROPONIN-T FRAGMENT T2 (RESIDUES 159-259) WITH TROPOMYOSIN IN THE PRESENCE OF TROPONIN-C AND -I. Joyce R. Pearlstone and Lawrence B. Smillie, MRC of Canada Group in Protein Structure and Function, Department of Biochemistry, University of Alberta, Edmonton, Canada T6G 2H7.

Present evidence is consistent with the view that the two chymotryptic fragments of troponin-T (Tn-T), T1 (residues 1-158) and T2 (residues 159-259), bind to separate sites on α-tropomyosin (TM), the former close to or at the head-to-tail overlap region and the latter near Cys-190. In the present study, the Ca²⁺-sensitivity of the interactions of T1 and T2 with TM in the presence of troponin-C (Tn-C) and -I (Tn-I) have been investigated using an α-TM-Sepharose 4B affinity column. Bound fragments were eluted using a 0.1 M to 0.5 M NaCl gradient. T2 and T1 were eluted at 0.21 M and 0.32 M NaCl respectively. The binding of T1 was not affected by the presence of Tn-C under ± Ca²⁺ conditions. The binding of T2 to TM was disrupted by the addition of Tn-C in the presence of Ca²⁺. Under these conditions T2 and Tn-C form a complex. In the absence of Ca²⁺, the addition of Tn-C did not affect the binding of T2. Similar results as with Tn-C were obtained when the Tn-C - Tn-I complex was added in the presence of Ca²⁺. In the absence of Ca²⁺, Tn-I and T2 formed a complex which was eluted at 0.47 M NaCl. These results are consistent with the previous conclusion that troponin binds to the thin filament through a Ca²⁺-insensitive site at the head-to-tail overlap region of TM and at a Ca²⁺-sensitive site in the region of Cys-190. (Supported by MRC of Canada.)

M-AM-Po58 PHOSPHORYLATION OF MYOSIN LIGHT CHAIN KINASE AND RELAXATION OF TRACHEAL SMOOTH MUSCLE.

J.R. Miller and J.T. Stull, Univ. Texas Health Science Center, Dallas, TX 75235

Myosin light chain kinase (MLCK) from smooth muscle is a substrate *in vitro* for cAMP-dependent protein kinase. Phosphorylation of MLCK renders it less sensitive to activation by Ca^{2+} -calmodulin (CM) and may thus contribute to relaxation of smooth muscle in response to increased cAMP formation. Phosphorylation of MLCK by cAMP-dependent protein kinase decreases the ratio of MLCK activities measured in the presence of 4 μM and 100 μM Ca^{2+} , at 1 μM CM. We have observed a decrease in this ratio from 0.79 to 0.21 with purified MLCK and from 0.71 to 0.30 in a tracheal smooth muscle homogenate. The effects of β -adrenergic stimulation upon the MLCK and phosphorylase *a* activity ratios in intact smooth muscle strips were then determined. Bovine trachealis muscle strips, under passive tension only, were quick-frozen after exposure to 0.3 μM isoproterenol for various times up to 5 min. At this concentration, isoproterenol causes near-maximal inhibition of a 0.1 μM carbachol-induced contraction. From a control value of 0.10, the mean phosphorylase *a* activity ratio was increased significantly at times > 1 min., and reached a value of 0.27 by 5 min. In contrast, the mean MLCK activity ratio measured in the same strips was unchanged from control over the entire time course. When trachealis muscle strips were exposed for 5 min. to a super-maximally effective concentration of isoproterenol (5 μM), the MLCK activity ratio was decreased only slightly, from 0.80 to 0.71; this effect was reversed upon removal of the agonist. Thus, β -adrenergic stimulation and presumably an increase in cAMP formation sufficient to induce relaxation in tracheal smooth muscle does not appear to result in phosphorylation of MLCK that decreases its sensitivity to activation by Ca^{2+} -CM. (Supported by NIH grants HL26043 and GM07062).

M-AM-Po59 CHANGES IN ACTIN STRUCTURE DURING POLYMERIZATION DETECTED USING A TRACE LABELING METHOD.

S. E. Hitchcock-De Gregori, S. Mandala, and G. A. Sachs, Carnegie-Mellon University, Pittsburgh, PA 15213

We have studied the structure of actin by measuring the relative reactivities of lysines with acetic anhydride using a trace labeling procedure (Hitchcock *et al.*, 1981) comparing monomeric G-actin, F-actin monomer (Rich and Estes, 1976, actin below critical concentration in 20 mM NaCl), F-actin polymerized with 100 mM NaCl, and F-actin polymerized with 100 mM NaCl, 2 mM MgCl_2 . We have identified 12 of the 19 lysines: 18, 50, 61, 68, 113, 191, 238, 291, 315, 326, 328, 359. In all conditions Lys (326, 328) is the most reactive peptide. In G-actin, Lys 18, 191, 291, 315, and 359 are less than 20% as reactive as Lys (326, 328); the remaining have intermediate reactivities. On polymerization in the presence of NaCl and Mg^{2+} , lysines 50, 61, 68, 113, and 291 become less reactive relative to Lys (326, 328) and Lys 238 becomes relatively more reactive. The changes in Lys 50, 61, and 113 are due largely to the polymerization event whereas those in Lys 68, 238, and 291 appear to be due to an effect of Mg^{2+} on the actin polymer. Lys 18, 191, and 359 increase in relative reactivity in the F-actin monomer and then become less reactive in the polymer showing no large overall change in reactivity relative to the G-actin monomer. Lysines that are reduced in reactivity upon polymerization indicate possible contact regions between actin monomers in the filament and suggest involvement of the N-terminal third of the protein. Supported by MDA and NIH.

M-AM-Po60 LUMINESCENCE OF ACTIN-BOUND TERBIUM IONS. L.D. Burtnick, Department of Chemistry, University of British Columbia, Vancouver, B.C., Canada V6T 1Y6.

Tb^{3+} replaces the tightly bound Ca^{2+} present in conventional preparations of muscle G-actin. An aromatic amino acid residue (probably a tryptophan) on actin lies sufficiently close to the bound Tb^{3+} that excitation of the aromatic chromophore at 295 nm (10 nm bandwidth) results in an approximately 100-fold enhancement of the Tb^{3+} emission at 544 nm over the emission level from the Tb^{3+} - containing buffer alone. On polymerization of the Tb^{3+} - substituted G-actin by the addition of KCl or MgCl_2 , a further enhancement of about 1.5-fold is observed in the emission intensity. However, the responses to addition of KCl or of MgCl_2 differ quantitatively. The addition of KI to 0.6 M to depolymerize Tb^{3+} - substituted F-actin samples leads to a further enhancement in the emission intensity, indicating that the structure of the actin monomers produced differs from that of either the G- or F- forms of actin unit. The binding of DNase I to Tb^{3+} - substituted G-actin results in a net decrease in the luminescence level of the sample, suggesting that complex formation results in a conformational change in actin in the vicinity of its divalent metal ion binding site.

Supported by grants from the British Columbia Health Care Research Foundation and the Natural Sciences and Engineering Research Council of Canada.

M-AM-Po61 FURTHER STUDIES OF X-RAY SCATTERING BY MYOSIN S1 AND THEIR IMPLICATIONS.

Robert A. Mendelson and Edward S. Giniger. University of California, San Francisco, CA. 94143

In order to define better the structure of myosin subfragment one and to ascertain the effect of light chain 2 (LC2) on its structure, we have compared the X-ray solution scattering curves of S1 prepared by chymotrypsin (+EDTA) and papain (+Mg) digestion of myosin. It was found that the scattering curves and radii of gyration (RG) were almost identical for the two preparations: $100(\Delta RG/RG) = +(1 \pm .5)\%$. This is to be compared with a +6% expectation for a uniformly enlarged S1 (based on MWs by Margossian *et al.*); thus S1 with LC2 is more symmetric than without. Scattering patterns and chord distributions (Patterson functions) were computed from S1 shapes derived from several helical EM reconstructions. Although there were some differences between the reconstructions of different workers, the S1 position on actin as suggested by Taylor and Amos always yielded a S1 which gave a better fit to scattering data than did a S1 derived using the position of Moore *et al.* Preliminary modeling shows that large distortions of S1, which plausibly could be responsible for force generation, make the agreement between EM and X-ray scattering worse. This suggests contraction mechanisms in which most, if not all, of the S1 mass moves as a rigid body on actin to generate force. (Supported by USPHS # HL-16683 and NSF grant # PCM 75-22698)

M-AM-Po62 PREPARATION AND CHARACTERIZATION OF FLUOROCHROME-LABELED TOAD STOMACH α -ACTININ. D. D. REES AND F. S. FAY, DEPT. OF PHYSIOLOGY, UNIV. OF MASS. MED. SCHOOL, WORCESTER, MASS. (INTRO. BY J. SINGER).

We propose to study the structure and function of the smooth muscle contractile apparatus by labeling the dense bodies of single, living smooth muscle cells of toad stomach with fluorescent tetramethylrhodamineisothiocyanate (TRITC)-labeled α -actinin. We have, therefore, isolated α -actinin from toad stomach and subjected it to DEAE-cellulose, Sepharose 6B-C1 and hydroxylapatite chromatography. Its subunit molecular weight, determined by SDS polyacrylamide gel electrophoresis (PAGE), is 100,000 daltons. At 40°C μ g quantities of toad stomach α -actinin greatly increase the viscosity of rabbit skeletal muscle F-actin (0.9 mg/ml F-actin in 100mM KCl, 1mM DTT, 20mM Tris-acetate, pH 7.5 [Viscosity Buffer]) measured with a falling ball viscometer. Although unaffected by Ca^{++} and Mg^{++} levels in the assay mixture, the α -actinin-induced viscosity increase is greatly inhibited by increasing the temperature to 23°C, increasing KCl to 200mM, or repeated freezing-thawing of the α -actinin. After conjugation of TRITC to α -actinin, the reaction mixture is applied to a Biogel P-6DG column to separate free TRITC from TRITC- α -actinin. The amount of fluorochrome noncovalently adsorbed to protein is quite low, as estimated from fluorescence of free TRITC after SDS PAGE of TRITC- α -actinin. No effect of fluorochrome-labeling on α -actinin's ability to increase F-actin viscosity in Viscosity Buffer at 4°C can be seen until the α -actinin is heavily conjugated. This demonstrates that an important characteristic of α -actinin, its ability to interact with actin, is preserved under these conditions in moderately labeled TRITC- α -actinin. (Supported by AM06568 (DDR) and HL14523 (FSF)).

M-AM-Po63 ¹⁹F NMR CHARACTERIZATION OF TWO HMM STATES AND THE EFFECT OF DIVALENT METAL IONS.

John W. Shriver[†], Lewis E. Kay, and Brian D. Sykes. Department of Chemistry, University of Alberta, Edmonton, Alberta; and [†]Department of Chemistry and Biochemistry and Department of Medical Biochemistry, Southern Illinois University, Carbondale, Illinois 62901.

A fluorine probe has been attached to the SH₁ position of the globular heads of HMM using N-(4-trifluoromethylphenyl)iodoacetamide. The ¹⁹F chemical shift of labeled HMM serves as a sensitive monitor of the conformational state of HMM. In the absence of divalent metal ion (0.1 M KCl, 50 mM PIPES pH 7.0) the heads may exist in two different interconvertible states that appear identical to those seen with S-1. However, the temperature driven transition between the two states can occur via two different paths and a hysteresis-like behavior is observed. One path is consistent with the two heads behaving independently similar to S-1 (HMM: $\Delta H^\circ = 39$ kcal/mole, $\Delta S^\circ = 131$ cal/deg/mole; S-1: $\Delta H^\circ = 34$ kcal/mole, $\Delta S^\circ = 120$ cal/deg/mole). The other path is consistent with the two heads behaving as a coupled cooperative unit ($\Delta H^\circ = 67$ kcal/mole, $\Delta S^\circ = 236$ cal/deg/mole). Addition of Ca(II) removes the hysteresis effect and only the apparently cooperative conformational change is observed ($\Delta H^\circ = 71$ kcal/mole, $\Delta S^\circ = 240$ cal/deg/mole). This work provides evidence for Ca(II) ion functioning as an effector which promotes the coupling of the two head groups of heavy meromyosin into a cooperative unit. A similar effect is seen with Mg(II) except that the stabilization of the cooperative unit occurs very slowly and is seen only after an hour at 20°C. (Supported by the MRC of Canada and the Alberta Heritage Research Foundation).

M-AM-Po64 POLYMERIZATION AND CROSS-LINKING OF ACTIN FILAMENTS MEASURED BY FLUORESCENCE PHOTOBLEACHING RECOVERY. Frederick Lanni and B. R. Ware, Department of Chemistry, Syracuse University, Syracuse, New York 13210.

We have adapted the technique of fluorescence photobleaching recovery for the study of polymerization and cross-linking of molecular species in solution. A photobleachable fluorescent dye is covalently attached to the species whose mobility is to be monitored. The solution of interest, in a micro-cuvette on the stage of a research microscope, is subjected to an intense pulse of light which has passed from a laser through a grating (Ronchi ruling), so that a striped pattern is created. The grating is then translated and the fluorescence monitored through the grating, so that a time-varying intensity is produced whose frequency is determined by the velocity and spacing of the grating and whose amplitude decays as the mobile species diffuse. From the time constant of the amplitude decay, the diffusion coefficient of the labelled species can be determined. The immobile fraction is evident from the persistent amplitude of the modulated signal. We have used this technique to measure accurate tracer diffusion coefficients of G-actin at low salt and to characterize the growth of actin filaments under higher salt (polymerizing) conditions. We have also used this approach to study the binding and crosslinking of actin filaments by actin-binding proteins and the inhibition of actin polymerization by various derivatives of the cytochalasin family. The FPR technique can be used to visualize the motion either of the polymerizing species or of any of the species which become bound to the supramolecular complex. Thus it serves as a species-specific assay of the assembly of the motile apparatus. (This work supported by a grant from the National Science Foundation.)

M-AM-Po65 THE REGULATION OF ACTIN POLYMERIZATION AND THE INHIBITION OF MONOMERIC ACTIN ATPASE ACTIVITY BY ACANTHAMOEBA PROFILIN. L.S. Tobacman and E.D. Korn. National Heart, Lung, and Blood Institute, NIH, Bethesda, Maryland 20205.

Profilin inhibits the rate of nucleation of actin polymerization and the rate of filament elongation and also reduces the concentration of F-actin at steady state. Addition of profilin to solutions of F-actin causes depolymerization. The same steady state concentrations of polymerized and non-polymerized actin are reached whether profilin is added before initiation of polymerization or after polymerization is complete. The K_D for formation of the 1:1 complex between *Acanthamoeba* profilin and *Acanthamoeba* actin is in the range of 4 to 11 μM ; the K_D for the reaction between *Acanthamoeba* profilin and rabbit skeletal muscle actin is about 60-80 μM , irrespective of the concentrations of KCl or MgCl_2 . The critical concentration of actin for polymerization and the K_D for the actin-profilin interaction are independent of each other; therefore, a change in the critical concentration of actin alters the amount of actin bound to profilin at steady state. At steady state, the concentration of F-actin $[A_f]$, the concentration of total profilin $[P_t]$, the actin critical concentration, $[A]_\infty$, and the K_D for the interaction of actin and profilin are related by the following equation:

$$[A_f] = [A_t] - [A]_\infty(1 + [P_t]/([A]_\infty + K_D)).$$

As a consequence, the presence of profilin greatly amplifies the effects of small changes in the actin critical concentration on the concentration of F-actin. Profilin also inhibits the ATPase activity of monomeric actin, the profilin-actin complex being entirely inactive.

M-AM-Po66 ON THE STABILITY OF THE MYOSIN COILED-COIL. EFFECTS OF HOFMEISTER ANIONS ON THE SUSCEPTIBILITY OF MYOSIN AND ROD TO PROTEOLYTIC DIGESTION. Walter F. Stafford, Department of Muscle Research, Boston Biomedical Research Institute, Boston, MA 01810 and Sarkis S. Margossian, Division of Cardiology, Montefiore Hospital and Medical Center, Bronx, NY 10467.

Myosin rod was found to be resistant to digestion by papain in 0.6M NaCl, 0.05M TRIS, pH 7.3 with little digestion (<5%) occurring within one hour (0.003g/L papain to 0.3 g/L rod, at 22°). However, when rod was exposed to increasing concentrations of phosphate, it became increasingly more susceptible to attack. In 0.6M KCl, 0.05M P_i , 0.01M EDTA, pH 7.3, some digestion to form LMM and an S2 was observed within 1 hr. As the P_i concentration was increased to 0.5M, digestion became more rapid and was essentially complete within 1 hr. In 1.0M P_i , digestion was very rapid with further complete digestion of LMM and S2 to smaller peptides within 15 min. Other anions of the Hofmeister series, notably sulfate and citrate, also enhanced the digestibility with similar results. In another set of experiments, whole myosin also was treated with trypsin in the 0.05M and 0.5M P_i buffers (0.01 g/L trypsin to 0.1 g/L myosin, at 25° and 35°). In 0.05M P_i at 25° digestion of heavy chain (HC) was ~40% and ~90% complete at 2 and 10 min., respectively, with the main products being rod, LMM and S2. At 35° HC was completely digested at 10 min. In 0.5M P_i at both 25° and 35°, at 2 min., HC was completely digested with only a trace of S2 and LMM remaining. These results suggest an increased lability of the coiled-coil in the presence of these anions and are consistent with the observation by Stafford and Margossian (Biophys. J. 30,243a,1981) of a rapidly reversible dissociation of myosin, rod and LMM in high phosphate.

Supported by NHLBI #HL-26229 to WFS; by NYHA, MDA and NHLBI #HL-26569 to SSM.

M-AM-Po67 TROPONIN I (TnI) BINDING SITES ON TnC. Z. Grabarek, J. Grabarek, P.C. Leavis and J. Gergely. Department of Muscle Research, Boston Biomedical Research Institute, Boston Mass.

Three of the eight α -helical regions in rabbit skeletal troponin C (TnC) are involved in interaction with TnI, viz the helices on the N-terminal sides of Ca^{2+} -binding loops II, III and IV (II_N , III_N and IV_N). Two, II_N and III_N , require binding of Ca^{2+} to the low and high affinity sites, respectively, for interaction with TnI (Grabarek et al. *J.Biol.Chem.* in press). We have studied interaction between these sites and TnI using tryptic fragments of TnC containing interaction site II_N alone (TR_1C , residues 9-84) or sites III_N plus IV_N (TR_2C , residues 89-159). Gel filtration studies indicate that the addition of TR_2C to the TR_1C -TnI complex results in dissociation of TR_1C . This suggests either that TR_2C and TR_1C compete for the same binding site on TnI or that TR_2C induces conformational changes in TnI that result in the release of TR_1C . The on-rates for TR_1C and TR_2C binding to TnI were determined by monitoring changes in the fluorescence of TnI labeled with N-(1-anilinonaphthyl)maleimide. The association of TR_1C and TR_2C followed first order kinetics with apparent first order rate constants 211s^{-1} and 47s^{-1} , respectively. Assuming the binding is a second order reaction and the first order rate constants are proportional to the protein concentration, viz $3.3\mu\text{M}$, the second order rate constants are 6.4×10^7 and 1.4×10^7 , respectively. The binding of TR_2C to the complex of TR_1C -TnI also followed first order kinetics with an apparent on rate constant 47s^{-1} . Since the dissociation rate of TR_1C -TnI complex as determined from exchange between added native TnI and labeled TnI in the complex is 20s^{-1} , the dissociation of TR_1C upon addition of TR_2C results from changes induced in TnI when TR_2C binds, rather than from competition for the same site. (Supported by NIH, MDA and AHA)

M-AM-Po68 STUDIES ON THE REVERSIBLE DISSOCIATION OF MYOSIN SUBFRAGMENT 1. Morris Burke and Mathoor Sivaramakrishnan. Department of Biology, Case Western Reserve University, Cleveland, Ohio 44106.

The reversible dissociation of the myosin subfragment 1 isoenzymes SF1(A1) and SF1(A2) has been studied by examining the kinetics of the isoenzyme to hybrid formation at elevated temperatures. The existence of a thermodynamic equilibrium for subunit dissociation was demonstrated by the observation that the rates of hybrid formation with and without preincubations of the isoenzymes were identical. Furthermore, the rate of hybrid formation was shown to be first order with respect to the isoenzyme, indicating that the rate limiting step is an intramolecular process and probably represents subunit dissociation. This analysis also yields K_D values of 1.9×10^{-7} and $3.6 \times 10^{-7}\text{M}$ for the dissociations of SF1(A1) and SF1(A2) respectively at 37° in 0.12M KCl, 10mM MgATP and pH 7.0. From the temperature dependence of hybrid formation the thermodynamic parameters ΔG° , ΔH° and ΔS° and T_m for these transitions for SF1(A1) and SF1(A2) have been evaluated and confirm that SF1(A2) is significantly less stable than SF1(A1). From the salt dependence of the process it appears that the transition to hybrid involves a net gain of about one molecule of KCl per isoenzyme. Supported by grants PCM-8007876 from the National Science Foundation and 2 R01 NS 15319-03A1 from the National Institutes of Health.

M-AM-Po69 UTILIZATION OF NUCLEOTIDE TRIPHOSPHATES BY CARDIAC AND SKELETAL MUSCLE SARCOPLASMIC RETICULUM AND PURIFIED NTPASE. R.J. Bick, W.B. Van Winkle, C.A. Tate and M.L. Entman. Sec. of Cardiovascular Sciences, Baylor College of Medicine, Houston, TX 77030.

In contrast to skeletal muscle sarcoplasmic reticulum (SR), cardiac SR hydrolyzes GTP in a manner quite distinct from ATP hydrolysis which we have designated "the alternative enzyme cycle". Cardiac SR hydrolysis of GTP is identical in rate to total ATP hydrolysis, shows a non-linear response with respect to nucleotide concentration, but is not calcium-dependent and gives rise to calcium accumulation but not translocation. Purification of the NTPase from both muscle sources results in an increase in specific activity and an alteration in the NTP concentration response compatible with a single high affinity binding site for ATP in cardiac SR and for both substrates in skeletal muscle SR. Both native skeletal muscle SR and the purified NTPase hydrolyze GTP and ATP, while in the purified cardiac NTPase there is no GTP hydrolytic activity. A23187 and oxalate increased cardiac NTPase activity with ATP as substrate but not with GTP, and nucleotide-dependent uptake of oxalate by cardiac SR was only present with ATP as substrate. E~P formation and decay were demonstrable with both substrates in skeletal muscle SR preparations, but only with ATP in the cardiac SR. After NTPase purification all "basic" activity was removed. From the standpoint of skeletal muscle SR, GTP is merely a less effective substrate for the same enzyme activities effected by ATP. In contrast, after purification, the cardiac NTPase is unable to utilize GTP as a substrate under any conditions. It is suggested that purification of the cardiac NTPase eliminates the alternative hydrolysis cycle not involving acyl phosphate formation or calcium translocation and that the "basic" Mg^{2+} ATPase may represent a less active manifestation of this alternative cycle. Supported by AHA (TX Affl.), HL 13870, HL 22855 and HL 17269.

M-AM-Po70 STUDIES ON THE HEAVY CHAIN-ALKALI LIGHT CHAIN INTERACTION IN MYOSIN SUBFRAGMENT 1.
Morris Burke and Hong Liyeuh Wang. Department of Biology, Case Western Reserve University,
Cleveland, Ohio 44106.

The influence of nitration of the three tyrosyl residues of A1 and A2 on the ability of these chains to reassociate with the heavy chains of myosin subfragment 1 has been investigated. Whereas all three tyrosyl residues in both these free light chains can be modified in 6M guanidine hydrochloride with tetranitromethane, only two can be modified in their native structure. By studying the sites of labeling at different extents of nitration it was shown that the two tyrosyl residues, nitratable in the native structure, are those located in the CB-1 and CB-3 cyanogen bromide peptides and that these are modified simultaneously and not sequentially. Although modification in 6M guanidine hydrochloride results in aggregation, this is not observed for nitration of these chains in their native structure. Monomeric forms of these light chains with two or three modified tyrosyl residues do not reassociate with the heavy chains of subfragment 1 by either the NH_4Cl or thermal hybridization procedures. Since quantitative reduction of the nitrotyrosyl groups to aminotyrosyl residues does not restore the heavy chain association function, it appears that regions in A1 and A2 at CB-1 and CB-3 of the common sequence segment exert an influence on the site for heavy chain association on these chains. Supported by grants PCM-800786 from the National Science Foundation and 2 R01 NS 15319-03A1 from the National Institutes of Health.